

Durham E-Theses

The application of radioactivity to studies of diffusion in solids

Ian M. Hoodles

How to cite:

Hoodles, Ian M. (1957) The application of radioactivity to studies of diffusion in solids. Doctoral thesis, Durham University.

Use policy

The full-text may be used and/or reproduced, and given to third parties in any format or medium, without prior permission or charge, for personal research or study, educational, or not-for-profit purposes provided that:

- a full bibliographic reference is made to the original source
- a <https://etheses.durham.ac.uk/id/eprint/8827/> is made to the metadata record in Durham E-Theses
- the full-text is not changed in any way

The full-text must not be sold in any format or medium without the formal permission of the copyright holders.

Please consult the [full Durham E-Theses policy](#) for further details.

THE APPLICATION OF RADIOACTIVITY TO STUDIES OF
DIFFUSION IN SOLIDS.

THESIS

submitted for the degree of

DOCTOR OF PHILOSOPHY

of the

UNIVERSITY OF DURHAM

by

IAN M. HOODLESS, B.Sc.

SEPTEMBER, 1957.



CONTENTS.

Page

	Acknowledgements.	
	Abstract.	
Chapter 1.	The Introduction.	1.
1.1.	Outline.	1.
1.2.	The Methods of Investigation of Ion Movement in Alkali Halide Crystals.	1.
1.3.	The Einstein Relationship.	2.
1.4.	The Structure-Sensitive Region.	4.
1.5.	Recent Experiments on the Structure- Sensitive Region.	7.
1.6.	The Evidence for Mosaic Structure in Single Crystals of Sodium Chloride.	8.
1.7.	The Effect of Fine Structure on Ion Movement.	10.
1.8.	The Present Work.	12.
Chapter 2.	The Growing of Single Crystals of Sodium Chloride.	14.
2.1.	Available Methods.	14.
2.2.	The Furnaces.	15.
2.3.	The Cooling System.	16.
2.4.	Temperature Control.	17.
2.5.	The Vessels for the Molten Sodium Chloride.	18.
2.6.	Seed Crystals.	18.
2.7.	Growing Technique.	18.
2.8.	Cleavage of Crystals.	19.
2.9.	The Purity of the Crystals.	20.

	<u>Page</u>
Chapter 3.	The Measurement of the Conductivity of Single Crystals of Sodium Chloride. 23.
3.1.	Introduction. 23.
3.2.	The Aim of the Conductivity Studies. 24.
3.3.	The Circuit. 24.
3.4.	The Crystal Unit. 26.
3.5.	The Temperature Measurement. 28.
3.6.	The Method of Measurement of the Conductivity. 29.
3.7.	The Electrode Materials. 31.
3.8.	The Calculation of the Conductivity from the Results. 36.
3.9.	The Results of the Conductivity Measurements. 37.
Chapter 4.	The Measurement of the Self-Diffusion of Sodium in Single Crystals of Sodium Chloride. 48.
4.1.	Introduction. 48.
4.2.	The Previous Methods of Measurement of Self-Diffusion in the Alkali Halides. 48.
4.3.	Outline of the Absorption Method of Measurement of the Self-Diffusion Coefficient. 51.
4.4.	The Details of the Diffusion Technique. 53.
4.5.	The Absorption Curve for Sodium-22. 57.
4.6.	The Calculation of Diffusion Coefficients. 59.
4.7.	The Results of the Diffusion Measurements. 65.
4.8.	The Nernst-Einstein Relationship. 72.

		<u>Page</u>
Chapter 5.	The Measurement of Surface Diffusion of Sodium on Single Crystals of Sodium Chloride.	75.
5.1.	Introduction.	75.
5.2.	Outline of the Method of Measurement.	75.
5.3.	The Details of the Diffusion Technique.	76.
5.4.	The Dimensions of the Surface Counting Arrangement.	79.
5.5.	The Calculation of the Surface Diffusion Coefficient.	81.
5.6.	The Results of the Surface Diffusion Measurements.	85.
Chapter 6.	The Surface Patterns on Cleaved Faces of Single Crystals of Sodium Chloride.	87.
6.1.	Introduction.	87.
6.2.	The Evaporation Vessel.	88.
6.3.	The Evaporation Technique.	89.
6.4.	The Results.	90.
Chapter 7.	Autoradiographic Studies of Diffusion in Single Crystals of Sodium Chloride.	92.
7.1.	Introduction.	92.
7.2.	Details of the Autoradiography Technique.	92.
7.3.	The Exposure and Development of the Nuclear Plates.	94.
7.4.	The Grinding of the Crystals.	95.
7.5.	The Sensitivity of the Method.	95.
7.6.	The Results.	96.

	<u>Page</u>
Chapter 8.	The Discussion of Results. 99.
8.1.	The Mosaic Block Theory. 99.
8.2.	The Theory of Seitz. 100.
8.3.	The Results of the Present Work. 101.
8.4.	Comparison of the Results with Other Workers. 103.
8.5.	Comparison of the Results with the Previous Theories. 105.
8.6.	The Presence of Altrivalent ions in the Crystal. 106.
8.7.	Interpretation of the Present Work. 108.
8.8.	Surface Diffusion and Grain Boundary Diffusion. 112.
8.9.	Future Work. 114.
Chapter 9.	Appendix. 116.
9.1.	The Labelling of Sodium. 116.
9.2.	Calculations on the Nernst-Einstein Relationship. 118.
	References. 121.

ACKNOWLEDGEMENTS.

I am deeply indebted to my supervisor, Dr. S.J. Thomson, for suggesting the problem and for his invaluable advice and encouragement at all times during the research.

I also wish to thank Mr. G.R. Martin for his advice on the conductivity measurements, and Mr. J.V. Major for his help and advice with the autoradiography experiments.

Finally I wish to acknowledge with gratitude a maintenance grant for my three years research from the Durham Colleges in the University of Durham.

Ian M. Hoodless

Ian M. Hoodless.

ABSTRACT.

The aim of the investigation was the study of the influence of crystal fine structure on conductivity and cation self-diffusion in single crystals of sodium chloride. Crystals were grown by the Kyropoulos technique and subjected to thermal treatments likely to alter the crystal fine structure. Both annealing and chilling of single crystals produced changes in the crystal conductivity and in sodium-22 self-diffusion rates at temperatures below 520°C. In the investigation of conductivity a study was made of electrode materials and for the diffusion measurements a sensitive absorption method was used.

The changes in diffusion rates and conductivity might have been the result of changes in internal surfaces and grain boundaries. The possibility of ion movement in grain boundaries was investigated by autoradiography of sections of crystal into which sodium-22 had penetrated. The rate of movement of sodium-22 on the surface of sodium chloride was also investigated and a limit set for the surface diffusion coefficient.

It was concluded that cation movement in sodium chloride single crystals does not take place more rapidly in the grain boundaries or on internal surfaces than it does through the bulk of the crystal. An explanation of the changes in diffusion rates and conductivity on thermal treatment of the crystal is offered in terms of vacancies, grain boundaries and impurity ions.

CHAPTER 1.

THE INTRODUCTION.

1.

INTRODUCTION.1.1. OUTLINE.

The experiments, which have been conducted in recent years, on the self-diffusion and conductivity in single crystals of the alkali halides by Mapother, Crooks and Maurer (1), Morrison et al. (2), Schamp and Katz (3), and Etzel and Maurer (4) have been interpreted in terms of vacancies in the otherwise perfect single crystal lattice. Seitz (5) has also recently published two reviews on ionic crystals in which ion mobilities are discussed from the standpoint of vacancies in the crystal lattice.

It is important to note, however, that, although these recent experiments have been interpreted in terms of lattice vacancies, there is a growing body of evidence which suggests that the single crystals of the alkali halides have discontinuities and boundaries in them. It was, therefore, the purpose of the present work to determine the effect of these boundaries on the self-diffusion and conductivity in the crystals.

1.2. THE METHODS OF INVESTIGATION OF ION MOVEMENT IN ALKALI HALIDE CRYSTALS.

Since the early 1920's, numerous investigations have been carried out on the movement of ions in ionic crystals and in particular on the movement in alkali halides. In early experiments the conductivity of the alkali halide crystals was measured. Turbandt (6) in a series of



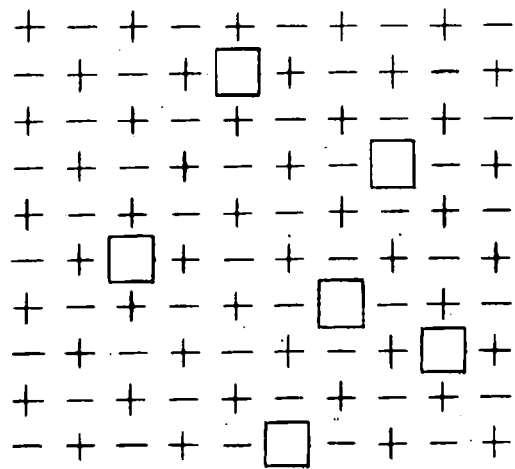


Fig. 1. Schottky defects.

measurements on the transport of matter under an applied electric field has shown that in the alkali halides, except at very high temperatures, the current is carried solely by the cation. In effect, therefore, the conductivity measured in the alkali halide crystals is the ionic conductivity of the cation in the crystal. More recently, with the increased availability of radioactive tracers, several investigations have been carried out on ion movements in crystals by self diffusion processes.

This movement of ions by diffusion or conduction in the crystal cannot be explained in terms of a perfect ionic crystal and so must be attributed to the presence of imperfections in the crystal. These imperfections fall into two classes namely, mosaic structure, dislocations, etc., and secondly, defects in the crystal because of ion vacancies.

1.3. THE EINSTEIN RELATIONSHIP.

The ion vacancies in the alkali halides are of the Schottky disorder type, Fig. 1. The disorder consists of anion and cation vacancies, present in equal numbers, and these can be considered to be formed by the removal of the ions from their normal lattice positions to the crystal surface. The movement of the ions, in diffusion or conductivity, can then be interpreted in terms of migration of these vacancies through the crystal.

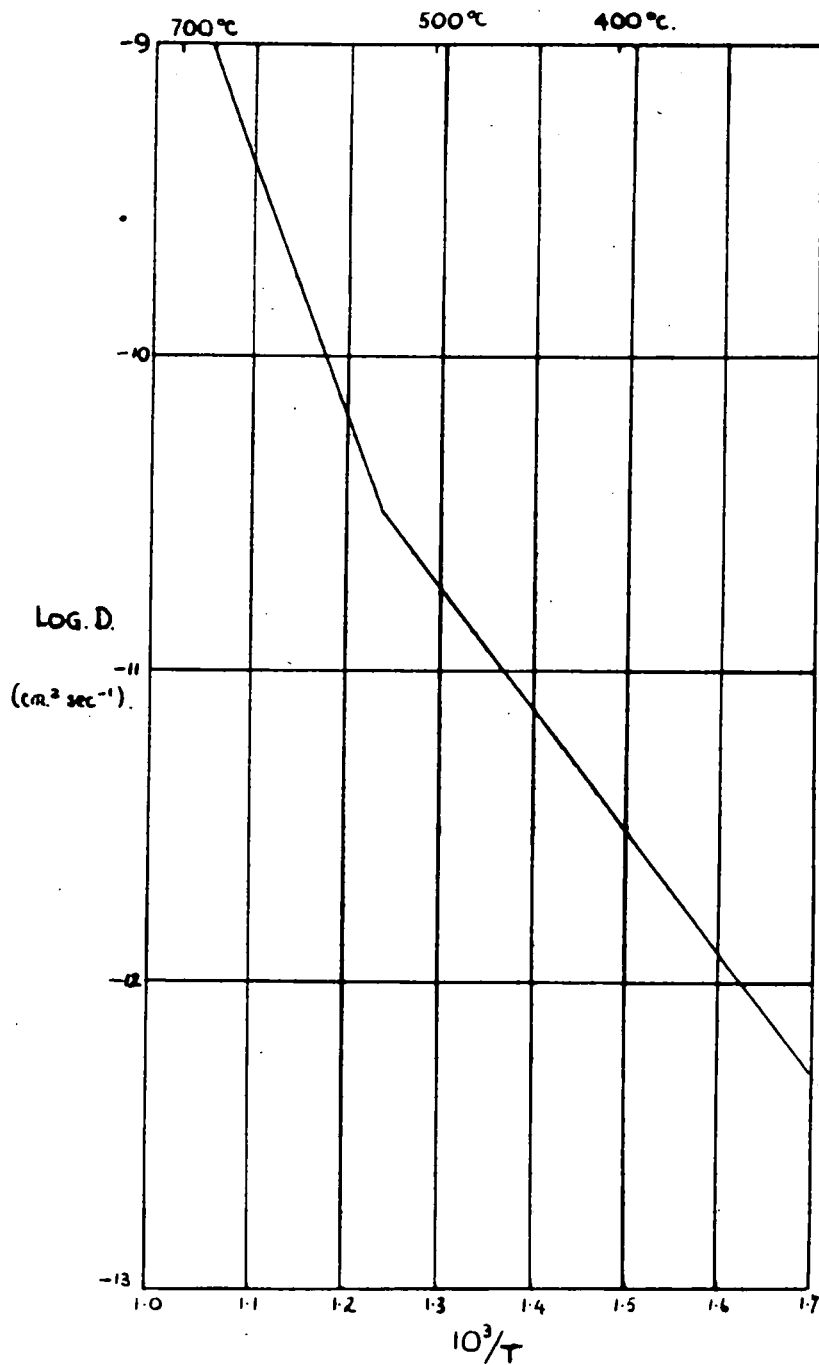


Fig. 2. Variation of the diffusion coefficient with temperature.

It is apparent that there is a close connection between the diffusion and the conductivity processes in the alkali halides since both are related to the movement of the cation in the crystal, the conductivity being accounted for by the ion movement under the influence of an electric field. A relationship has been derived by Nernst (7) and Einstein (8) to connect diffusion and conductivity. It is,

$$\sigma/D = Ne^2/kT \quad (\text{Eqn. 1})$$

In the expression σ is the ionic conductivity, D , the self-diffusion coefficient, and N , the number of ion pairs per cm.³.

In recent years, several notable experiments have been carried out to verify this relationship by measurement of the self-diffusion of sodium in sodium chloride and bromide crystals and the conductivity of these crystals at various temperatures (1,3,4). The graphs obtained by plotting the logarithm of the conductivity or the diffusion coefficient against the reciprocal of the absolute temperature invariably gave two distinct straight lines, Fig. 2. The knee in the graph for sodium chloride appears at 550°C. Above this point, consistent values of the conductivity or diffusion coefficient are obtained independent of the past history of the crystal specimens and in this region the Einstein relationship (Eqn. 1) is found to hold true, so proving that the ionic movement in this region is due to the

diffusion of lattice defects of the Schottky type, which were previously described. Below 550°C , the conductivity or the diffusion coefficient vary from one specimen to another and are dependent on the degree of purity and the past thermal history of the crystal. The region is known as the structure-sensitive region. It has been found that the directly measured self-diffusion coefficient is always larger than the diffusion coefficient calculated from conductivity results thus showing the Einstein relationship does not hold in this region.

1.4. THE STRUCTURE-SENSITIVE REGION.

Several theories have been put forward to explain conductivity and diffusion in this structure-sensitive region since the sharpness in the knee of the curve suggests that the mechanism for the ionic movement in the two regions must be different. The theories will be discussed in terms of the variation in conductivity observed for specimens examined in this structure-sensitive range.

The first theory was proposed by Smekal (9) who suggested that the structure-sensitive conductivity could be explained by the movement of a small number of suitably placed ions, in this case the Na^+ ions, along the grain boundaries in the crystal. This type of movement would probably have a low activation energy as would be expected in this low temperature region. Furthermore, different crystals would probably have different mosaic structures so

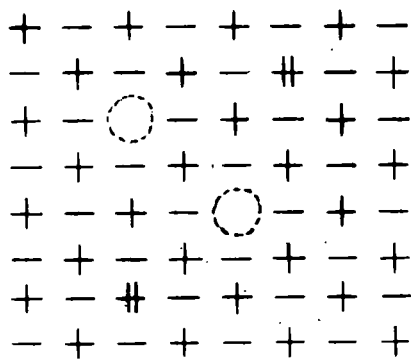


Fig. 3. The effect of divalent cations in the lattice.

explaining the variation of conductivity from one specimen to another. It would seem reasonable to suppose that the thermal history of the crystal and its degree of purity may affect the mosaic structure and results from the microscopic examination of crystal surfaces seem to support this view. These results will be described in a later chapter.

Jost (10), on the other hand, suggested the concept of "frozen equilibrium" based on the idea of Order-Disorder transitions. He suggested that on cooling a crystal from a high temperature, a point would be reached where the equilibrium distribution of disorders could not be attained in a reasonable time and so these disorders would be "frozen in" in the crystal. Changes in temperature below this point would have no effect on the number of defects. In this case, a rapidly quenched crystal would be expected to show an increased ionic conductivity.

A third hypothesis, first put forward by Koch and Wagner(11) suggested that the structure-sensitive region would depend on the presence of altermvalent ions as impurities in the lattice. Consider the case of the presence of a divalent cation in a lattice position, Fig. 3. To maintain electrical neutrality another cation vacancy must be formed in the crystal. These vacancies would be present at all temperatures and would affect the conductivity and diffusion in the low temperature region where, from thermodynamical

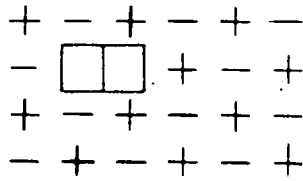


Fig. 4. Neutral pair vacancy.

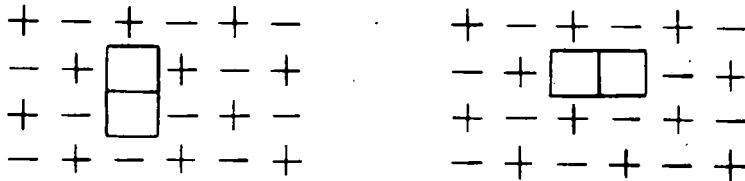
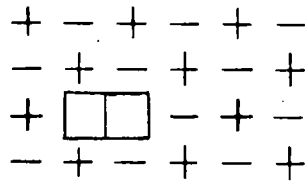


Fig. 5. Diffusion by neutral pair mechanism.

considerations, the concentration of Schottky defects must be low. Hence the degree of purity of the crystal would have a great effect on the ionic movement in the structure sensitive region, while the past thermal history of the crystal would be expected to have no effect.

More recently two proposals based on the Koch-Wagner hypothesis have been put forward to explain this structure-sensitive region. The first interpretation, which was put forward by Seitz (5), is to explain this structure-sensitive behaviour in terms of neutral pairs of vacancies formed by a cation and an anion vacancy.

Since a cation vacancy has an effective negative charge and an anion vacancy a positive charge, they will be attracted to one another and tend to form a vacancy pair which would be neutral, Fig. 4. This vacancy pair would then be able to move through the crystal, Fig. 5, and so contribute to diffusion but because of its neutrality it would not contribute to the conductivity. Hence this would explain why the directly measured self-diffusion coefficient would be larger than that calculated from conductivity measurements.

Mapother, Crooks and Maurer (1), however, proposed that a fraction of the divalent impurity ions, present in the crystal, would be associated with vacancies to form a complex in which a positive ion vacancy was a nearest neighbour of the impurity ion (Fig. 6). Such complexes would not contribute to the conductivity but would contribute to the self-diffusion.

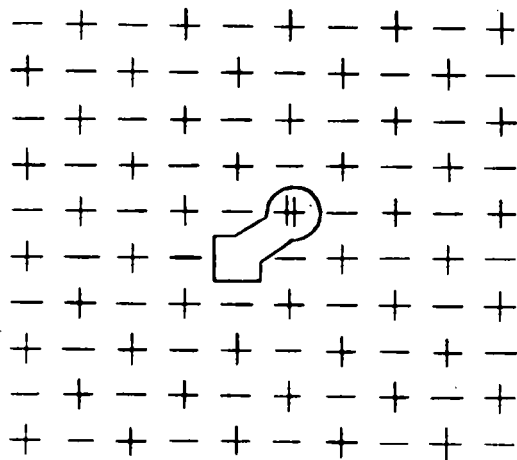


Fig. 6. The divalent impurity ion-vacancy complex.

Both these proposals explain, therefore, the discrepancy between the measured diffusion rate and that calculated from conductivity measurements. They also explain the dependence of the structure-sensitive region on the past history and degree of purity of the crystal since the number of complexes formed will be dependent on the divalent cation impurity present in the crystal and both the formation of the neutral pairs and the complexes will be dependent on the past thermal history of the crystal.

1.5. RECENT EXPERIMENTS ON THE STRUCTURE-SENSITIVE REGION.

The recent experiments of Mapother, Crooks and Maurer (1) on structure-sensitive self-diffusion and conductivity in single crystals of sodium chloride and sodium bromide have been interpreted in terms of the formation of divalent impurity ion-vacancy complexes. This theory has been supported by the work of Etzel and Maurer (4), who have measured the effect of the addition of divalent cations on the conductivity of single crystals of sodium chloride.

The possibility of the neutral pair mechanism in the alkali halide crystals in the structure-sensitive region has been disproved by the work of Schamp and Katz (3) who have measured the self-diffusion of bromide ions in single crystals of sodium bromide and by Morrison et al. (2) who carried out the same measurements for the chloride ions in sodium chloride crystals. It was found in both these measurements that the anion diffusion was too small to

account for diffusion by a neutral pairs mechanism.

The recent experiments have therefore all been interpreted in terms of vacancies in the otherwise perfect crystal lattice, but recent advances in the theories of dislocations in crystals have shown that the possible influence of these dislocations on the diffusion and conductivity cannot be ignored. The evidence for the dislocations in sodium chloride single crystals will be dealt with in the next section.

1.6. THE EVIDENCE FOR MOSAIC STRUCTURE IN SINGLE CRYSTALS OF SODIUM CHLORIDE.

The existence of discontinuities within rock-salt crystals has been shown by heating the crystals in a sodium vapour (12). The sodium aggregates along faults in the crystal and these faults may be traced by using an ultramicroscope. Amelinckx, Van der Vorst, Gevers and Dekeyser (13) have recently published photographs of dislocation networks in natural and artificial single crystals of sodium chloride by an additive coloration technique.

Further evidence for fine structure in single crystals of sodium chloride is available from investigations on the scattering of light by the crystals. These experiments have been carried out by Humphreys-Owen (14), Schneider and Parker (15), and Taurel (16). The variation in intensity of the scattering has been interpreted as being due to small cracks or fissures in the crystal and they have been able to make estimates of the size of these mosaics.

X-ray studies on single crystals have also indicated the presence of crystallites in natural and artificial sodium chloride crystals,(17,18). Jones and Smith(19) have employed the X-ray technique of Guinier and Tennevins (20) to determine the cross sectional area of the crystallites in single crystals of sodium chloride grown by the Kyropoulos technique.

Evidence for the existence of inhomogeneities in sodium chloride crystals has also come from a study of freshly cleaved crystal surfaces. Amelinckx (21) has carried out a detailed study on the cleaved surfaces of sodium chloride crystals by an etching process followed by viewing under a microscope and his experiments have revealed the presence of grain boundaries and slip lines on the surface. On theoretical grounds, the existence of small surface cracks has also been suggested by Lennard-Jones (22). He assumes that these cracks occur as a result of unbalanced forces at the crystal surface and may extend into the interior of the crystal so forming a mosaic structure.

A number of investigators have measured the size of these mosaics, and in Table 1, a summary of these results of crystallite size in single crystals of sodium chloride is given.

TABLE 1.

Investigator	Method of Measurement.	Length of Side of Crystallite.
Furth and Humphreys Owen (14)	Light scattering	2000Å
Taurel (16)	"	1800Å
Parker and Schneider (15)	" #	2000Å
Amelinckx (21)	Etching	3.5μ.
Smith and Jones (19)	X-ray	.15 - .41 cm. (in area.)
Renninger (23)	"	10 ⁻⁴ - 10 ⁻³ cm.
Goldsztaub and Kern (24)	Toepler method	1 cm.

Measurement for potassium chloride.

The variation in crystallite size is probably the result of studying crystals grown in different laboratories for, as Smith and Jones (19) have shown, there is even a difference in crystallite size along the axis of single crystal boules of sodium chloride grown by the Kyropoulos technique.

1.7. THE EFFECT OF FINE STRUCTURE ON ION MOVEMENT.

The preceding section has outlined the large amount of evidence for fine structure in single crystals of sodium chloride. Since it is generally true in diffusion that energy of activation for surface diffusion is less than the energy of activation for grain boundary diffusion

which is less than the energy of activation for bulk diffusion (25), the fine structure would be expected to have a considerable influence on the conductivity and diffusion in the crystals.

A detailed study of the literature on the influence of fine structure on the conductivity in ionic crystals leads to a series of conflicting reports. Von Hevesy (26), for instance, has shown that single crystals of sodium nitrate, because of their smaller internal surface, show a lower conductivity than the polycrystalline mass solidified from the melt. Tammann and Veszi (27) have shown an analogous case with sodium chloride, the polycrystal being formed in this case by compression of powdered salt, while a comparison of the conductivity of a sodium chloride polycrystal and a single crystal grown from solution has shown that the latter is a hundred times less than the former (28). These experiments point to the internal surface being of great importance in conductivity measurements.

Etzel and Maurer (4), on the other hand, found that the conductivity of "pure" sodium chloride single crystals and crystals containing less than 0.2 moles per cent of cadmium was not affected by heat treatment. They allowed a crystal to cool rapidly in air from 770°C and found it had the same conductivity as a crystal cooled at a rate of 1°C per minute. Quenching of crystals containing more than 0.2 moles per cent of cadmium did increase the

conductivity by as much as 70 per cent. This latter observation has been verified by Goodfellow (29) and Schneider and Cunnell (30) on crystals containing manganese as impurity. Schneider and Cunnell (30) however have also found that the conductivity of "pure" sodium chloride crystals is affected by quenching, which is the converse of Etzel and Maurer's results. Schneider and Cunnell have interpreted their results in terms of an effective block structure in single crystals resulting from a non-uniform distribution of impurities, while Etzel and Maurer have explained their results in terms of impurity-vacancy complexes.

1.8. THE PRESENT WORK.

In view of the discrepancies in the reports on the effect of the annealing of crystals on their conductivity and in the lack of information on these types of studies on self-diffusion in sodium chloride crystals, it was the immediate aim of the present work to carry out a detailed study of the effect of fine structure on the conductivity and self-diffusion in single crystals of sodium chloride.

It was proposed to carry out the investigation along the following lines:-

- a) Single crystals of sodium chloride were to be grown from the melt by the Kyropoulos method, then, for the sake of purity, the crystals were to be melted down and regrown from this new melt.
- b) After making a careful study of electrode materials, the conductivities of specimens from the same single

crystal were to be measured after various heat treatments which were likely to alter the fine structure of the crystal. Chilling of the crystals was to be carried out at a temperature at which vacancies would not be "frozen in" in the crystal.

c) The self-diffusion of sodium was to be studied in chilled and annealed specimens taken from the same single crystal as was used in the conductivity studies. A radioactive technique was to be used which would give the best comparison of diffusion rates after the various treatments of the crystal. It was also proposed to study the surface migration of radioactive sodium on the crystal.

d) The possibility of migration of sodium in the grain boundaries of a single crystal of sodium chloride was to be studied by an autoradiographic technique.

It was hoped that the results of these investigations would give a much clearer picture of the role of the fine structure in diffusion and conductivity in single crystals of sodium chloride.

CHAPTER 2.

THE GROWING OF SINGLE CRYSTALS OF
SODIUM CHLORIDE.

2. THE GROWING OF SINGLE CRYSTALS OF SODIUM CHLORIDE.

2.1. AVAILABLE METHODS.

The choice of method for the growing of large single crystals of sodium chloride lay between the Stober process and the Kyropoulos process, which are described by Menzies and Skinner. (31) .

In the Stober process a crucible containing the molten alkali halide is cooled in a slowly changing thermal gradient. This is brought about by keeping the temperature at the top of the melt constant while the temperature at the lowest point of the melt is slowly reduced by cooling. In this way the isothermal planes move up through the material. The position of the isothermal corresponding to the melting point of the material determines, at any time, the location of the solid-liquid boundary. Crystallisation begins when this isothermal plane reaches the lowest point of the crucible and then moves upwards through the melt.

In the Kyropoulos process a seed crystal is lowered into the molten salt, maintained at a temperature approximately 50° above the melting point of the salt. The seed is cooled and crystallisation of the melt tends to take place on the seed. The crystal is then raised gradually, keeping the lower surface always in contact with the melt. This is continued until a large enough crystal has been obtained and then the crystal is removed from the melt.

It was decided to use the Kyropoulos process since this process has advantages over the other method in that it is possible to observe the growth of the crystal; furthermore if the seed is a single crystal it is extremely likely that the crystal growing on the seed will be single, as the crystal tends to follow the same crystallographic orientation as the seed.

2.2. THE FURNACES.

The furnace, in which the sodium chloride was to be melted, consisted of a cylindrical fire-clay core, 5 in. internal diameter by 10 in. in length, wound with heavy "Nichrome wire", .039 in. in diameter. The total resistance of the furnace, at room temperature, was 60 ohms. The windings were covered with a thick paste made by mixing Thermal Syndicate Ltd. C60 alumina cement with water. The cement was dried by passing a low current, sufficient to give a furnace temperature of 150°C , through the furnace for 24 hours and then fired by taking the temperature up to 800°C for 8 hours.

A circular base plate, about 3 in. thick, was moulded from Messrs. Morgan's Plastic Mouldable and then baked out at 150°C . The furnace rested securely on this base plate. The upper end was closed by covers of $\frac{1}{2}$ in. Sindanyo sheet, obtained from Turners Asbestos Cement Co. Ltd.

The furnace was then fitted into a cylindrical steel

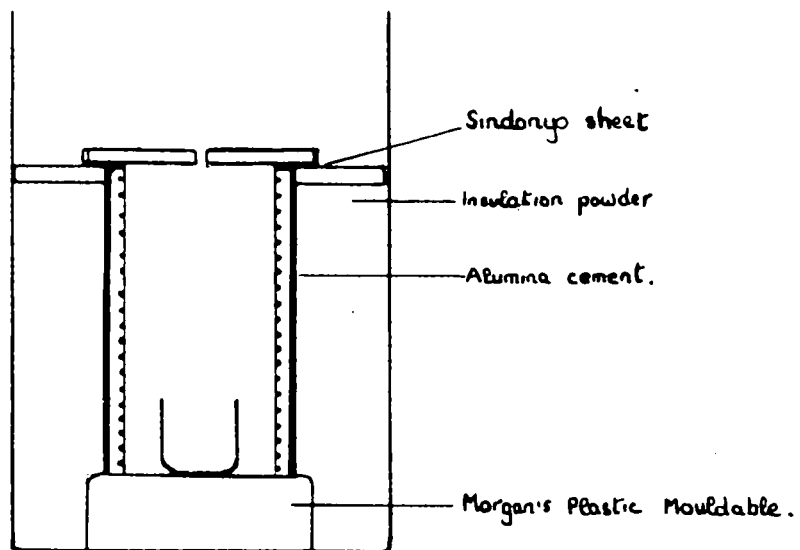


Fig. 7. The furnace.

container, 12 in. diameter by 24 in. long, the space between the furnace and the container being filled with a magnesia-pipeclay lagging. It was most important that the furnace was uniformly lagged, for if the temperature variations were not symmetrical about the vertical axis then uneven growth occurred, the crystal tending to grow most rapidly towards the coolest side of the furnace. The top of the furnace was made from a circular disc of $\frac{1}{2}$ in. Sindanyo sheet which fitted securely into the container, the disc having a 6 in. diameter hole cut in its centre to allow access to the furnace interior. The leads to the furnace were brought out through insulated holes in the steel container and connected to the mains through a variac and the temperature controller; the maximum input was 1250 watts. Illumination of the interior of the furnace was provided by a galvanometer lamp fitted above the furnace.

The completed furnace is shown in Fig. 7.

A similar type of furnace was constructed to run at 600° - 700° C for annealing the crystals. This had a maximum input of 850 watts.

2.3. THE COOLING SYSTEM.

The cooling system for holding the seed crystal is shown in Fig. 8. This consisted of a nickel tube 0.4 in. diameter which was silver-soldered to a nickel head. The head was made from a solid nickel bar, 1 in. diameter, and had a cylindrical hole, $\frac{1}{2}$ in. diameter by $\frac{1}{2}$ in. in length,

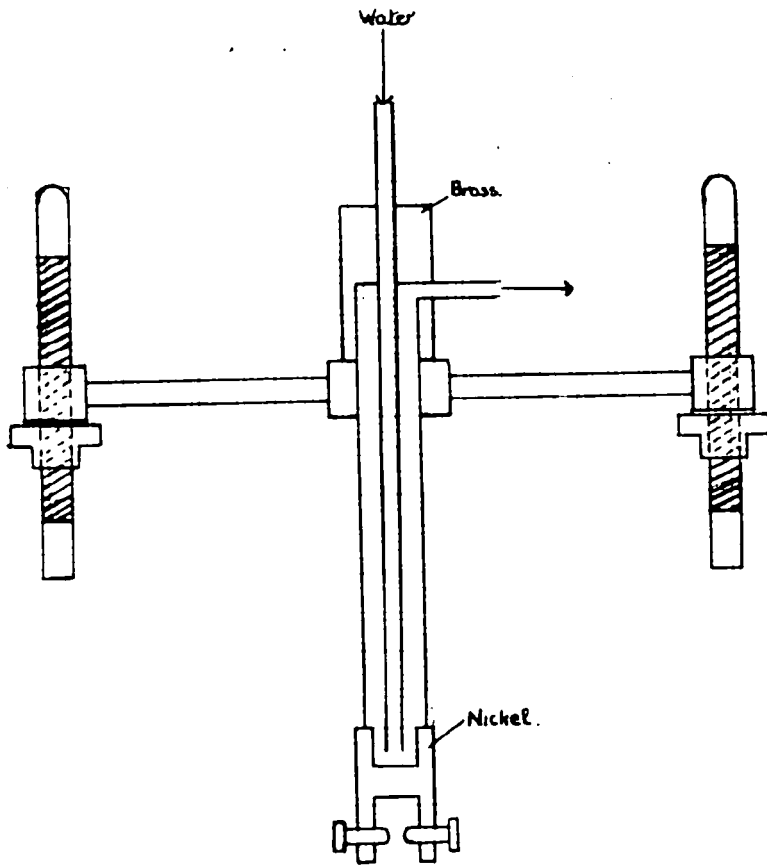


Fig. 8. The cooling system.

at its lower end. Four nickel grub-screws were mounted at 90° to one another in this end so that a seed crystal of rectangular dimensions could be held. The tube was fitted to a brass-block, through which a thin brass tube, 0.2 in. diameter, ran; the internal tube continued down to within $\frac{1}{2}$ in. of the nickel head. Water could be passed down this central tube to cool the head and the seed crystal.

The brass block was connected by steel bars to two vertical steel bars, which had a thread cut over 6 in. of their upper ends. The height of the cooler was adjusted by two heavy-brass knurled nuts which ran on these threads. The framework was fitted to the wall of the laboratory to ensure rigidity.

2.4. TEMPERATURE CONTROL.

Temperature control of the "growing" furnace was maintained by using a "SUNVIC" Resistance Thermometer Controller Type RT.2. and a platinum resistance thermometer.

The platinum resistance thermometer, which had a resistance of 10 ohms at 0°C , was fitted into the furnace and protected by a nickel tube. The leads from the thermometer were sheathed against induction and connected to the appropriate range terminals of the RT.2 controller. The controller could then be adjusted to the desired temperature. The furnace temperature was controlled to within $\pm 2^{\circ}\text{C}$ of the desired value. Failure to maintain these temperature limits caused faulty "melting back" of the seed crystal so

leading to a polycrystalline growth.

2.5. THE VESSELS FOR THE MOLTEN SODIUM CHLORIDE.

Initially 400 ml. glazed porcelain beakers were used to hold the sodium chloride in the furnace. These suffered from the disadvantages that the solidification of the melt on cooling smashed the beaker so a new beaker was required for each day's crystal growing and furthermore it appeared that impurities in the wall of the beaker diffused into the melt. In later work a 200 ml. platinum beaker was used; this could be cleaned before each growth.

2.6. SEED CRYSTALS.

In the initial experiments it was found convenient to use single crystal pieces of some natural rock-salt crystals as seed crystals. The crystals grown from these were split and used as the seeds for further crystals. The average size of seed crystal used was 0.5 cm. x 0.5 cm. x 2.0 cm.

2.7. GROWING TECHNIQUE.

The beaker was filled with "ANALAR" sodium chloride and placed in the furnace, which was then brought up to a temperature approximately 50°C above the melting point of sodium chloride. The seed crystal was then fixed securely in the nickel head by means of the grub-screws and the whole cooling system lowered by means of the brass nuts into the furnace until the seed crystal dipped into the melt. The rate of water passing through cooling tube was

adjusted until the water just boiled in the cooler. In this way the faces of the seed crystal were allowed to melt away so forming fresh, clean faces. When this was adjudged to have happened, usually after some fifteen minutes, the rate of water was increased and the growing commenced.

The crystal grew downwards, and outwards and when the latter growth was sufficient the seed was raised slightly. This process was repeated until a large enough crystal was grown. In the later stages of growth it was sometimes necessary to lower the furnace temperature slightly and also slow down the lifting rate. By this means crystals 2 in. in height and $1\frac{1}{2}$ in. in diameter were grown.

After growth of the crystal the cooling system was raised, the grub-screws were loosened and the crystal transferred rapidly by means of tongs to a platinum beaker in the "annealing" furnace, which was at 600°C . The crystals were then allowed to cool to room temperature over a period of twelve hours by gradually reducing the current supplied to the furnace. After cooling the crystals were stored in a calcium chloride desiccator until required.

2.8. CLEAVAGE OF CRYSTALS.

The crystals, which were cylindrical in shape, were then cleaved into specimens, suitable for use in the experiments. This was carried out most conveniently by cleaving with a mallet and chisel. With practice it was

found that it was very easy to cleave cleanly along the (100) planes provided the crystals were sufficiently annealed. Smaller specimens (less than 1 in. square) could be cleaved by using a razor blade and a hammer. Unless the blade was parallel to the cleavage plane the crystal shattered or produced a series of steps on the cleaved face. It was found that the cleaved faces were effective enough without polishing for the needs of the experiments.

Polycrystals were very difficult to cleave, usually the crystal being shattered in the process. Examination of the polycrystals under a polarising microscope showed that they cause a change in the plane of polarisation of the light.

2.9. THE PURITY OF THE CRYSTALS.

An essential feature of the work was to have the crystals of as high a degree of purity as possible and attempts were made to purify the "ANALAR" sodium chloride by a zone melting technique. This method of purification has been used very successfully in the case of a number of metals. (32)

The basis of the method is to have the material to be purified in the form of a bar and to slowly move a small furnace, capable of melting the material, along the bar. In this way a molten zone will travel along the bar and results show that the impurities in the material move towards one end of the bar, so leaving the other end in a much purer state.

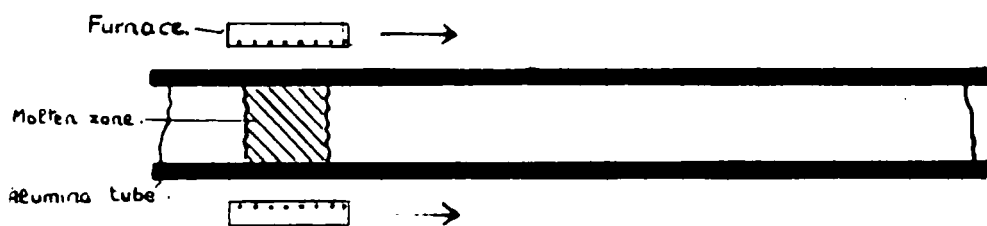


Fig. 9. The zone-melting apparatus.

An alumina tube, 1 in. in diameter and 24 in. in length, was cleaned by immersing in molten sodium chloride. It was then filled with "ANALAR" sodium chloride and set up so that a small furnace, 3 in. in length, could pass along it, Fig. 9. The furnace was maintained at 850° - 900° C, a temperature high enough to melt the sodium chloride fairly rapidly, and then passed along the tube at a speed of 4 in. per hour. The traverse was then repeated, the furnace passing once again in the same direction. The tube was then broken and samples of the sodium chloride were removed and spectroscopically analysed. The results, shown in table 2, did not show any evidence of purification. (See Table 2 overleaf).

The experiments were repeated using a platinum tube, 12 in. length and $\frac{1}{2}$ in. diameter, in place of the alumina tube and with the number of traverses of the furnace increased. It proved, however, extremely difficult to melt out definite sections of the bar of sodium chloride at the end of the experiment and it was impossible to prevent the contamination of one section by its neighbour during this melting out.

However a certain amount of purification of the crystals has been possible since Schulman⁽³³⁾ and McFee⁽³⁴⁾ have observed that the impurity content of an alkali halide crystal grown by the Kyropoulos technique was of the order of one tenth of the impurity concentration in the melt.

The crystals used in the experiments were grown, melted down and regrown from this once purified melt so obtaining crystals which were about one hundred times purer than "ANALAR" sodium chloride.

TABLE 2.

Sample B: Zone 8 in. from end A - once melted.

Sample F: Zone 15 in. from end A - twice melted.

Sample E: Zone 20 in. from end A - twice melted.

Sample G: Original "ANALAR" sodium chloride.

	Sample B	Sample E	Sample F	Sample G
Potassium	.002%	Not detected	.0005%	Not detected
Aluminium	.0005%	.001%	.0005%	.0005%
Lithium	.0001%	.0001%	.0001%	Not detected
Silver	.0003%	.0001%	.0001%	.0001%
Copper	.0001%	.0001%	.0001%	.0001%
Iron	trace	Not detected	Not detected	Not detected
Calcium	Less than .0005%, if any, in all samples.			
Magnesium	Less than .0005%, if any, in all samples.			

CHAPTER 3.

THE MEASUREMENT OF THE CONDUCTIVITY OF
SINGLE CRYSTALS OF SODIUM CHLORIDE.

3. THE MEASUREMENT OF THE CONDUCTIVITY OF SINGLE CRYSTALS OF SODIUM CHLORIDE.

3.1. INTRODUCTION.

The measurements of Turbandt (6) on the transport of matter by passage of a current have established that, except at high temperature, only the sodium ion is mobile in sodium chloride. Measurement of the conductivity of a sodium chloride crystal is therefore a measure of the movement, under the influence of an electric field, of a sodium ion in the crystal.

Early experiments (35) have shown that the conductivity varies with temperature and when the logarithm of the conductivity is plotted against the reciprocal of the absolute temperature, the graphs invariably possessed a "knee" dividing the graph into two distinct parts. The graphs may be fitted to an equation of the form,

$$\sigma = A_1 e^{-E_1/RT} + A_2 e^{-E_2/RT} \quad (36)$$

where $A_1 < A_2$ and $E_1 < E_2$. The "knee" in the graph for sodium chloride occurs at approximately 550°C. Above this temperature the conductivity is reproducible and independent of the past history of the crystal specimen, the ionic movement obeying the Nernst-Einstein relationship, i.e. $\sigma/D = Ne^2/kT$ (Eqn.1), which relates diffusion to conductivity. In the low temperature range, however, the conductivity is much less reproducible and is dependent on the past thermal history and the degree of purity of the crystal. In this range the Nernst-Einstein

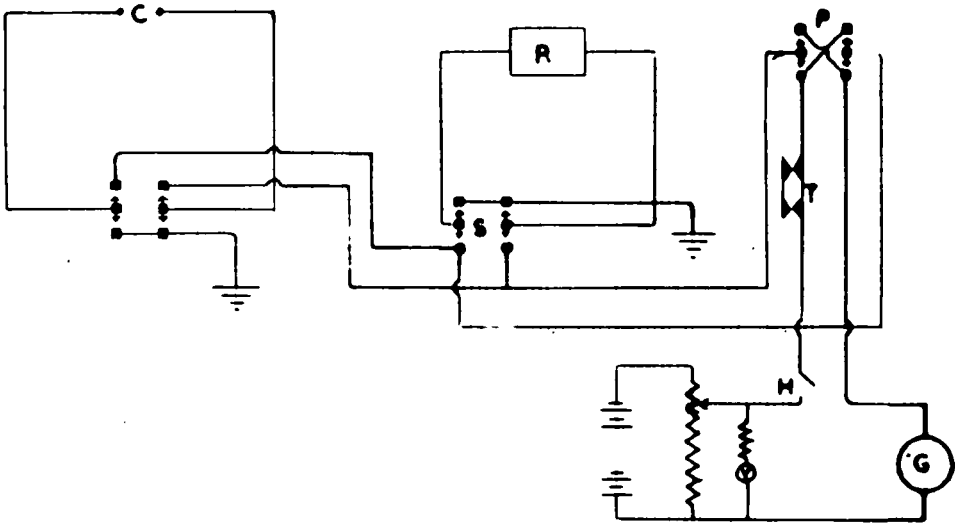


Fig. 10. The conductivity circuit.

relationship is not obeyed. These observations, which have been noted by numerous workers, have led to the conclusion that in the upper temperature range ionic transport in the crystals is explained by the diffusion of lattice defects, mentioned in the thesis introduction, but in the low temperature region much more complicated processes occur.

3.2. THE AIM OF THE CONDUCTIVITY STUDIES.

The aim of the conductivity measurements was to determine the effect of the fine structure on the crystal conductivity in the low temperature range. Pieces of the same crystal were to be given a series of heat treatments, which would be expected to alter the size of the mosaic structure without "freezing in" vacancies in the crystal, and their conductivities compared. Furthermore particular care was to be taken in the measurement of conductivity by inter alia making accurate temperature measurements and by a critical examination of a variety of electrode materials to be applied to the sodium chloride crystals.

3.3. THE CIRCUIT.

The circuit, shown in Fig. 10, was similar to that used by Mapother, Crooks and Maurer (1). The principle behind the method was to measure the deflection produced on a galvanometer by passing a pulse of d.c. current through a crystal slice, then to replace the crystal by a variable resistance box and to adjust this until the same deflection was obtained with a similar pulse of d.c. current.

The pulse of current was produced by a timing switch, T, connected to a 120 volt H.T. battery and a potentiometer so that the voltage could be varied from 0 to 40 volts. The timing switch consisted of two rotating cams geared to a small electric motor; each cam closed a pair of platinum points once during each revolution and these cams were geared so that a pulse of d.c. current, lasting 0.2 second, could be delivered once every 17 seconds. The timing switch was brought in for each pulse by a manually operated switch, H. The pulse was fed through a polarity switch, P, to a manually operated reversing switch, S, where, either the crystal unit, C, described in section 4, or the resistance box, R, could be brought into circuit. The deflection produced by passing the pulse through the circuit was measured by a Pye mirror ballistic galvanometer, G, whose deflection was noted on a 50 cm. scale placed one metre away from the mirror. The galvanometer had a period of 10.5 seconds and gave a deflection of 300 cms. on the scale by a passage of 1 micro-coulombs. This proved, however, to be too sensitive to external effects and so the galvanometer was damped by having a 22,000 ohm resistance in parallel.

The resistance box, R, which was capable of measuring from 1000 ohms to 55 megohms, consisted of a series of high stability carbon resistors with a tolerance of 1 per cent. The 1000 ohm and 10,000 ohm ranges were two Muirhead Decade Resistance Boxes, type A26, and the remaining 100,000 ohm, 1 megohm

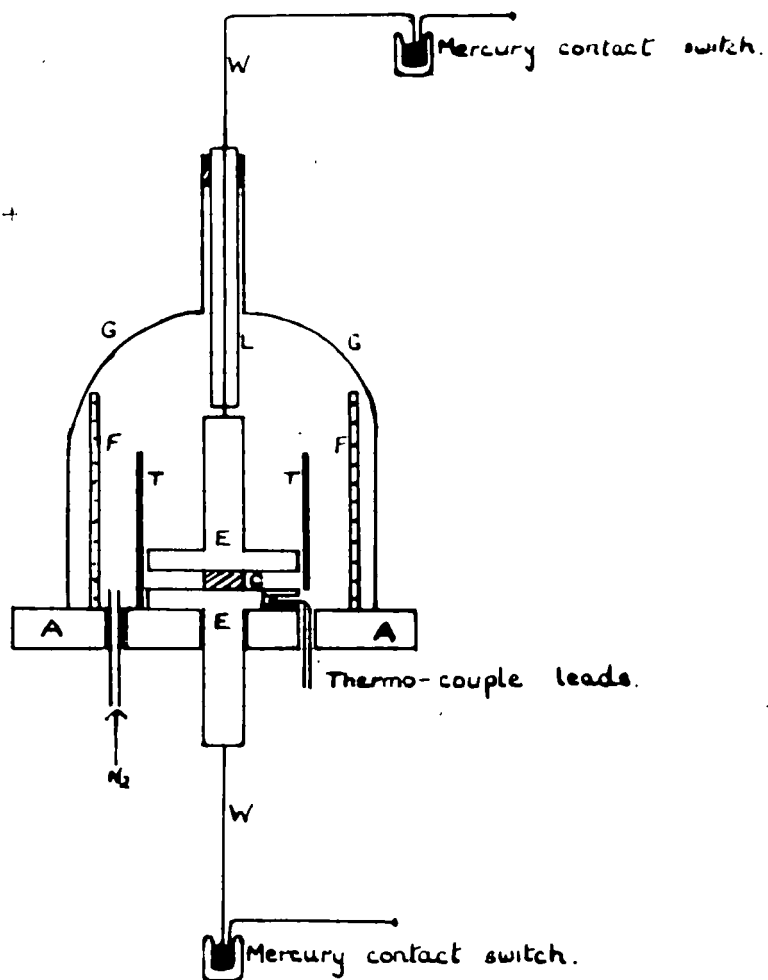


Fig. 11. The crystal unit.

and 5 megohm ranges were Welwyn resistors, types C22 and SA3623. These resistors were connected in series so that ten 1000 ohm, ten 10,000 ohm, nine 100,000 ohm, nine 1 megohm and nine 5 megohm values were available for use. Special care was taken to eliminate any resistances in the switches of the resistance box by using high quality rotary "wafer" switches.

Initially, measurements with the circuit were not satisfactory but these troubles were traced to leakage currents and contact potentials. These were eliminated by having the apparatus mounted on blocks of paraffin wax, while the galvanometer was mounted on a plate glass base. Insertion of mercury switches wherever possible in the apparatus reduced the contact potential difficulties.

3.4. THE CRYSTAL UNIT.

The first experiments on the measurement of conductivity revealed several disadvantages in the early designs of the crystal unit. The electrodes tended to be unsteady and the movement of these electrodes during measurements caused changes in the conductivity due to changes of pressure on the crystal. The faults were eliminated in the final design, which is shown in Fig. 11. The unit has proved satisfactory for all the conductivity measurements.

A base-board, A, of $\frac{1}{2}$ in. Sindanyo asbestos sheet was rigidly fixed to a wall framework and had a hole drilled

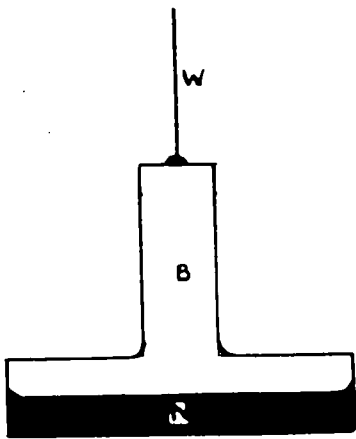


Fig. 12. The electrode.

in the centre of the board so that the lower electrode, E, fitted securely into it. A tightly fitting Pyrex tube, T, surrounded the electrode and crystal so that the upper electrode when fitted in position had no freedom of movement. The tube and the electrodes were surrounded by the furnace, F, capable of producing temperatures of up to 600°C.

The furnace was made from Nichrome wire, of resistance 27 ohms per yard, wound on an insulated steel core, 8 cm. diameter and 10 cm. in length, to give a total resistance of 50 ohms at room temperature. The windings were well lagged with asbestos paper and tape. The power was fed to the furnace through a variac from the mains, the leads connecting the furnace to the variac being slotted through the base-board, A.

The crystal temperature was measured by an iron-constantan thermo-couple mounted in the lower electrode and passing through a hole in the base-board, while oxygen-free nitrogen could be passed into the apparatus through an inlet tube in the base-board.

The electrodes were of a circular T shape, Fig. 12, and consisted of a nickel face plate, N, 1 in. in diameter, silver-soldered to a brass head. In early experiments the nickel face plate was covered with a platinum foil but later work showed that the foil was unnecessary, the nickel face presenting a satisfactory electrical contact. The nickel wires, W, silver-soldered to the electrodes and passing into mercury contact switches, provided the connection with the main circuit; the contact wire from the upper electrode was enclosed by a capillary tube, L, which fitted into a bung

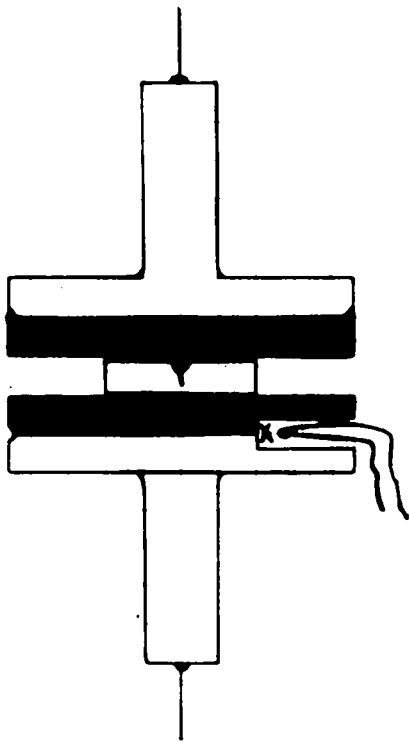


Fig. 13. The Thermocouple Position.

in this neck of the Pyrex vessel, G, which surrounded the apparatus.

The type of unit restricted movement of the electrodes during the measurements and also had the advantage that it was very much less subject to external fluctuations in temperature since it was shielded against outside draughts by the Pyrex vessel, G. Further temperature control was maintained by having the apparatus housed in a thermostatted room.

3.5. THE TEMPERATURE MEASUREMENT.

Temperature measurements, as previously stated, were made with an iron-constantan thermo-couple, whose hot junction was mounted in the lower electrode, Fig. 13. The cold junction was maintained at 0°C in an ice bath. The e.m.f. produced in the thermo-couple by the temperature at X, was read off directly, with an accuracy of .005 millivolt, on a Pye slide wire potentiometer, No. 7556, calibrated in millivolts. The potentiometer was calibrated against a Weston standard cell before each reading.

Because of the likelihood of temperature gradients between the crystal position, Y, and the thermo-couple position, X, great care was taken in the measurement of temperature. The thermo-couple was periodically calibrated against another calibrated iron-constantan thermo-couple, which was placed in the position of the crystal, Y, in the apparatus. In this way,

any thermal gradient in the apparatus could be allowed for accurately. The maximum error in the temperature measurements for the crystal position was estimated at $\pm 2^{\circ}\text{C}$.

3.6. THE METHOD OF MEASUREMENT OF THE CONDUCTIVITY.

The crystal, whose size was of the order of .75 cm. x .50 cm. x .15 cm., was placed in the conductivity apparatus and a stream of dry, oxygen-free nitrogen passed through the crystal unit. The temperature of the crystal was then raised to the desired value and maintained at this for twenty minutes, the temperature being checked every few minutes. The crystal was then switched into the conductivity circuit and subjected to a pulse of d.c. current lasting 0.2 second; the size of the pulse was varied by trial and error to obtain a suitable deflection. The resulting galvanometer deflection and the crystal temperature were noted. The crystal unit was switched out of circuit and replaced by the resistance box which was adjusted, with the voltage pulse value the same as for the crystal, until the same deflection was obtained.

The conductivity measurements were taken both after increasing and after decreasing the crystal temperature, the direction of the current being reversed after each reading to prevent polarisation of the crystal.

The crystal size was accurately measured after a conductivity run with a 1 in. micrometer screw gauge calibrated in thousandths of an inch.

The results of a typical experiment are shown in Table 3. In this case the crystal was coated with "Melton" liquid silver paint and then baked out at 600°C. The edges of the crystal were cleaved away and the crystal transferred to the apparatus.

TABLE 3.

Crystal dimensions - .2442 in. x .1478 in. x .0489 in.

Voltage applied to the crystal	Galvanometer deflection. cms.	Thermo-couple milli-voltage	°C	Resistance. ohms.
8	9.7	11.42	320	14.411×10^6
5	21.4	13.44	367	4.041×10^6
1	18.8	16.04	427.5	0.916×10^6
$\frac{1}{2}$	8.1	16.37	435	0.741×10^6
$\frac{1}{2}$	20.4	17.13	453	0.587×10^6
5	8.9	11.87	330	10.112×10^6

The accuracy and the reproducibility of the apparatus was tested by measuring the spread of the deflections produced by passing a voltage pulse through the resistance box.

The resistance box was set at a definite value and subjected to a pulse of d.c. current, the pulse was adjusted previously to give a 10-20 cms. deflection. The deflection was noted, then the direction of the pulse reversed and the resistance again subjected. This was carried out until eight readings of the deflection were obtained.

This procedure was repeated for a widely spread series of resistance values. The results are shown in Table 4.

TABLE 4.

Resistance ohms.	Deflection with reversing key up. cms.	Deflection with reversing key down. cms.
1.011×10^6	21.4	21.4
	21.3	21.2
	21.5	21.3
	21.4	21.1
5.011×10^6	13.4	13.3
	13.6	13.3
	13.4	13.3
	13.4	13.3
20.011×10^6	15.9	15.8
	15.6	15.6
	15.7	15.6
	15.9	15.7
$.411 \times 10^6$	15.3	15.4
	15.3	15.6
	15.4	15.6
	15.3	15.6

The table shows that the results were reproducible and that the maximum error in the spread of the deflections was 3 mms. in 133 mms.

3.7. THE ELECTRODE MATERIALS.

Good electrical contact between the surface of the crystal and the electrodes was needed for the measurement

of the crystal conductivity and so it was necessary to coat the crystal faces, which were to be in contact with the electrodes, with a suitable conducting material. A wide variety of materials have been described in the literature and it was decided to make a careful study of these with a view to examining stability over periods of heating and annealing, chemical attack on the crystal, and reproducibility.

a). In the early measurements it was decided to coat the crystals with a suspension of colloidal graphite, which was the method used by Mapother, Crooks and Maurer (1) in their measurements. The suspension of graphite in white spirit was commercially known as "dag" dispersion 2404 and was available from the Acheson Colloids Ltd.

The dag was applied to the crystal with a small camel hair brush and then the crystal heated to 150°C . to remove the white spirit, the graphite forming a uniform film which firmly adhered to the crystal. The edges of the crystal were cleaved away to remove any graphite on the sides and then the crystal was placed between the nickel electrodes.

Many crystals, treated in this way, gave reasonable conductivity results below 400°C but at higher temperatures reproducible results could not be obtained. This was attributed to the disappearance of the coating from the crystal surfaces at these higher temperatures and an experiment was carried out to show this effect.

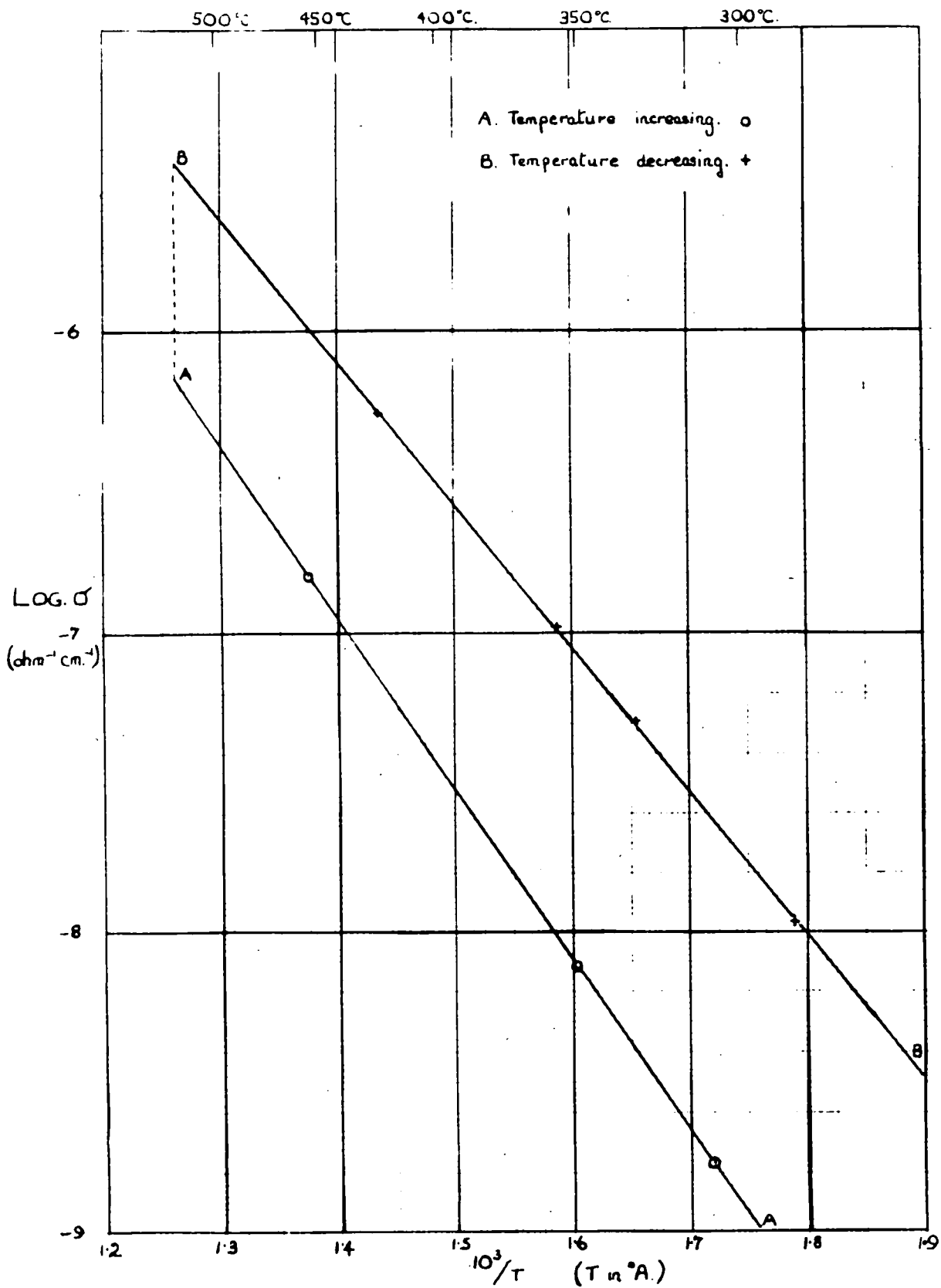


Fig. 14. The variation of conductivity with temperature for a crystal coated with "dag".

The temperature of a crystal, coated with "dag" dispersion, was raised from 300°C to 520°C in 45 minutes, the conductivity being taken as the temperature was increasing. The crystal was maintained at 520°C for 30 minutes and then cooled down to 300°C over a period of 30 minutes. Four conductivity measurements were made as the temperature was decreasing. The logarithm of the conductivity was plotted against the reciprocal of the absolute temperature and the results are shown in Fig. 14 .

The graph shows the large change in conductivity after heating at 520°C for 30 minutes. The results below 420°C fall on to the two straight lines showing that there was no evaporation below this temperature.

The temperature measurements in this experiment were only approximate because of the rapid rate of heating and cooling which did not allow the furnace temperature to stabilise.

b). Attention was next turned to the use of platinum as a suitable coating for the crystal-electrode faces. The platinum has been applied to the crystal by two different methods, primarily by painting on to the crystal a solution of Johnson-Matthey's Liquid Bright Platinum and secondly by evaporation from a platinum filament.

The Liquid Bright Platinum could be applied to the crystal in the same manner as the "dag" dispersion. The

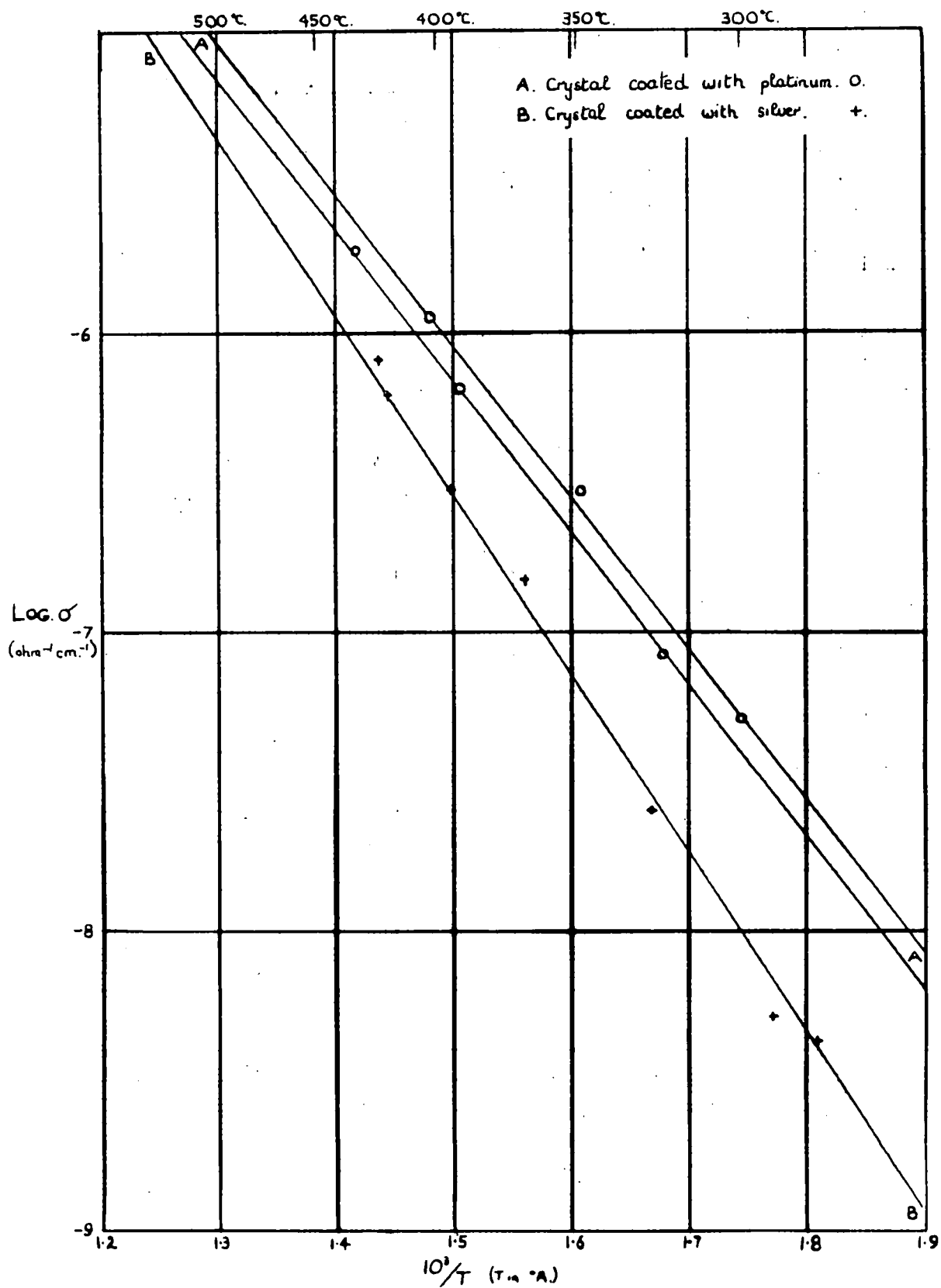


Fig. 15. The variation of crystal conductivity with temperature.

crystal was then heated to 400°-500°C to remove the solvent and the edges of the crystal cleaved away to prevent conduction around these sides. The platinum has also been applied to the crystal by an evaporation technique, under high vacuum, using a platinum filament. Initially a tungsten filament, covered with platinum foil, was used but there was evidence of tungsten and platinum both being evaporated on to the crystal. After cleavage of the edges the crystal was placed between the nickel electrodes.

The conductivity measurements, using a platinum coating on the crystal, was unsatisfactory and in all cases a white crustation, which had formed on the crystal surface, was observed when the crystal was removed from the apparatus.

Moreover when the results of the few measurements possible were plotted on a log. σ vs $1/T^\circ$ graph they fell into two definite parallel straight lines, Fig. 15. It was very significant that alternate points fell on the same straight line so it would appear that there was a greater passage of current in one direction than the other. A further example of this phenomena is given in Fig. 16.

This was a definite property of the platinum-coated crystal since the graph plotted for results obtained on a piece of the same crystal, this time coated with liquid silver, fall on to one straight line, (Fig. 15). A further check was carried out on the resistances but they gave the same deflection independent of the current direction, thus showing the apparatus was not at fault.

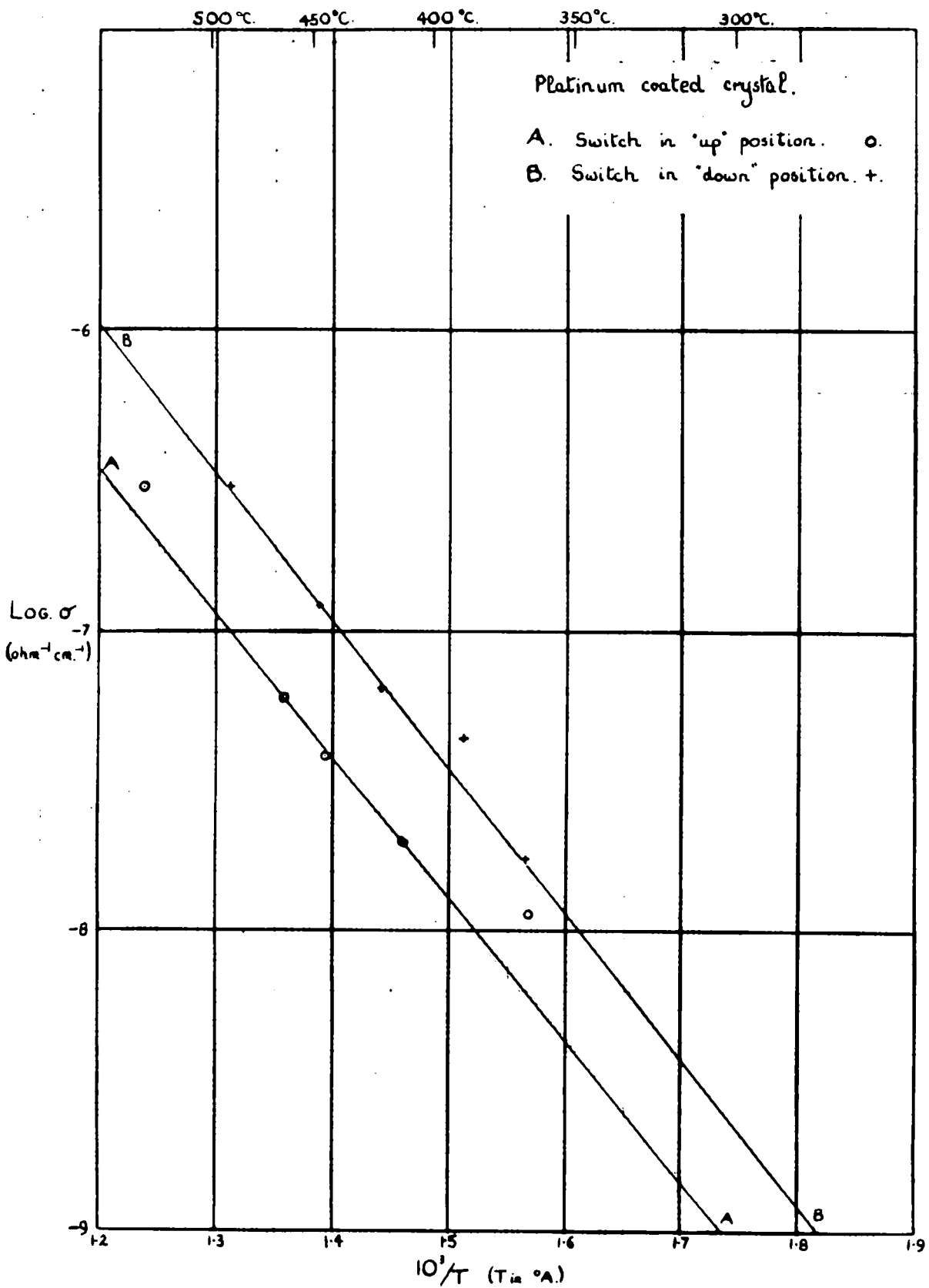


Fig. 16. The variation of conductivity with temperature for a crystal coated with platinum.

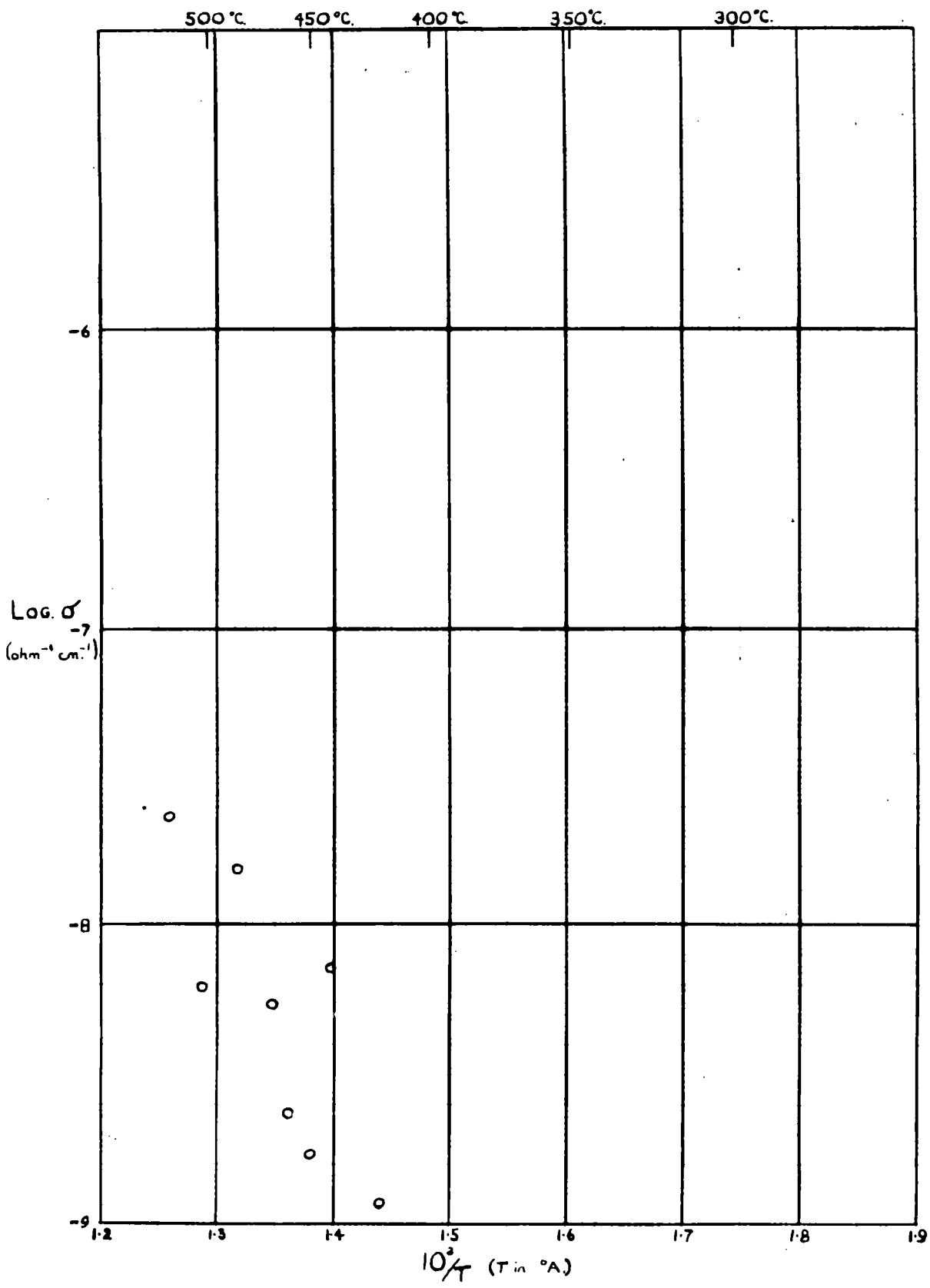


Fig. 17. The variation of conductivity with temperature for a crystal coated with gold.

c). Gold, which was applied to the crystal by a high vacuum evaporation technique, has also been tried as a suitable electrode coating. It proved extremely difficult to obtain a good film on the crystal and any film obtained appeared to react with the crystal when measurements were made above 400°C forming the chloride. The results of the $\log. \sigma$ against the reciprocal of absolute temperature plot is shown in Fig. 17.

d). Goodfellow (29), in his work on the measurements of conductivity produced in alkali halide crystals by mechanical deformation, applied a silver coating to his crystals. This coating has been most satisfactory for the measurements to be described in this thesis.

The silver could be obtained in the form of a solution, (Melton "Liquid Silver" Q50 grade), which could be applied to the crystal surface with a small paint brush. The crystal was then taken up to a temperature of 600°C , reducing the solution to a film of metallic silver. After cleavage of the edges, the crystal was placed between the nickel electrodes.

Crystals, treated in this way, gave satisfactory reproducible results over the required temperature range, (200° - 550°C). This type of film had also many advantages over the other coatings; the film was not easily damaged and was stable on annealing for long periods at 620°C .

This allowed a series of annealing studies to be carried out on the same piece of crystal without recoating the surfaces, the film having no chemical effect on the crystal at this temperature. The $\log \sigma$ vs $1/T$ graph for a silver-coated crystal is shown in Fig. 18.

3.8. THE CALCULATION OF THE CONDUCTIVITY FROM THE RESULTS.

It is a well known physical law that the resistance of any conductor varies directly as its length (1 cm.) and inversely as its area (A sq. cm.); that is

$$R = S \frac{1}{A} \quad (\text{Eqn. 2})$$

where S is a constant and is known as the specific resistance. It is the resistance in ohms of a specimen 1 cm. in length and 1 sq. cm. in cross section of the material.

The results of the experiments are interpreted in terms of the specific conductivity (σ ohms⁻¹ cm.⁻¹) which is defined as the reciprocal of the specific resistance, i.e.

$$\sigma = 1/S$$

Therefore from (Eqn. 2),

$$\sigma = 1/S = 1/A.R. \quad (\text{Eqn. 3})$$

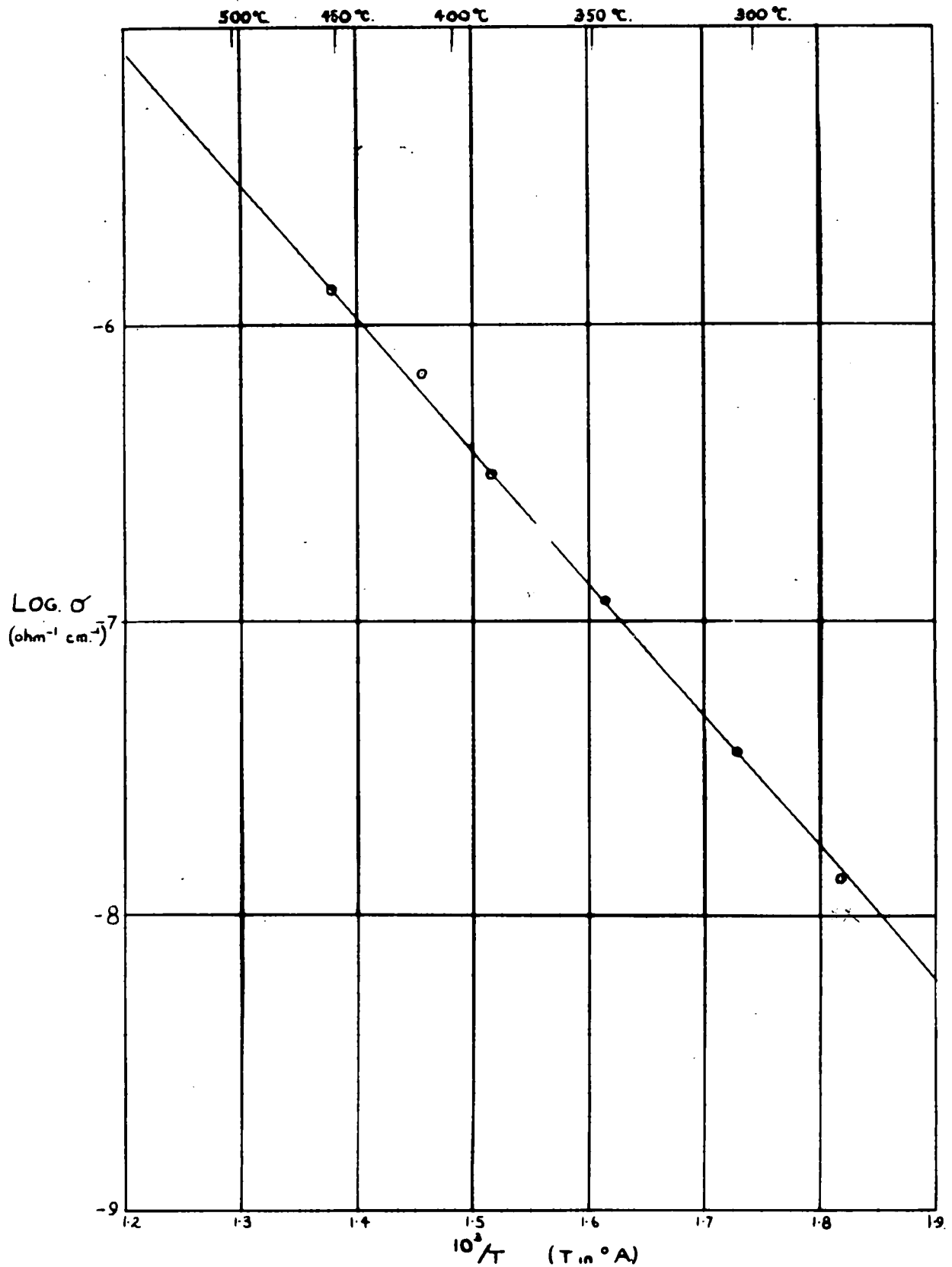


Fig. 18. The variation of conductivity with temperature for crystal 3.

3.9. THE RESULTS OF THE CONDUCTIVITY MEASUREMENTS.

a) General.

It has been found, in agreement with previous workers, that the conductivity results, of which measurements on crystal 3 (Fig. 18) are a typical example, can be expressed by an equation of the form

$$\sigma = A_1 e^{-E_1/RT} + A_2 e^{-E_2/RT} \quad (36)$$

where $A_1 < A_2$ and $E_1 < E_2$. The results of the present conductivity work are therefore represented in the form of graphs of the logarithm of the conductivity against a thousand times the reciprocal of the absolute temperature.

For the reasons stated in section 7 of this chapter, the crystals have been coated with "Melton" Liquid Silver in all of the measurements which follow. The measurements have all been carried out in the structure-sensitive temperature range, i.e. below 550°C.

b) The Chilling and Annealing Studies.

I. The first set of measurements were carried out on the same single crystal piece. The conductivities of the untreated crystal, the same crystal piece after 14 hours annealing at 600°C in air and then after 30 hours annealing at 600°C in air have been measured. The crystal was cooled after each annealing by switching off the furnace and allowing it to cool to room temperature over a period of four hours. The results are summarised in Table 5.

TABLE 5.

Silver coated crystal in atmosphere of nitrogen.

Crystal dimensions 0.49 cm. x .389 cm. x .1263 cm.

A. Untreated Crystal.

$^{\circ}\text{C}.$	Resistance Ohms.	σ $\text{Ohm}^{-1} \text{ cm.}^{-1}$
276	150.96×10^6	4.389×10^{-9}
316	67.774×10^6	9.777×10^{-9}
370	16.311×10^6	4.062×10^{-8}
401	5.311×10^6	1.247×10^{-7}
434	2.551×10^6	2.597×10^{-7}
463	1.591×10^6	4.165×10^{-7}
503	0.680×10^6	9.744×10^{-7}
480	1.002×10^6	6.615×10^{-7}
455	1.791×10^6	3.70×10^{-7}
420	4.101×10^6	1.616×10^{-7}
378	13.301×10^6	4.982×10^{-8}
346	33.211×10^6	1.995×10^{-8}

B. Crystal Annealed for 14 hours at $600^{\circ}\text{C}.$

$^{\circ}\text{C}$	Resistance Ohms.	σ $\text{Ohm}^{-1} \text{ cm.}^{-1}$
354	36.411×10^6	1.82×10^{-8}
377	22.341×10^6	2.966×10^{-8}
443	4.711×10^6	1.407×10^{-7}
470	2.761×10^6	2.40×10^{-7}
504	1.741×10^6	3.807×10^{-7}
458	4.571×10^6	1.45×10^{-8}
410	13.271×10^6	4.993×10^{-8}

C. Crystal Annealed for 30 hours at $600^{\circ}\text{C}.$

$^{\circ}\text{C}$	Resistance Ohms.	σ $\text{Ohm}^{-1} \text{ cm.}^{-1}$
396	30.811×10^6	2.151×10^{-8}
415	20.311×10^6	3.263×10^{-8}
463	6.411×10^6	1.034×10^{-7}
504	2.693×10^6	2.46×10^{-7}
488	3.635×10^6	1.823×10^{-7}
438	12.611×10^6	5.255×10^{-8}

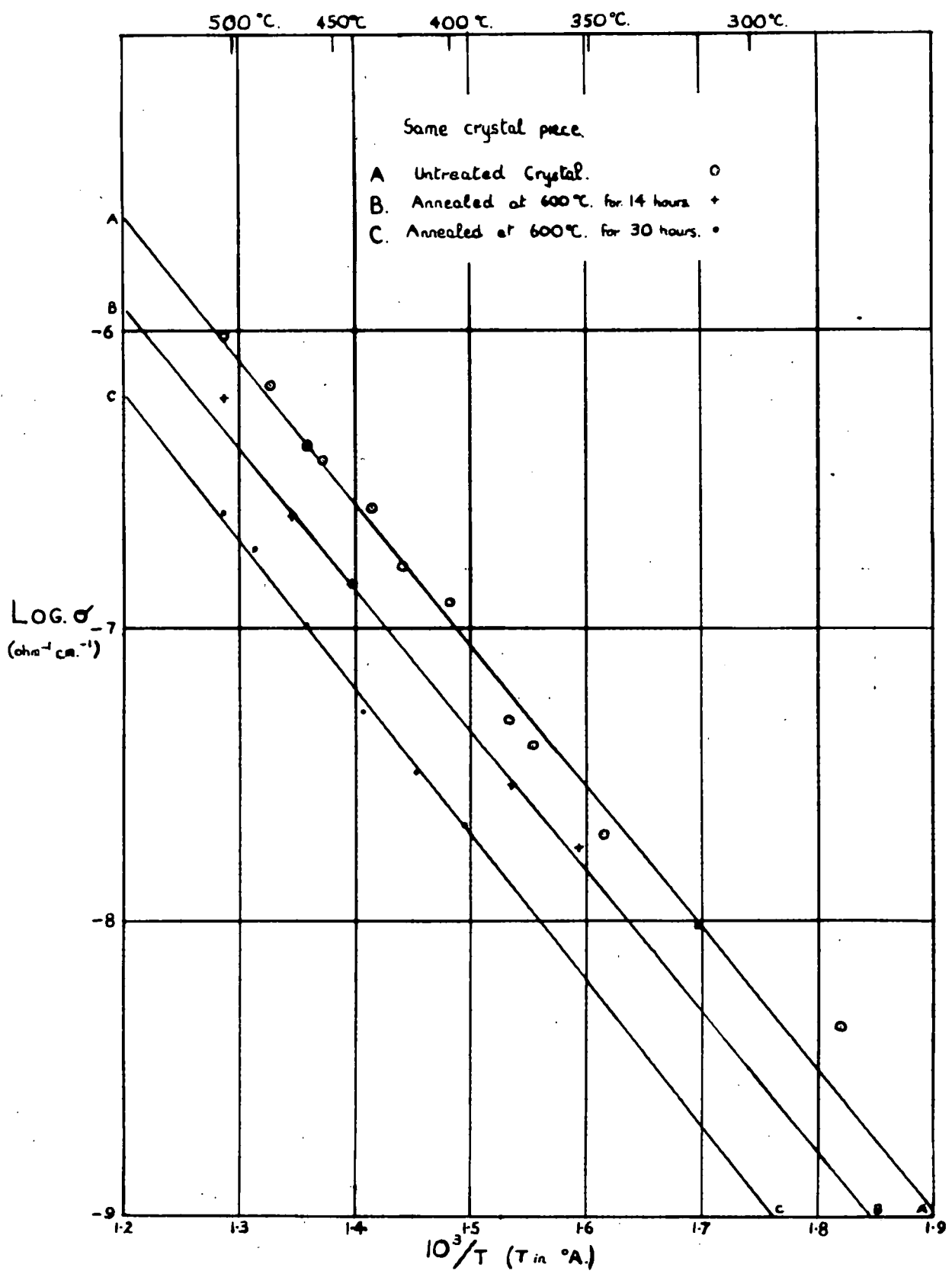


Fig. 19. The effect of annealing on the crystal conductivity.

The results are shown graphically in Fig. 19.

The crystal conductivity was, therefore, considerably reduced by annealing, even for short periods at 600°C. Comparison of the results at 441°C, ($1000/T = 1.4$), showed the conductivity of A, B and C to be $2.76 \times 10^{-7} \text{ ohm}^{-1} \text{ cm.}^{-1}$, $1.45 \times 10^{-7} \text{ ohm}^{-1} \text{ cm.}^{-1}$ and $6.31 \times 10^{-8} \text{ ohm}^{-1} \text{ cm.}^{-1}$ respectively. This amounted to a decrease of 47.5 per cent in the conductivity on annealing for 14 hours and a decrease of 77.2 per cent for 30 hours annealing.

It was questionable, however, whether this decrease in conductivity on annealing was in fact a property of the crystal and not due to the crystal plus silver coating. Etzel and Maurer (4) have observed in their work on sodium chloride crystals containing cadmium, that at least part of the decrease in the conductivity on annealing these crystals was due to the electrodes which they applied before this annealing process.

It was decided, therefore, that in all of the annealing studies, the electrode material should not be applied until after annealing.

II. The effect on the conductivity of annealing and chilling crystal pieces of the same single crystal has been investigated in conjunction with these types of experiments in diffusion.

To obtain an exact comparison between the conductivity and the diffusion results the heat treatments were carried

out on large single crystal pieces of crystal 5, so that after the treatment these pieces could be cleaved and part of the specimen used for the conductivity measurements and part for the diffusion measurements.

Two pieces of this crystal (No. 5) have been annealed at 620°C for different lengths of time, while another piece of the crystal was sealed in a dry tube and cooled rapidly from room temperature to -193°C by immersing it in liquid nitrogen for three minutes.

The results are shown in Table 6.

TABLE 6.

A. Untreated crystal slice of crystal 5.

Crystal dimensions .3783 cm. x .4572 cm. x .1270 cm.

°C	Resistance Ohms	σ Ohm ⁻¹ cm. ⁻¹
282	70.899 x 10 ⁶	1.036 x 10 ⁻⁸
320	27.211 x 10 ⁶	2.698 x 10 ⁻⁸
410.5	2.961 x 10 ⁶	2.48 x 10 ⁻⁷
444	1.441 x 10 ⁶	5.096 x 10 ⁻⁷
474	0.781 x 10 ⁶	9.401 x 10 ⁻⁷
417.5	2.541 x 10 ⁶	2.89 x 10 ⁻⁷

B. Slice of crystal 5 sealed in a tube and cooled in liquid nitrogen for three minutes. The crystal was cleaved to obtain fresh faces, the liquid silver applied and the conductivity measured.

Crystal dimensions .620 cm. x .3754 cm. x .1242 cm.

°C	Resistance Ohms	σ Ohm ⁻¹ cm. ⁻¹
279	60.149 x 10 ⁶	8.87 x 10 ⁻⁹
320	14.411 x 10 ⁶	3.703 x 10 ⁻⁸
367	4.041 x 10 ⁶	1.32 x 10 ⁻⁷
427.5	0.916 x 10 ⁶	5.825 x 10 ⁻⁷
435	0.741 x 10 ⁶	7.201 x 10 ⁻⁷
453	0.587 x 10 ⁶	9.09 x 10 ⁻⁷
330	10.112 x 10 ⁶	5.28 x 10 ⁻⁸

- C. Neighbouring slice of crystal 5 annealed for 69 hours at 600°C in an atmosphere of nitrogen and then the furnace switched off and cooled down to room temperature over four hours.

Crystal dimensions. $6.171 \text{ cm.} \times .546 \text{ cm.} \times .1427 \text{ cm.}$

$^{\circ}\text{C}$	Resistance Ohms	σ $\text{Ohm}^{-1} \text{ cm.}^{-1}$
286	36.011×10^6	1.176×10^{-8}
323	9.562×10^6	4.429×10^{-8}
356.5	3.800×10^6	1.115×10^{-7}
395.5	1.348×10^6	3.142×10^{-7}
415.5	0.831×10^6	5.097×10^{-7}
369	2.627×10^6	1.613×10^{-8}
342	5.643×10^6	7.505×10^{-8}

- D. Crystal slice of 5 was sealed in pyrex vessel under one atmosphere of nitrogen and annealed for 256 hours at 620°C - 640°C . The crystal was allowed to cool to room temperature over a period of four hours.

Crystal dimensions $.5887 \text{ cm.} \times .7598 \text{ cm.} \times .1547 \text{ cm.}$

$^{\circ}\text{C}$	Resistance Ohms	σ $\text{Ohm}^{-1} \text{ cm.}^{-1}$
257	57.98×10^6	5.963×10^{-9}
295	16.011×10^6	2.159×10^{-8}
345	3.541×10^6	9.764×10^{-8}
385	1.279×10^6	2.703×10^{-7}
421	0.516×10^6	6.7×10^{-7}
456	0.277×10^6	1.248×10^{-6}

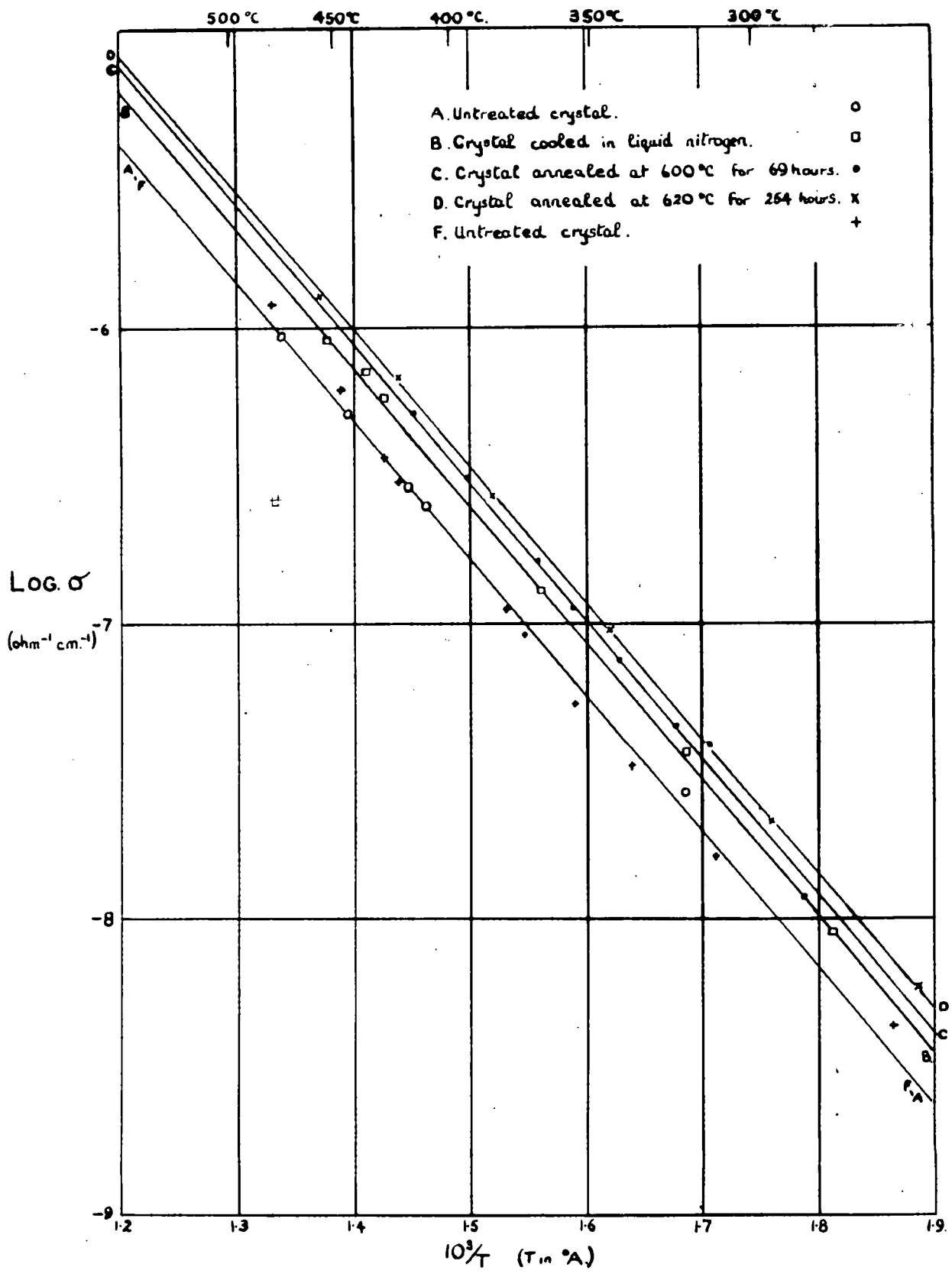


Fig. 20. The effect of various heat treatments on the conductivity of crystal 5.

F. Untreated piece of crystal 5.

Crystal dimensions .5974 cm. x .5658 cm. x .1417 cm.

$^{\circ}\text{C}$	Resistance Ohms.	σ $\text{Ohm}^{-1} \text{ cm.}^{-1}$
263	96.18×10^6	4.36×10^{-9}
311	26.211×10^6	1.6×10^{-8}
379	3.769×10^6	1.113×10^{-7}
428	1.171×10^6	3.58×10^{-7}
447	0.691×10^6	6.067×10^{-7}
479	0.348×10^6	1.205×10^{-6}
422	1.401×10^6	2.993×10^{-7}
374	4.591×10^6	9.132×10^{-8}
357	8.021×10^6	5.226×10^{-8}
337	12.841×10^6	3.265×10^{-8}

The results are shown in graphical form in Fig. 20. The results for both untreated crystals lie on the same line.

As the graph shows, the conductivity was increased by both the chilling and the annealing of the crystal pieces. A typical result was taken at 441°C ($1000/T = 1.4$), where the conductivities of A, B, C and D were $4.79 \times 10^{-7} \text{ ohm}^{-1} \text{ cm.}^{-1}$, $7.59 \times 10^{-7} \text{ ohm}^{-1} \text{ cm.}^{-1}$, $9.12 \times 10^{-7} \text{ ohm}^{-1} \text{ cm.}^{-1}$ and $1 \times 10^{-6} \text{ ohm}^{-1} \text{ cm.}^{-1}$ respectively. This shows that, at this temperature, the chilling of the crystal increases the conductivity by 58.47 per cent, while the annealing of the crystal, for 69 hours and 256 hours at 620°C , increases the conductivity by 90.4 per cent and 108.8 per cent respectively.

III. It was decided that the results obtained for heat treatments of crystals should be checked: to do this the

experiments were repeated as before.

The results are summarised below in Table 7 and are shown graphically in Fig. 21.

TABLE 7.

G. Untreated piece of crystal 5.

Crystal dimensions .5618 cm. x .4895 cm. x .09244 cm.

$^{\circ}\text{C}$	Resistance Ohms	σ $\text{Ohm}^{-1} \text{ cm.}^{-1}$
278	23.277×10^6	1.444×10^{-8}
332.5	4.061×10^6	8.28×10^{-8}
378	1.251×10^6	2.688×10^{-7}
428	0.384×10^6	8.756×10^{-7}
403	0.641×10^6	5.245×10^{-7}
347.5	2.606×10^6	1.29×10^{-7}

H. Piece of crystal 5 annealed in an atmosphere of nitrogen at 620°C for 48 hours and allowed to cool over a period of four hours.

Crystal dimensions .3197 cm. x .3899 cm. x .09244 cm.

$^{\circ}\text{C}$	Resistance Ohms	σ $\text{Ohm}^{-1} \text{ cm.}^{-1}$
314.5	12.511×10^6	5.933×10^{-8}
367	3.531×10^6	2.102×10^{-7}
406	1.504×10^6	4.936×10^{-7}
455	0.573×10^6	1.295×10^{-6}
381	2.701×10^6	2.747×10^{-7}
349	6.381×10^6	1.078×10^{-7}

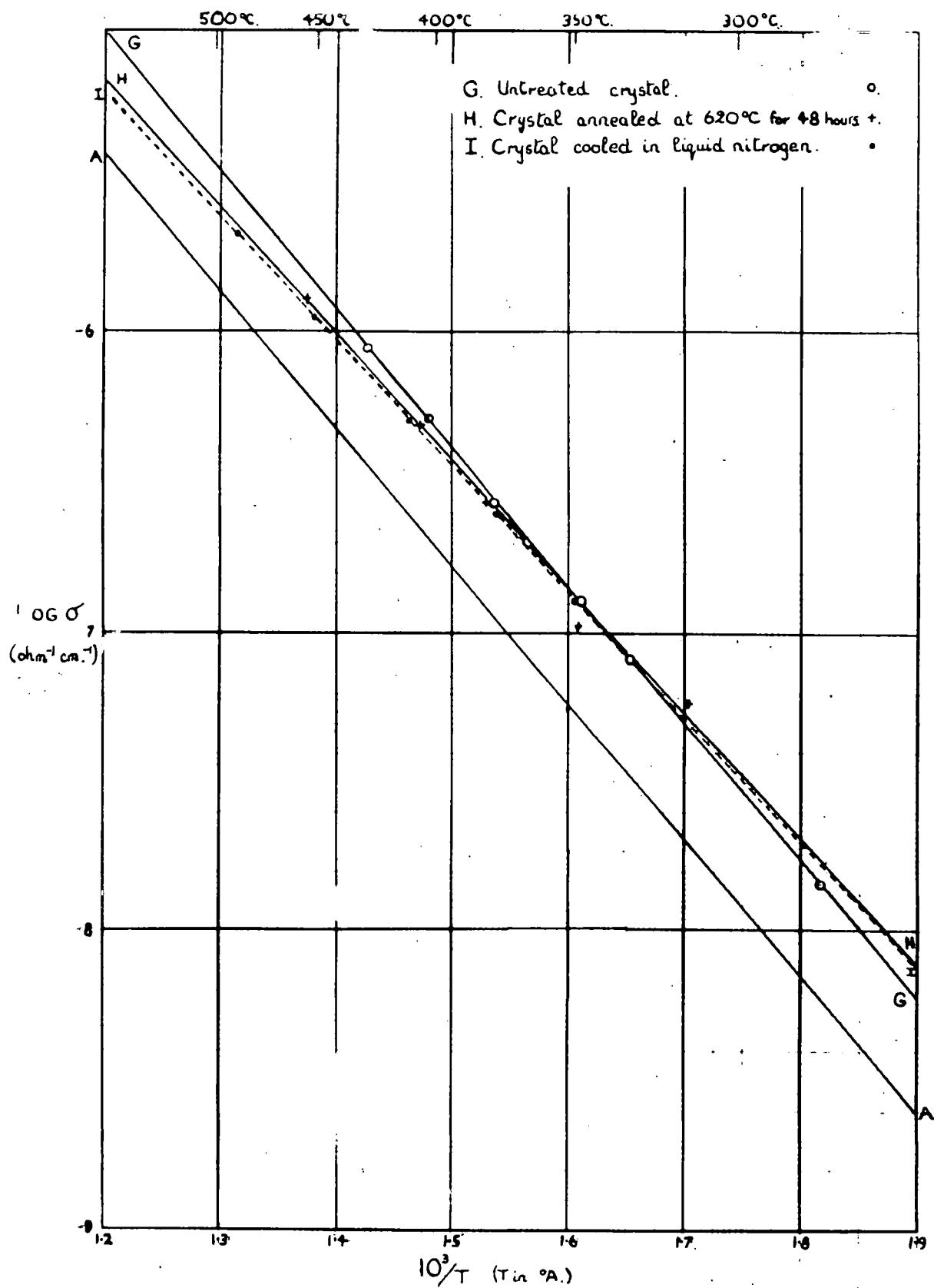


Fig. 21. The effect of various heat treatments on the conductivity of crystal 5 (repeat).

- I. The neighbouring piece of crystal was sealed in a pyrex tube and cooled from room temperature to -193°C by cooling in liquid nitrogen. The crystal was then cleaved, the liquid silver applied and the conductivity of the cleaved slice measured.

Crystal dimensions .2659 cm. x .3662 cm. x .1567 cm.

$^{\circ}\text{C}$	Resistance Ohms.	σ $\text{Ohm}^{-1} \text{ cm.}^{-1}$
349	12.711×10^6	1.266×10^{-7}
376.5	6.311×10^6	2.55×10^{-7}
411	3.091×10^6	5.206×10^{-7}
452	1.412×10^6	1.14×10^{-6}
488	0.758×10^6	2.123×10^{-6}

The results of these measurements were unsatisfactory for as can be seen from Fig. 21, the graph of the untreated crystal, G, had a much higher conductivity than the untreated crystal, A, which was used in the previous experiments. This was probably due to the fact, that, although the piece used was from the same crystal as the previous experiments, it was not from the same section of the crystal as the pieces A, B, C, D and F.

It was extremely difficult, however, to account for the graphs of the treated crystals (H and I) being at a much different slope to that of the untreated specimen. It was possible that the position of the thermocouple had been accidentally altered between the measurements on G and those on H and I. This would have given rise to errors in the temperature measurement, which would cause a change in the slope of the graphs.

It was therefore doubtful whether any dependence could

be placed on these results, but it was significant to note that the graph for the annealed crystal was nearer to the graph of the chilled crystal than in the previous experiments. This was what would be expected with a shorter annealing time.

IV. The previous results having proved unsatisfactory, it was decided to recheck the effect on the conductivity of chilling a crystal in liquid nitrogen. The experiment had to be carried out on another crystal, (crystal 6), as there was no more of crystal 5 available. Prior to these measurements the conductivity circuit was checked and all the contacts cleaned. The thermo-couple joints were also checked and then its hot junction was placed in its original position in the electrode. The results of the measurements are given in Table 8.

TABLE 8.

Y. Untreated specimen of crystal 6.

Crystal dimensions .4863 cm. x .6648 cm. x .1102 cm.

$^{\circ}\text{C}$	Resistance Ohms.	σ $\text{Ohm}^{-1} \text{ cm.}^{-1}$
262	20.221×10^6	1.658×10^{-8}
320	2.671×10^6	1.276×10^{-7}
379	$.541 \times 10^6$	6.303×10^{-7}
354	$.962 \times 10^6$	3.544×10^{-7}

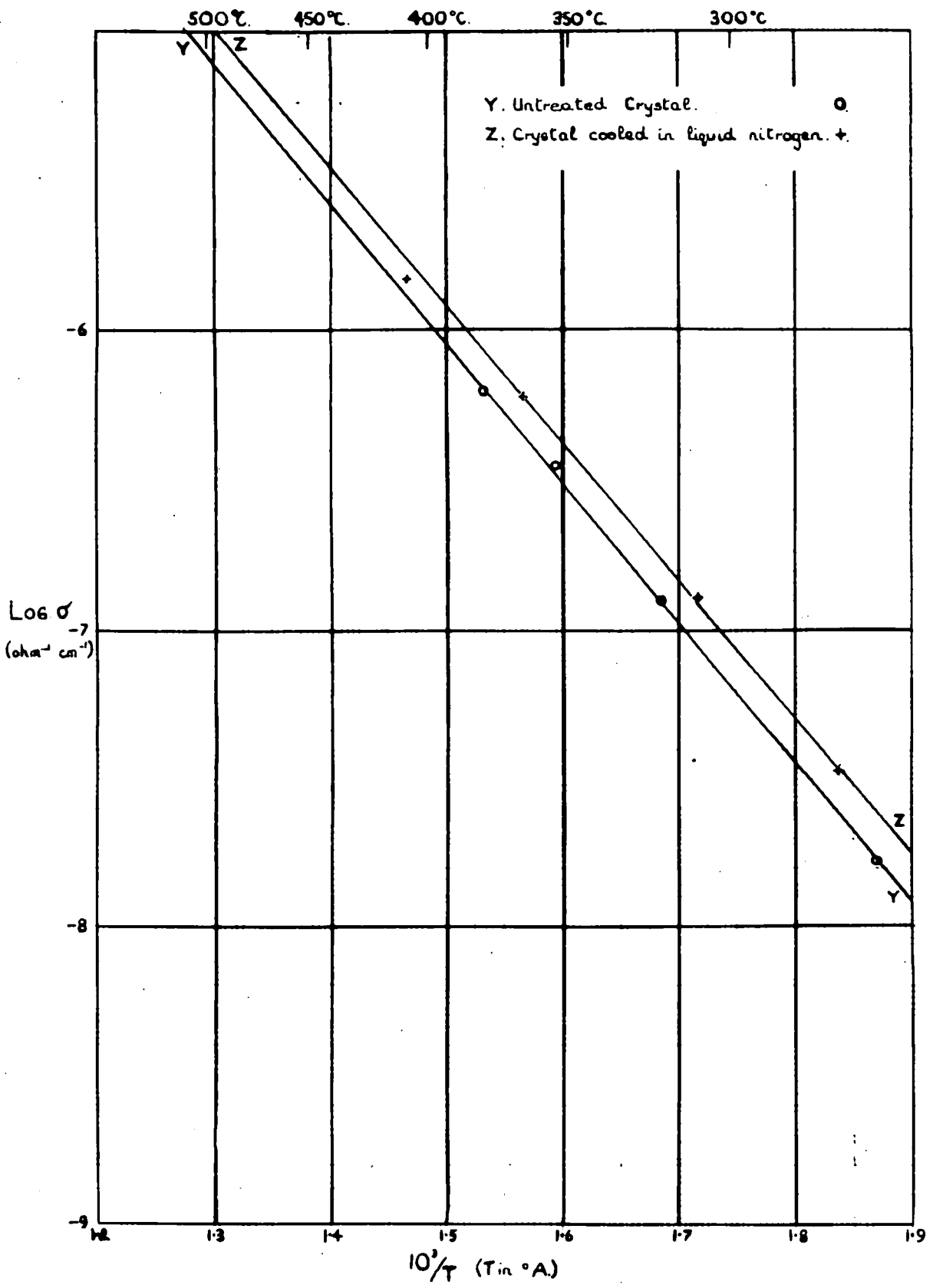


Fig. 22. The effect of chilling in liquid nitrogen on the conductivity of crystal 6.

Z. Neighbouring specimen of crystal 6 sealed in a tube and immersed in liquid nitrogen for 3 minutes. It was coated with the liquid silver and then the conductivity measured.

Crystal dimensions .637 cm. x .5576 cm. x .2464 cm.

$^{\circ}\text{C}$	Resistance Ohms.	$\text{Ohm}^{-1}\text{cm.}^{-1}$
271	20.511×10^6	3.382×10^{-8}
309	5.331×10^6	1.301×10^{-7}
365	1.154×10^6	6.01×10^{-7}
408	$.476 \times 10^6$	1.457×10^{-6}

The results of these experiments are shown in Fig. 22.

Comparison of these results with the results of Experiment II, shows that the graphs have the same slope, although the absolute values of the conductivities are different. This was, of course, an expected result since a different crystal was used in these experiments. The results did show, however, that the chilling of the crystal increased the conductivity. A typical result is given at 441°C ($1000/T = 1.4$) where the conductivities of the untreated and chilled crystal were $2.6 \times 10^{-6} \text{ ohm}^{-1} \text{ cm.}^{-1}$ and $3.467 \times 10^{-6} \text{ ohm}^{-1} \text{ cm.}^{-1}$ respectively. This amounts to an increase of 33.36 per cent in the conductivity.

The results of these conductivity measurements are summarised below.

- a) In two out of three specimens annealed, the conductivity has increased on annealing, the increase depending on the time of annealing.
- b) In two out of three specimens chilled in liquid nitrogen, the conductivity has increased.

- c) The third specimen has given anomalous results in the measurements on the untreated crystal, the chilled crystal and the annealed crystal.
- d) It was doubtful whether any dependence could be placed on the annealing studies carried out on a crystal already coated with the electrode material before annealing.

The results will be discussed in a later chapter.

CHAPTER 4.

THE MEASUREMENT OF THE SELF-DIFFUSION OF SODIUM IN
SINGLE CRYSTALS OF SODIUM CHLORIDE.

4. THE MEASUREMENT OF THE SELF-DIFFUSION OF SODIUM IN SINGLE CRYSTALS OF SODIUM CHLORIDE.

4.1. INTRODUCTION.

It was now proposed to carry out a series of studies on self-diffusion in conjunction with the conductivity studies, described in Chapter 3. The self-diffusion of "labelled" sodium was to be investigated in specimens from the same single crystal of sodium chloride as was used in the conductivity experiments, the specimens having been subjected to a variety of heat treatments as before. The measurement of the self-diffusion was to be carried out by an "absorption technique", designed to give the best possible intercomparison of diffusion rates.

4.2. THE PREVIOUS METHODS OF MEASUREMENT OF SELF-DIFFUSION IN THE ALKALI HALIDES.

In previous investigations of the self-diffusion in ionic crystals the depth of penetration of the radioactive material has been determined by measuring the radioactivity in slices or layers of the crystal either by a microtoming (1) or by a grinding technique (3). The only notable exception to this type of procedure was the work of Morrison et al. (2) who have determined the chloride ion self-diffusion in sodium chloride crystals by an isotopic exchange between the chloride ions in the crystal and a surrounding layer of chlorine gas. No further description of this method will be given as it was not a method which could be applied

to the present work.

Mapother, Crooks and Maurer (1) have employed the microtoming technique to measure the self-diffusion of sodium in single crystals of sodium chloride and sodium bromide. After the diffusion had taken place the crystal was mounted in a vice on a microtome carriage, which moved in a horizontal direction across a knife edge. The crystal was adjusted, by means of grub-screws on the vice, so that the face, on which the active material had been deposited, was in the plane swept out by the knife edge. This mounting was checked by reflection of a beam of light from a mirror resting on the crystal face. Before each passage of the knife over the crystal, a strip of adhesive tape was pressed on to the crystal face and the material sectioned off by the knife edge adhered to the tape in the form of a fine powder. The samples were mounted on brass rings and their radioactive intensity measured. The height of the knife blade was adjusted by a precision screw after each traverse so that the thickness of the individual slices was about 5×10^{-4} cm.

Schamp and Katz (3), on the other hand, employed a grinding technique in their investigation of the bromide ion diffusion in single crystals of sodium bromide. The sectioning was carried out by a ground glass plate passing across the face of the crystal, which was held in a vice and properly orientated with respect to the plate by an optical lever

system. Layers of 2-3 microns thick were removed and these adhered to the plate in a rectangular smear quite reproducible in shape and size. These samples were then counted.

It is the present authors' opinion that these sectioning methods are likely to give rise to considerable errors in the determination of the self-diffusion coefficient, D , especially in the low temperature range where penetration depths are small. The mounting of the crystals for sectioning seems extremely critical and slight misalignments in the mounting, which would not necessarily be detectable by the optical lever system, would give rise to errors in the measurement of depth of penetration. Schamp and Katz have in fact observed a tilting of the crystal after slicing in one of their experimental determinations. They have also pointed out that the roughness of the crystal surface after removal of a layer of material gives rise to errors, which are not easily estimated, in the determination of the self-diffusion coefficient.

It would also seem likely with these techniques that there will be a loss of radioactive material from each slice, during the sectioning and mounting, by either a transfer of some of the material to the sides of the underlying crystal or by a complete loss of some of the material because it seems unlikely that all of it would adhere to the Scotch tape (1) or to the plate (3). These errors have been estimated by Schamp

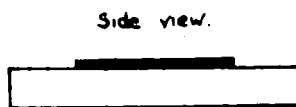
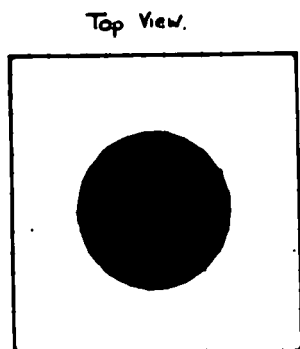


Fig. 23. Before diffusion.

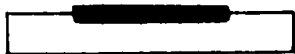


Fig. 24. After diffusion.

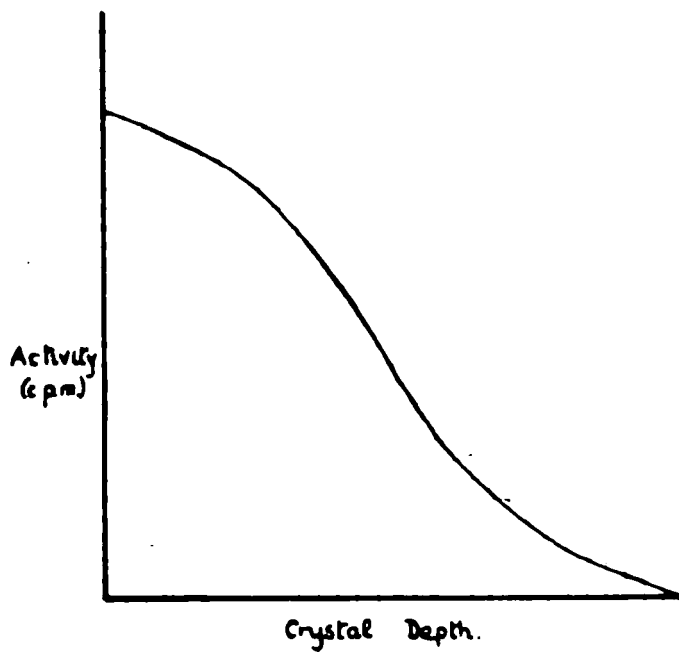


Fig. 25. Variation of activity in the crystal.

and Katz to be as much as 80 per cent in the low temperature region while Mapother, Crooks and Maurer estimate the error at 10-20 per cent.

In view of these observations a technique, based on absorption measurements, was devised to give a much more accurate comparison of diffusion rates, though not necessarily good absolute values. (After this work had been completed it was found that the method had already been used in a metallic system by Steigman, Shockley and Nix (37)).

4.3. OUTLINE OF THE ABSORPTION METHOD OF MEASUREMENT OF THE SELF-DIFFUSION COEFFICIENT.

In the experiments on the self-diffusion it was necessary to use a radioactive isotope to follow the diffusion process and in the present work sodium-22, which emitted β^+ particles and γ -rays, was used.

A layer of sodium chloride, labelled with sodium-22, was evaporated on to the face of a single crystal of sodium chloride, Fig. 23 . The activity of this face was then measured by counting the rate of β^+ emission from the face with a thin, end-window Geiger counter. The crystal was sealed in a tube under a pressure of approximately one atmosphere of an inert gas and placed in a furnace at the desired temperature. After leaving for a known time the tube was removed from the furnace, cooled and the activity of the crystal face again measured by counting as before.

During diffusion the active sodium would have penetrated

into the crystal, Fig. 24, so that there would be a variation of the activity with depth of the crystal as depicted in Fig. 25. Since the β^+ -particles emitted by the sodium-22 were of low energy, 0.56 MeV., some of these particles, which originated in the inner layers of the crystal would be absorbed by the intervening layers before they reached the outside face. Consequently the count rate at the outside face was found to be diminished after the diffusion.

For the evaluation of diffusion coefficients it was necessary to know the extent of the absorption of the β^+ particles in varying thicknesses of sodium chloride. This information was obtained experimentally, Fig. 29, and from the graph it was possible to calculate the activity produced at the surface by an active layer of material at any depth. From a knowledge of this absorption and the decrease in activity at the face it was then possible to evaluate the self-diffusion coefficient. The complete calculation will be described in section 6 .

This method of measurement was especially useful with low energy β -particles where there would be a sharp "fall-off" in activity at the surface with penetration depth due to their ease of absorption. The type of absorption curve shown in Fig. 29 would be steeper the softer the β -particle energy so increasing the accuracy of the measurements. There would of course be a limit to

the softness of the β -particle for below an energy of 0.25 MeV. it would be difficult to obtain thin enough absorbers to determine the absorption curve.

Surface migration of the active material was shown to be unlikely to introduce large errors into the measurements since the trial experiments on surface diffusion, which are described in Chapter 5, showed that it was not much more rapid than bulk diffusion.

It was also necessary to test for any evaporation of the active deposit during the diffusion as this would introduce large errors in the determination of the diffusion coefficient. This was carried out by having an inactive crystal mounted near the active crystal during the diffusion run. Any evaporation of the active deposit would be shown on the inactive crystal; in only one experiment has this been found to occur.

This absorption method should be very good for comparing diffusion penetrations, for there was no need for sectioning of the crystals which may lead to a possible loss of material as described in section 2.

4.4. THE DETAILS OF THE DIFFUSION TECHNIQUE.

(a) The Mounting of Samples for Counting.

Since the application of the method depended on measuring small changes in count rates it was of the utmost importance that the crystal samples for counting could be mounted in a reproducible position. The brass plate, shown in Fig. 26, was constructed for mounting the crystals. The crystal

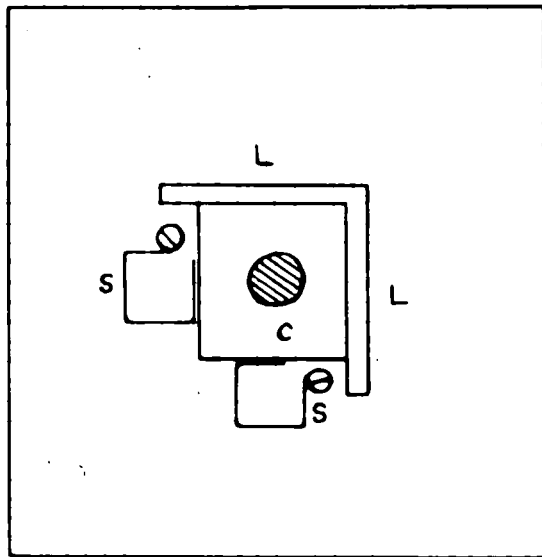


Fig. 26. The crystal plate.

could be fitted into the metal right angle, L, brazed on the plate in such a position that the crystal was directly under the counter window. The crystal was held in position on the plate by the two spring clips, S, and the plate could then be fitted into the shelf of a counter holder.

(b) The Counting of the Samples.

The samples were counted by an end-window Geiger-Muller counter with a window thickness of 7 mgm. per cm.², the counter plateau being checked before each measurement. In the early experiments 3,000-5,000 counts were taken on each sample but in the later experiments, where the comparison of diffusion rates was being made, 10,000 counts were taken on each, so ensuring a 1 per cent statistical accuracy. The counter was always standardised before and after each measurement by taking at least 10,000 counts on a standard active crystal. The complete counting apparatus was left untouched between experiments.

(c) The Measurement of the Diffusion.

The active sodium chloride, incorporating sodium-22, was evaporated on to the freshly cleaved face of single crystal, approximately 2 cm. x 2 cm. x 0.2 cm. in size, by a technique which will be described in Chapter 6. By careful shielding of the crystal the active deposit, weighing approximately 20 mgm., was obtained on a clearly defined area. In this way an activity of 1,000-3,000 counts per minute was obtained on the crystal face.

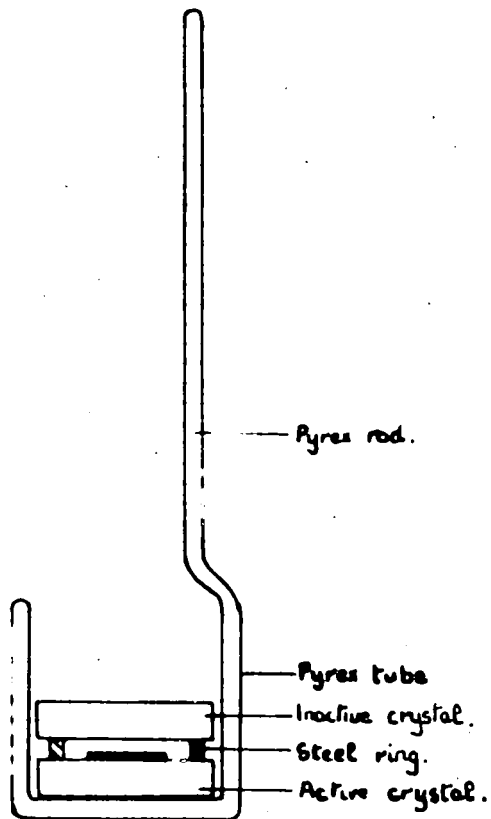


Fig. 27. The crystal holder.

The active face of the crystal for the diffusion study was then counted and the crystal placed active face upwards in the bottom of a pyrex tube, 3 cm. in diameter and 4 cm. in height. A thin mild steel ring, 2 cm. diameter and .15 cm. in height, was placed on the active crystal and this ring supported an inactive crystal of sodium chloride. This crystal acted as a monitor against evaporation during the diffusion run. The arrangement is shown in Fig. 27.

The small tube was lowered into the large pyrex vessel, 60 cm. in length and 4 cm. in diameter, fitted with a B-34 socket. An adaptor, consisting of a B-34 cone joined by a constriction to a B-12 socket, was waxed into the large tube's B-34 socket and the apparatus attached to a vacuum line by the B-12 socket. The vessel was pumped to sticking vacuum and, after being filled with slightly less than one atmosphere of oxygen-free nitrogen, the constriction was sealed off, Fig. 28. The nitrogen was used in order that there would be no oxidation or chemical reaction with the surrounding gas during the diffusion. Also the pressure of the nitrogen at the working temperature would be approximately 2.5 atmospheres, so reducing any chance of evaporation of the active deposit off the crystal.

A furnace, identical to the one used for crystal growing, was brought up to the required temperature and controlled to within $\pm 3^{\circ}\text{C}$ of this temperature by the Sunvic Resistance Thermometer Controller Type RT.2, the temperature of the furnace being measured by a 550°C mercury-in-glass

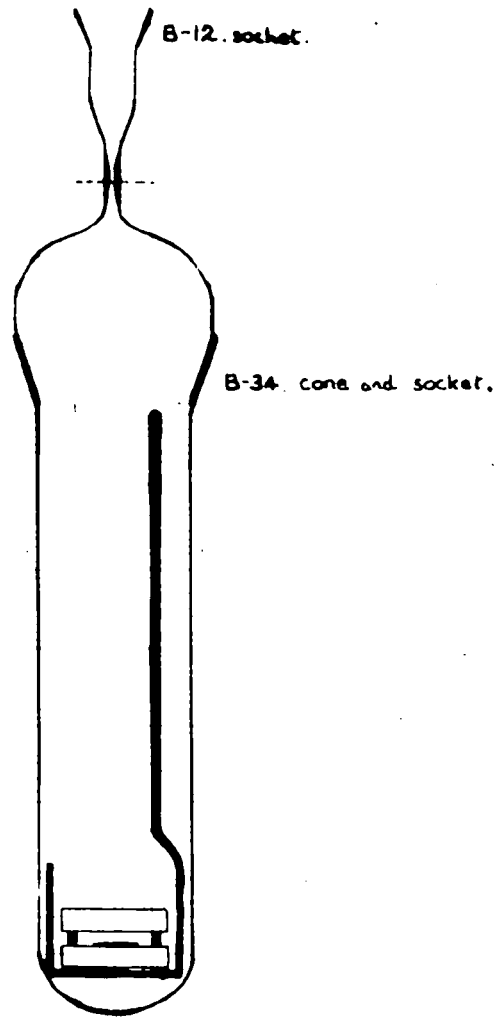


Fig. 28. The diffusion tube.

thermometer. The thermometer was placed in contact with the lower part of the tube in the furnace. The upper part of the tube, which extended about 30 cm. out of the furnace, was shielded against outside draughts and the heat of the furnace by asbestos screens. In this way it was found that the upper end was never warm enough for the wax to soften.

A typical set of readings of the variation in temperature during a diffusion run is shown in Table 9 .

TABLE 9.

Hours of Heating	Temperature °C
3	504
7	506
9	505.5
24	508
26	505
48	508
54	507
72	508
76	506
96	507
107	503
120	508
126	506
144	508
150	504
168	503
189	506

After allowing diffusion to take place for a certain time the tube was removed from the furnace, cooled to room temperature in air and opened. The active face of the crystal was then counted with the crystal in the identical position to the previous count and also the blank crystal and ring were examined for any activity which might have evaporated on to them.

To allow for slight variations in the sensitivity of the Geiger counter and so that all counting results should be strictly comparable, a radioactive standard was prepared as follows. A crystal of sodium chloride was taken and a deposit of active sodium chloride evaporated on to it as before. This crystal was kept at room temperature in a desiccator as a counting standard and all counts were related to this standard. The standard crystal was counted before and after every diffusion count.

4.5. THE ABSORPTION CURVE FOR SODIUM-22.

Before any calculation of diffusion coefficients could be made it was necessary to prepare an absorption curve for the β^+ + γ radiations of sodium-22 in sodium chloride. The β^+ -particle has an energy of only 0.56 MeV. and it was found impossible to prepare thin enough sections of sodium chloride to use as absorbers. Absorption measurements were therefore made with uniform thin aluminium foils and the corresponding absorption curve for sodium chloride calculated from comparison of the densities of aluminium and sodium chloride. This may

have introduced small errors into the absolute values obtained for the self-diffusion coefficient but it did not affect comparison of the coefficients thus obtained.

The absorption measurements were carried out on the standard crystal mounted on the plate, Fig. 26, in order that the counter geometry would be identical to that of the diffusion measurement counting. The aluminium foils, which were cut in squares of 2 cm. side were placed on the metal right-angle support and the screw clips so that the foil completely covered the crystal surface. To ensure a 1 per cent statistical accuracy, 10,000 counts were taken for each thickness of foil after which the foil was accurately weighed on a micro balance. The corresponding thickness of sodium chloride was calculated from these weights. The results are given in Table 10 and the absorption curve is shown in Fig. 29.

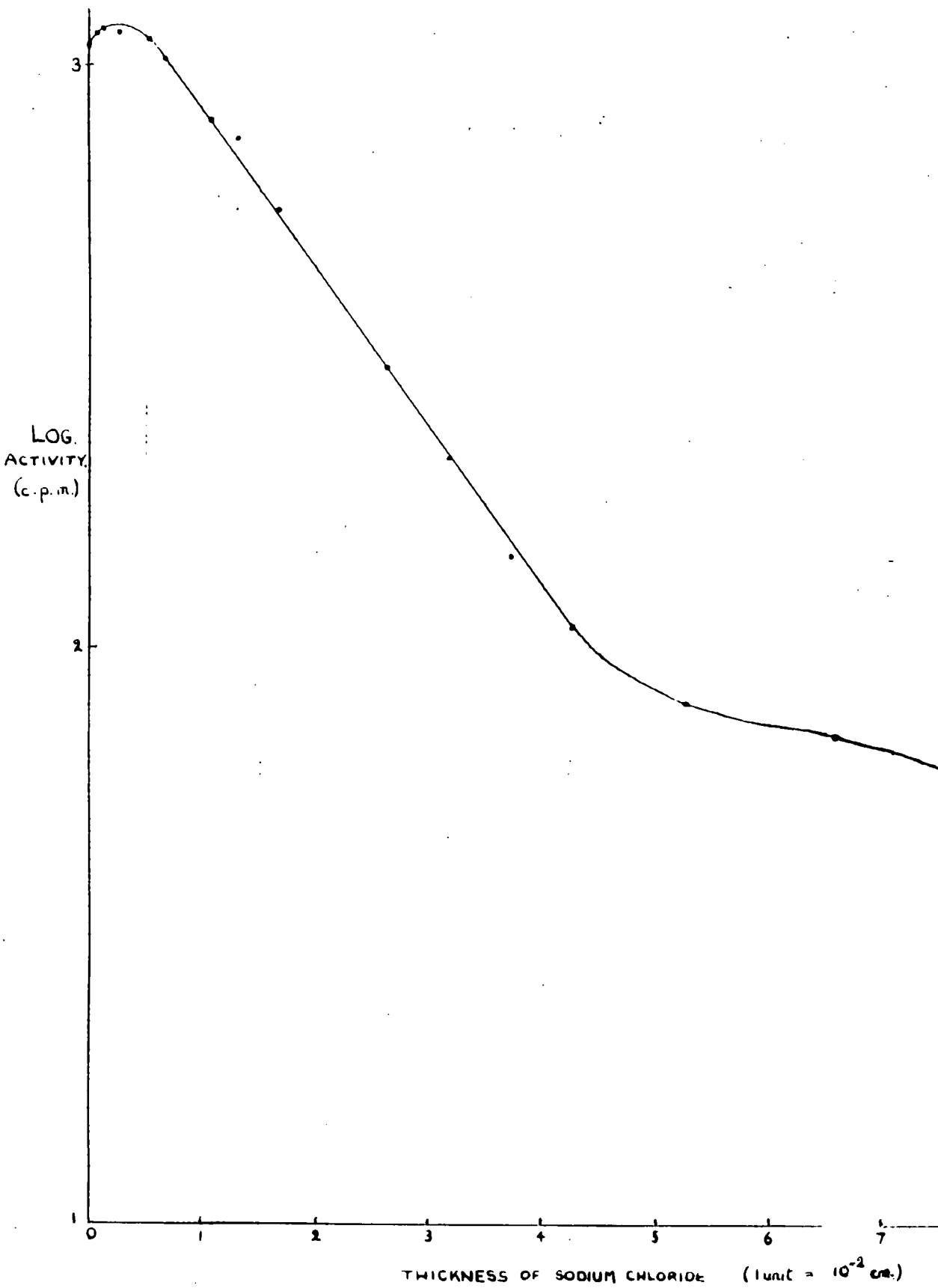


Fig. 29. The absorption curve for sodium-22.

TABLE 10.

THE ABSORPTION OF THE RADIATIONS OF SODIUM-22 IN
SODIUM CHLORIDE.

Weight of Aluminium Foil in Mgm. per cm. ²	Corresponding Thickness of Sodium Chloride in cm.	Counts per Minute Corrected to Standard Count.
Zero	Zero	1088
1.4875	.0006873	1136
2.975	.001374	1157
5.95	.002748	1141
11.7966	.00545	1107
14.7716	.006821	1024
23.5932	.0109	806
28.4638	.01314	747
35.3898	.01635	564
56.9276	.02629	302
68.7242	.03174	211
80.5208	.0372	143
92.3174	.04264	109
113.8552	.0526	80
142.31875	.0651	70
170.788	.07887	58

4.6. THE CALCULATION OF DIFFUSION COEFFICIENTS.

From the measurements made of the decrease in count rate after diffusion and of the

absorption of the sodium-22 radiations in sodium chloride it was now possible to calculate the diffusion coefficient, D . The basis of the diffusion equation and a typical example of the calculation involved in the determination of D will be given.

a.) The Diffusion Equation.

Let the source of active sodium chloride go on to the crystal as a layer Δx cm. thick (where Δx is 10^{-5} - 10^6 cm.)

Fick's first law of diffusion states that,

$$\partial C / \partial t = D \cdot \partial^2 C / \partial x^2$$

where C = concentration of active material (counts per min./cm.),

t = time in seconds,

D = Diffusion coefficient,

and x = depth in cm.

The solution of this law, applicable to this diffusion case, is given by the equation (38),

$$C_x = \frac{Q}{(\pi Dt)^{1/2}} e^{-x^2/4Dt}$$

where C_x = concentration of active material at a depth x cm.,

and Q = the initial amount deposited

$$= C_{t=0} \Delta x$$

$$= C_0 \Delta x$$

$$= R_0 \text{ (the initial counting rate)}$$

The equation can be rewritten as

$$C_x = \frac{R_0}{(\pi Dt)^{\frac{1}{2}}} e^{-x^2/4Dt}.$$

b) An Example of the Type of Calculation.

Crystal C.

Initial active face count	= 1037 c.p.m.
Active face count after 254.5 hours at 511°C	= 801 c.p.m.
Count corrected to standard	= 806 c.p.m.
Decrease in count at active face	= 231 c.p.m.

$$\text{Now } C_x = \frac{Q}{(\pi Dt)^{\frac{1}{2}}} e^{-x^2/4Dt}$$

where C_x = concentration of active material at a depth x . cm.,

x = depth in cm.,

D = diffusion coefficient,

t = time in sec. = $254.5 \times 60 \times 60 = 9.162 \times 10^5$ sec.

Q = initial count rate = 1037 c.p.m.

A value of D was then chosen and variation of C_x with x calculated from the equation.

Take $D = 7 \times 10^{-11}$ cm.²/sec.

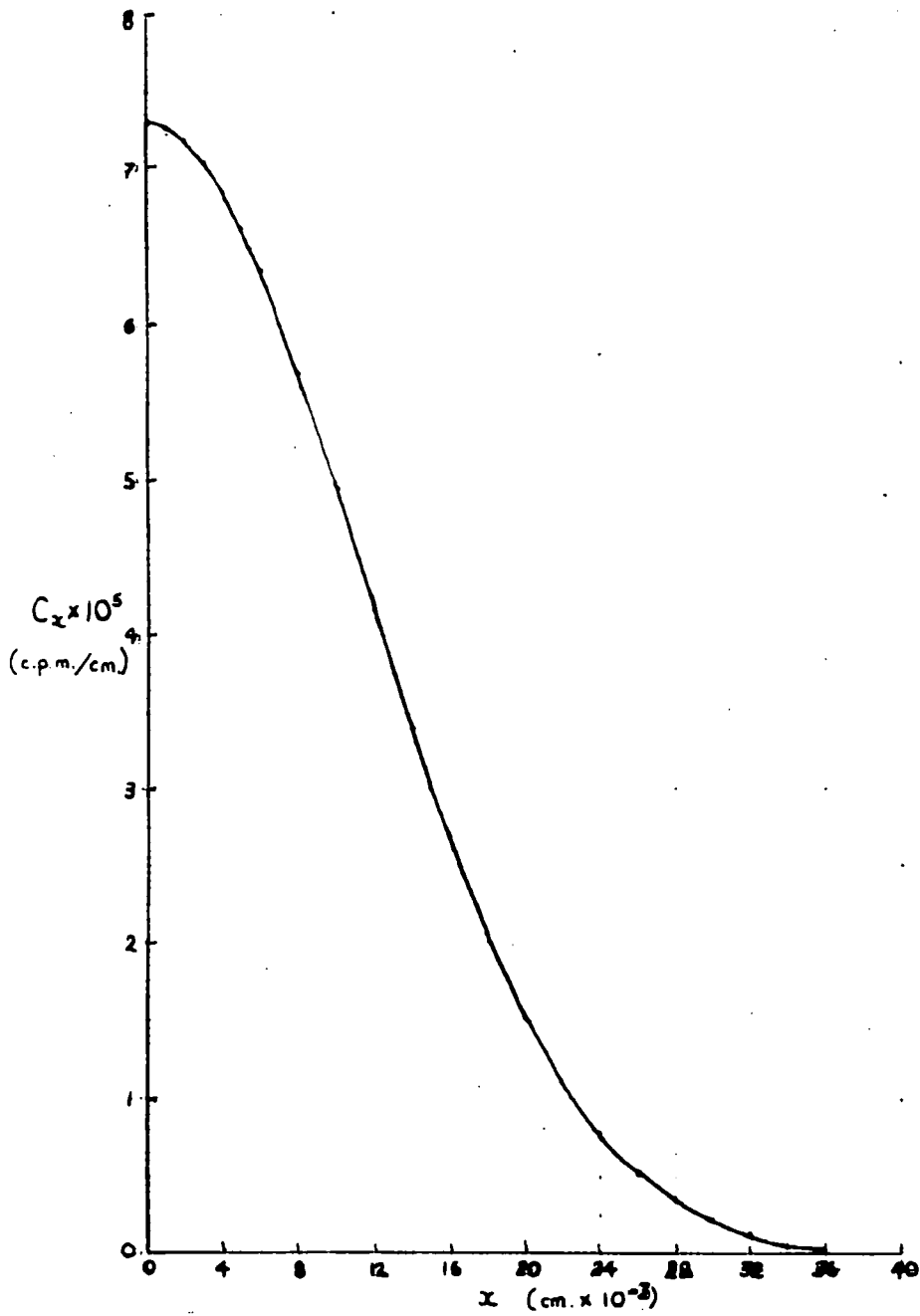


Fig. 30. The variation of activity with depth of crystal

x cm.	$Cx \times 10^5$ c.p.m./cm.	x	$Cx \times 10^5$
0	.7303	2×10^{-2}	.1536
1×10^{-3}	.7272	2.2×10^{-2}	.1108
2×10^{-3}	.7190	2.4×10^{-2}	.0774
3×10^{-3}	.7052	2.6×10^{-2}	.0525
4×10^{-3}	.6861	2.8×10^{-2}	.0355
5×10^{-3}	.6625	3.0×10^{-2}	.0219
6×10^{-3}	.6346	3.2×10^{-2}	.0135
8×10^{-3}	.5690	3.4×10^{-2}	.0057
1×10^{-2}	.4941	3.6×10^{-2}	.0047
1.2×10^{-2}	.4167		
1.4×10^{-2}	.3402		
1.6×10^{-2}	.2693		
1.8×10^{-2}	.2066		

A graph was then drawn of Cx against x showing the variation in concentration of active material with depth of penetration, Fig. 30, and the x -axis was divided into strips of 1×10^{-3} cm. width. The value of Cx corresponding to the mid-point of each strip was then read off. By consultation of the sodium chloride absorption curve (Fig. 29) the contribution of each strip to the surface count was calculated. The calculation was continued until a depth of x was obtained which gave no measurable count rate at the surface. A table was drawn up showing the results.

TABLE 12.

Depth x cm.	Cx x 10 ⁵	C.p.m. at surface i.e. (Cx)x(width of strip)x(absorption factor.)
.0005	.729	74.71
.0015	.726	77.74
.0025	.713	76.67
.0035	.6965	74.26
.0045	.675	71.04
.0055	.648	65.81
.0065	.620	60.40
.0075	.587	53.41
.0085	.5515	46.89
.0095	.514	40.86
.0105	.475	35.59
.0115	.435	30.59
.0125	.397	26.20
.0135	.358	22.21
.0145	.3185	18.5
.0155	.285	15.59
.0165	.250	12.87
.0175	.220	10.62
.0185	.191	8.637
.0195	.164	6.979
.0205	.139	5.570
.0215	.119	4.473
.0225	.101	3.574
.0235	.086	2.846
.0245	.070	2.181
.0255	.058	1.701
.0265	.049	1.347
.0275	.040	1.033
.0285	.032	0.7765
.0295	.0275	0.6268

Total count
at surface

855 c.p.m.

Therefore if the diffusion coefficient had been 7×10^{-11} cm.² per sec. the count at the surface would have been 855 c.p.m. The actual count was 806 c.p.m. so the diffusion coefficient must be greater than 7×10^{-11} cm.² per sec. A larger diffusion coefficient was then chosen and a similar calculation carried out. The results

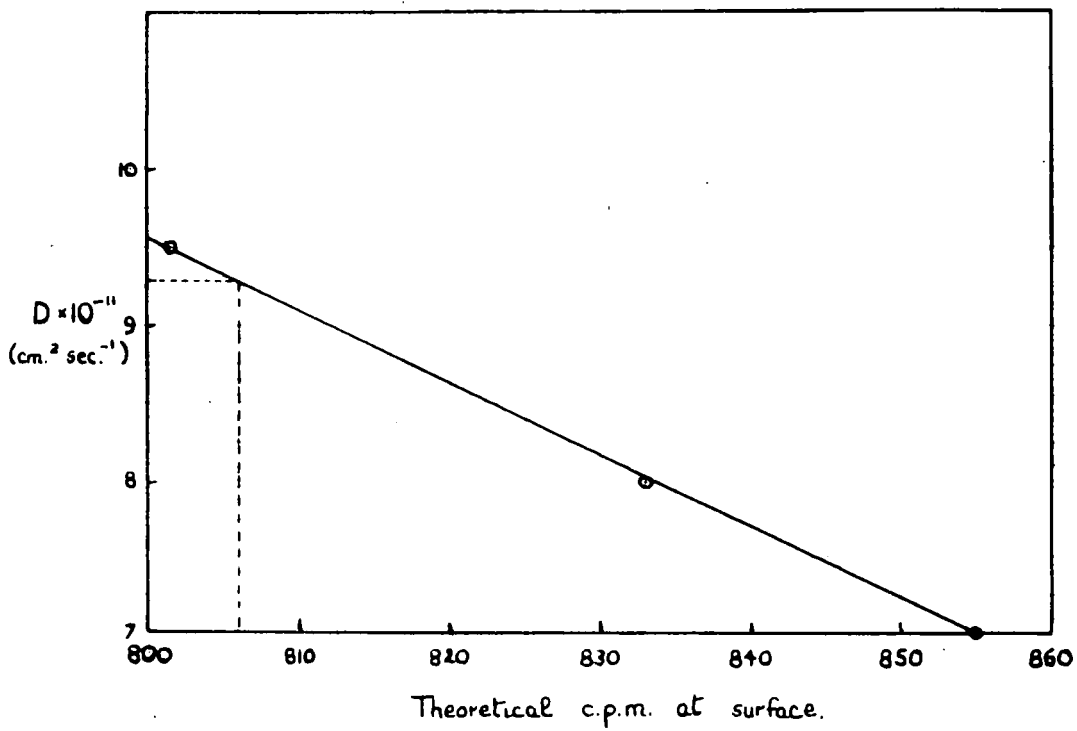


Fig. 31. The variation of c.p.m. at surface with diffusion coefficient.

are summarised in Table 13.

TABLE 13.

D. cm. ² per sec.	Theoretical c.p.m. at surface
7×10^{-11}	855
8×10^{-11}	833
9.5×10^{-11}	801.3

A graph was now drawn of c.p.m. at surface against diffusion coefficient (Fig. 31) and the value of D corresponding to a surface count of 806 c.p.m. was read off.

The value of D was found to be 9.28×10^{-11} cm.² per sec. Therefore the diffusion coefficient at 511°C of crystal C was 9.28×10^{-11} cm.² per sec.

The method was fairly sensitive and as the above calculation shows a change 2.6 per cent in the counting rate brought about a change 13.3 per cent in the diffusion coefficient.

4.7. THE RESULTS OF THE DIFFUSION MEASUREMENTS.

The trial experiments in bulk-diffusion were carried out on single crystals 1 and 2, which were grown in the laboratory. The results of the experiments are given in Table 14, but because of the nature of the experiments, which were aimed at standardising the technique and at determining suitable temperatures and times of diffusion, the diffusion coefficients calculated from the results could not be regarded as accurate data.

TABLE 14.

CRYSTAL 1.

Diffusion temperature and time.	Face Count. Counts per minute.	Standard Crystal c.p.m.	Face Count Corrected to standard 2514 c.p.m.	Inactive crystal c.p.m.	Pressure of nitrogen in diffusion tube at room temperature. cm. of mercury.
Initially	6719	2514	6719	16 (background)	(76)
After 184½ hours at 400°C.	6614	2633	6298	15 (background)	(10 ⁻²)
Further 168 hours at 490°C.	4248	2714	3925	374 evaporation	(75)
Further 168 hours at 520°C.	3642	2772	3294	18 (background)	

CRYSTAL 2.

Diffusion temperature and time.	Face Count. Counts per minute.	Standard Crystal c.p.m.	Face Count Corrected to standard 2514 c.p.m.	Inactive crystal c.p.m.	Pressure of nitrogen in diffusion tube at room temperature. cm. of mercury.
Initially	1675	2514	1675	16 (background)	(76)
After 184 $\frac{1}{2}$ hours at 400°C.	1746	2633	1667	15 (background)	(10 ⁻²)
Further 168 hours at 490°C.	1516	2714	1405	15 (background)	

CRYSTAL 1.

184 $\frac{1}{2}$ hours heating at 400°C.

$$D = 4.1 \times 10^{-11} \text{ cm.}^2 \text{ sec.}^{-1}$$

CRYSTAL 2.

184 $\frac{1}{2}$ hours heating at 400°C.

$$D = 1.45 \times 10^{-11} \text{ cm.}^2 \text{ sec.}^{-1}$$

These results are very approximate but one important fact, which did arise out of these measurements, was that the diffusion runs could not be carried out under vacuum because under these conditions evaporation of the active deposit took place. This was shown by the second heating of crystal 1 (Table 14). There was no evidence of any evaporation when a pressure of approximately one atmosphere, at room temperature, was used.

These experiments were carried out in conjunction with some trial measurements on the surface diffusion, (Section 6, Chapter 5), and as the results of the latter work have shown that this type of diffusion was less than 100 times the bulk diffusion, the effective area of the deposit would not be radically changed, so altering the counter geometry, during the experiments.

The method, having been shown to be very promising, was further tested by two diffusion runs, at a higher temperature, on crystals 3 and 4, grown in the laboratory. The results are given in Table 15. Comparison of the directly measured diffusion coefficient of crystal 3 was to be made with the diffusion coefficient calculated from the conductivity measurements on the crystal, (Fig. 18, Chapter 3).

TABLE 15.

CRYSTAL 3.

Diffusion temperature and time.	Face Count. Counts per minute.	Standard Crystal c.p.m.	Face Count Corrected to standard 4999 c.p.m.	Inactive crystal c.p.m.	Pressure of nitrogen in diffusion tube at room temperature. cm. of mercury.
Initially	2098	4999	2098	No inactive crystal present	← (74)
After 156 hours at 502°C.	1669	5001	1669	"	

156 hours at 502°C.

$$D = 1.26 \times 10^{-10} \text{ cm.}^2 \text{ sec.}^{-1}$$

TABLE 15.

CRYSTAL 4.

Untreated crystal which was used in the trial experiments in autoradiography.

Diffusion temperature and time.	Face Count. Counts per minute.	Standard Crystal c.p.m.	Face Count Corrected to standard 4999 c.p.m.	Inactive crystal c.p.m.	Pressure of nitrogen in diffusion tube at room temperature. cm. of mercury.
Initially	1559	4999	1559	No inactive crystal present.	(74)
After 156 hours at 502°C.	974	5001	974	"	

156 hours at 502°C.

$$D = 2.34 \times 10^{-10} \text{ cm.}^2 \text{ sec.}^{-1}$$

The effect of fine structure on the diffusion rate was then measured using three specimens taken from the same single crystal (No. 5). These experiments were carried out in conjunction with the study of the effect of chilling and annealing the crystal on the crystal conductivity. A set of similar experiments to those carried out on diffusion in crystal 5 have been made on the conductivity in crystal 5, (Fig. 20, Section 9, Chapter 3), so that an exact comparison can be made of these effects.

Great care was taken in these final experiments to,

- (a) avoid evaporation of the active deposit,

- (b) use a standard reproducible procedure, and
 (c) to ensure a 1 per cent statistical accuracy in all the counting results.

The single crystal 5 was grown in the laboratory, annealed for six hours at 600°C. and then allowed to cool down to room temperature.

The results of the diffusion experiments are given in Tables 16, 17, and 18.

TABLE 16.

CRYSTAL 5A.

Untreated specimen of crystal 5.

Diffusion temperature and time.	Face Count. Counts per minute.	Standard Crystal c.p.m.	Face Count Corrected to standard 1045 c.p.m.	Inactive crystal c.p.m.	Pressure of nitrogen in diffusion tube at room temperature. cm. of mercury.
Initially	952	989	1006	16 (background)	73.5
After 189 hours at 511°C.	854	1045	854	16 (background)	
Further 254½ hours at 511°C.	678	1020	695	16 (background)	

Coefficient of self-diffusion (First heating) calculated for 189 hours at 511°C.

$$D = 7.90 \times 10^{-11} \text{ cm.}^2 \text{ sec.}^{-1}$$

Coefficient of self-diffusion calculated for 443½ hours at 511°C.

$$D = 9.0 \times 10^{-11} \text{ cm.}^2 \text{ sec.}^{-1}$$

TABLE 17.

CRYSTAL 5B.

Specimen of crystal 5, which was sealed in a pyrex tube, and then immersed in liquid nitrogen for three minutes. The crystal was cleaved to give fresh faces and the active deposit evaporated on to one of the freshly cleaved faces.

Diffusion temperature and time.	Face Count. Counts per minute.	Standard crystal c.p.m.	Face Count Corrected to standard 1045 c.p.m.	Inactive crystal c.p.m.	Pressure of nitrogen in diffusion tube at room temperature. cm. of mercury.
Initially	3583	989	3791	15 (background)	(73.5)
After 189 hours at 511°C.	3167	1045	3167	15 (background)	(75)
After further 254½ hours at 511°C.	2519	1020	2583	15 (background)	

189 hours at 511°C.

$$D = 8.7 \times 10^{-11} \text{ cm.}^2 \text{ sec.}^{-1}$$

443½ hours at 511°C.

$$D = 9.37 \times 10^{-11} \text{ cm.}^2 \text{ sec.}^{-1}$$

TABLE 18.

CRYSTAL 5C.

Specimen of crystal 5 which has been annealed for 256 hours at 620°C in an atmosphere of nitrogen and cooled to room temperature over 12 hours.

Diffusion temperature and time.	Face Count. Counts per minute.	Standard crystal c.p.m.	Face Count Corrected to standard 1045 c.p.m.	Inactive crystal c.p.m.	Pressure of nitrogen in diffusion tube at room temperature. cm. of mercury.
Initially	1023	1031	1037	Background count	(75)
After 254½ hours at 511°C.	809	1049	806	Background count	

254½ hours heating at 511°C.

$$D = 9.28 \times 10^{-11} \text{ cm.}^2 \text{ sec.}^{-1}$$

It can be observed from the results that both the chilling and the annealing of the crystal increase the self-diffusion coefficient. The annealing of the crystal increases the self-diffusion coefficient from $7.9 \times 10^{-11} \text{ cm.}^2 \text{ sec.}^{-1}$ to $9.28 \times 10^{-11} \text{ cm.}^2 \text{ sec.}^{-1}$, a change of 17.47 per cent, while the chilling of the crystal increases the coefficient by 7.34 per cent.

Further agreement for this effect of increase of diffusion coefficient with heating time has come from the results on the second heating of the untreated and the chilled crystals. There has been an increase from

$7.9 \times 10^{-11} \text{ cm.}^2 \text{ sec.}^{-1}$ to $9.0 \times 10^{-11} \text{ cm.}^2 \text{ sec.}^{-1}$ (13.9 per cent) in the former and in the latter an increase from $8.7 \times 10^{-11} \text{ cm.}^2 \text{ sec.}^{-1}$ to $9.37 \times 10^{-11} \text{ cm.}^2 \text{ sec.}^{-1}$ (7.7 per cent).

Comparison of these results with the experiments of Mapother, Crooks and Maurer (1), who observed a self-diffusion coefficient of approximately $3 \times 10^{-11} \text{ cm.}^2 \text{ sec.}^{-1}$ at 511°C , shows a discrepancy of approximately three. It is possible, however, that part of this may be accounted for by the fact that their maximum heating time was 120 hours compared with a minimum time of 189 hours in this work, and as the results of these experiments show the self-diffusion coefficient does increase with the length of heating time.

The results and the conclusions drawn from them will be discussed in a later chapter.

4.8. THE NERNST-EINSTEIN RELATIONSHIP.

The results of the directly measured self-diffusion coefficient have been compared with the self-diffusion coefficient calculated from the conductivity by means of the Nernst-Einstein relationship, which is described in section 3 of Chapter 1. The relationship states that,

$$\sigma/D = Ne^2/kT \quad (\text{Eqn. 1})$$

The calculations have been carried out on the conductivity measurements, described in section 9 of Chapter 3, on crystal 3 and the pieces of crystal 5, which have been subjected to various heat treatments. The

calculated self-diffusion coefficients were compared with the directly measured self-diffusion coefficients described in this chapter.

The results of these calculations are summarised in Table 19 (the complete calculations are given in the appendix).

TABLE 19.

Crystal	Temp. of measurements °C.	Conductivity $\text{ohm}^{-1}\text{cm.}^{-1}$.	Observed self-diffusion coefficient $\text{cm.}^2\text{sec.}^{-1}$.	Calculated self-diffusion coeff. $\text{cm.}^2\text{sec.}^{-1}$	$\frac{D_{\text{observed}}}{D_{\text{calculated}}}$
Crystal No. 3	502	3.428×10^{-6}	1.26×10^{-10}	6.401×10^{-11}	1.968
Crystal No. 5 Untreated slice 5A.	511	1.82×10^{-6}	7.9×10^{-11}	3.438×10^{-11}	2.298
Slice cooled in liquid nitrogen 5B.	511	2.884×10^{-6}	8.7×10^{-11}	5.45×10^{-11}	1.596
Slice annealed at 620°C for $254\frac{1}{2}$ hours 5C.	511	3.802×10^{-6}	9.28×10^{-11}	7.183×10^{-11}	1.292

It can be seen from the results of crystal 5 that the effect of the heat treatments on the crystal was to lower the D_{observed} to $D_{\text{calculated}}$ ratio. Chilling of the crystal decreased the ratio by 30.43 per cent while

annealing of the crystal for $254\frac{1}{2}$ hours at 620°C caused decrease of 43.48 per cent.

These results will be discussed in a later chapter.

CHAPTER 5.

THE MEASUREMENT OF SURFACE DIFFUSION OF SODIUM ON
SINGLE CRYSTALS OF SODIUM CHLORIDE.

5. THE MEASUREMENT OF SURFACE DIFFUSION OF SODIUM ON SINGLE CRYSTALS OF SODIUM CHLORIDE.

5.1. INTRODUCTION.

The experiments on diffusion, described in the previous chapter, have been aimed at determining the effect of fine structure on the diffusion rate in the crystal. These changes in fine structure would only affect the rate of diffusion in the crystal if grain boundary diffusion took place and if the rate of this type of diffusion was more rapid than that of bulk diffusion. In measurements of diffusion in metals, it is generally found that grain boundary diffusion is more rapid than bulk diffusion, while surface diffusion is even more rapid than the grain boundary diffusion.

It was decided to carry out a series of measurements to determine the surface diffusion coefficient of sodium on the same crystal and at the same temperature as the bulk diffusion measurements. It should then be possible to estimate the approximate rate of grain boundary diffusion from the expected difference in the surface and bulk diffusion rates. From these results the significance of grain-boundary diffusion on the self-diffusion in sodium chloride crystals could be determined.

5.2. OUTLINE OF THE METHOD OF MEASUREMENT.

A long narrow rectangular deposit of sodium chloride, with the sodium labelled, was evaporated on to one surface

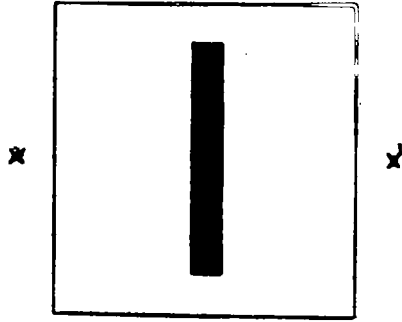


Fig. 32. The active deposit.

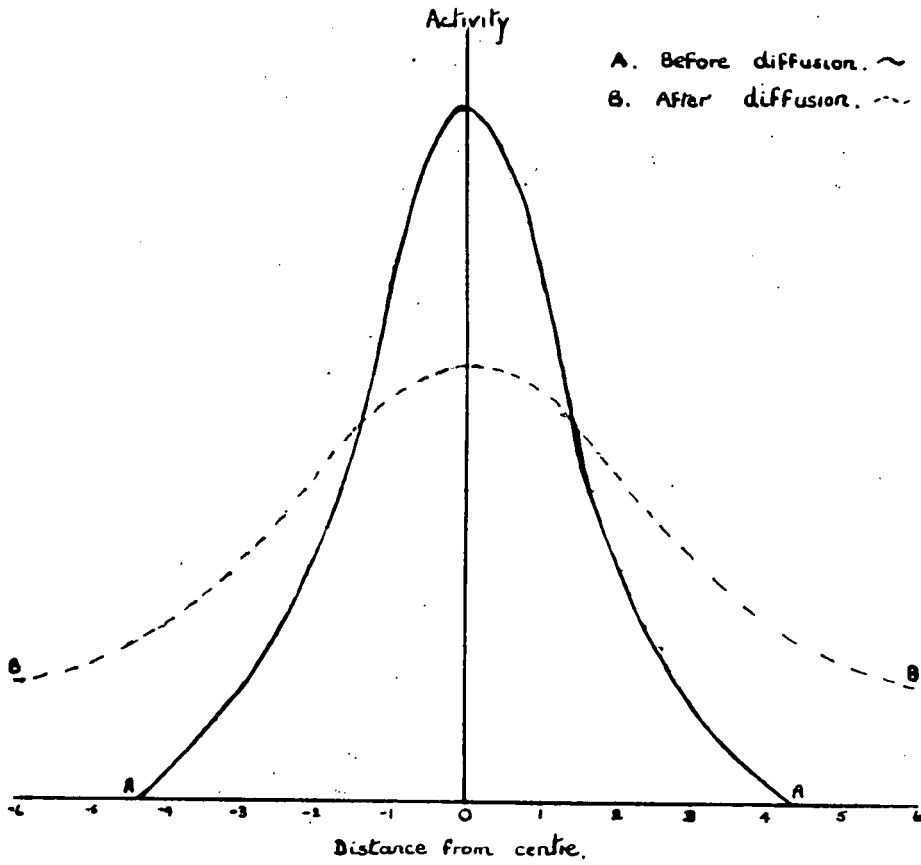


Fig. 33. Variation of activity over the crystal surface.

of the crystal, Fig. 32. A deposit of this shape was required so that the only significant diffusion would be in the X-X direction. The variation in activity in this direction across the surface was then measured by a scanning apparatus, which will be described in the next section. The graph of this variation in activity across the surface is shown in Fig. 33.

The crystal was transferred to a pyrex vessel, sealed off under a pressure of nitrogen gas and placed in a furnace at the desired temperature. After leaving for a known time, the vessel was removed, cooled and the surface scan of the crystal face repeated.

If any surface diffusion had taken place, the width of the active deposit would have increased and so a type of graph, shown in Fig. 33, would now be obtained. The result will be complicated by the bulk-diffusion during this time, but any surface diffusion would be detected by the change in shape of this graph of the variation in activity with distance across the surface.

5.3. THE DETAILS OF THE DIFFUSION TECHNIQUE.

a) The Scanning Apparatus.

The apparatus is shown in Fig. 34. A brass base-plate, B, 8cm. x 10cm. in size, had mounted on it a movable steel plate P. This plate was moved by means of a calibrated screw, S, one full turn of which moved the plate .0835 cm. The crystal was fitted into steel right angle, L, which was brazed on

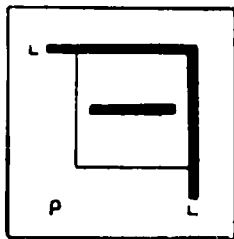
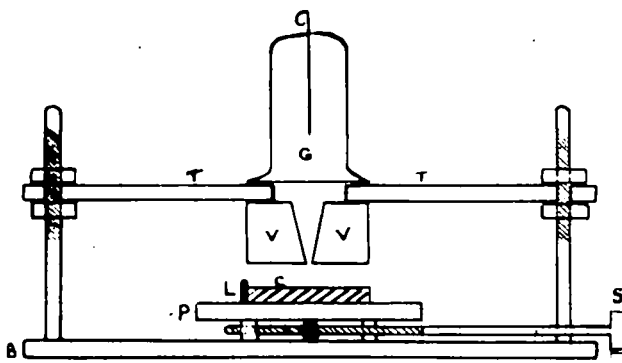


Fig.34. The scanning apparatus.

to the steel plate, P; the position of the steel right angle was such that the crystal, when in position, could be moved under the field of view of an end window Geiger-Muller counter, G, which had a window thickness of 7 mgm. per sq. cm. The counter was fitted above a circular aperture, 3 cm. in diameter, in the upper brass plate, T.

The field of view of the counter was restricted by a V-shaped lead slit, V, which was 1.4 cm. in depth and whose width varied from .0508 cm. at the lower end to .37 cm. at the top. This enabled the activity of a strip of crystal, .13 cm. in width, to be measured during each count. The upper plate was screwed down on the four supports from the lower plate until the slit was as near to the crystal as possible.

The accuracy of this type of scanning apparatus has been tested by Sherwood (39), who, on a similar apparatus, compared accurately the width of the active deposit obtained by the surface scan with the actual width of the deposit, and he has shown that the two measurements were identical.

b) The Technique of Measurement.

In the early measurements of surface diffusion, sodium chloride, labelled with sodium-24, was used as the tracer material but, as this had a very short half-life (14.8 hours), the period of diffusion was limited to the inadequate time of 60 hours. Consequently, in later work, the sodium

chloride was labelled with sodium-22 which has a half-life of 2.6 years.

The active sodium chloride was evaporated from a platinum boat on to a rectangular area, approximately 1.5 cm. x .2 cm. in size, of a freshly cleaved face of a single crystal, 2 cm. x 2 cm. x .2cm. in size, by the method described in Chapter 6. The total activity deposited on the crystal face was determined by counting it under an end window Geiger counter with a 7 mgm. per sq. cm. window thickness. A surface scan of the crystal face was then made, with the apparatus described in Section 3, to determine the distribution of activity.

This was carried out by first adjusting the movable plate so that one edge of the crystal was directly under the counter slit. A count was then taken, after which the crystal was moved .0835 cm. by giving the movable plate screw one full turn; a count was again taken. This procedure was repeated until the complete crystal surface had been scanned. Near the centre of the crystal, where the activity was highest, the crystal was only moved half a turn of the screw per count. Sufficient counts were taken at each point to ensure a statistical accuracy of at least 2 per cent in the counting.

The crystal was placed in a pyrex glass holder and a monitoring inactive crystal was supported above the active face of the first crystal. Direct contact between the two crystals was avoided by having a thin mild steel ring,

2.5 cm. in diameter and .15 cm. thick, placed between them. The holder was fitted into a long pyrex tube and connected to a vacuum line. The vessel was pumped to sticking vacuum and then filled with approximately one atmosphere of oxygen-free nitrogen; this gave a pressure of 2.7 atmospheres at the diffusion temperature. The vessel was sealed off and placed in the temperature controlled furnace. This procedure is described fully in section 4c of Chapter 4.

The temperature for the surface diffusion runs was measured by a 550°C mercury-in-glass thermometer, which was in contact with the lower end of the tube, and was noted frequently during the time of diffusion. Temperature control was maintained to within $\pm 3^\circ\text{C}$ of the desired value during the diffusion run. After it had been left for the desired time, the tube was removed from the furnace, cooled down to room temperature in air and the scan of the activity variation over the crystal surface repeated.

The inactive crystal and the ring were examined for activity by a thin end window counter. In only one case has the blank crystal become active due to evaporation of the deposit and this was when a run was carried out with a pressure in the diffusion tube of only 1×10^{-2} atmospheres.

5.4. THE DIMENSIONS OF THE SURFACE COUNTING ARRANGEMENT.

In order to calculate the surface diffusion coefficient it was essential to know the width of the crystal viewed by the counter, the width of the active deposit on the crystal

Scale 1cm. = 1mm. of apparatus.

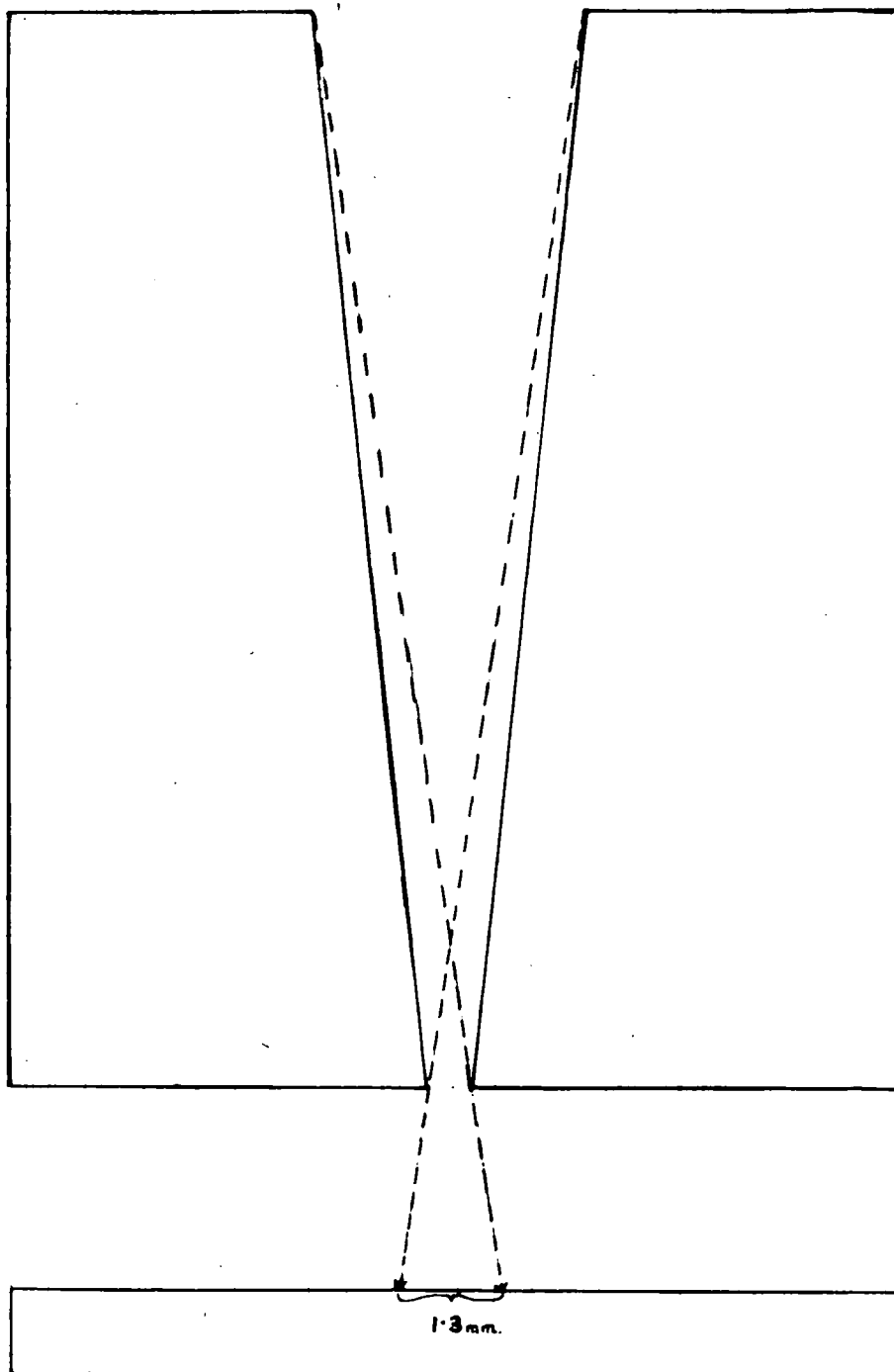


Fig. 35. Scale diagram of the lead slit-system.

and the distance moved by the crystal after each count.

The dimensions of the V-shaped lead slip and the distance from the slit to the crystal face were accurately measured with a thickness gauge. The details are given below:-

Slit width at bottom	=	0.0508 cm.
Slit width at top	=	0.37 cm.
Depth of the slit	=	1.4 cm.
Distance from movable plate to slit	=	0.3746 cm.
Thickness of crystal	=	0.1113 cm.

A scale diagram of the experimental arrangement is shown in Fig. 35. From an examination of this diagram it was observed that the counter viewed a strip of crystal 0.13 cm. in width each count.

The width of the deposit on the crystal has been measured with a Vernier gauge. The result was identical to that obtained for the slit width of the box, in which the crystal was housed for the evaporation process.

Width of active deposit on crystal = 0.26 cm.

The movement of the crystal mounting plate was determined by measuring the distance moved for a number of turns of the screw. This was repeated several times.

Distance moved by plate for one full turn
of the screw = 0.0835 cm.

5.5. THE CALCULATION OF THE SURFACE DIFFUSION COEFFICIENT.

The equation for surface diffusion is derived from Fick's first law of diffusion. This states that,

$$\frac{\partial c}{\partial t} = D \frac{\partial^2 c}{\partial x^2}$$

where c = concentration of active material (counts per min./cm.),

t = time in seconds,

D = diffusion coefficient in $\text{cm.}^2 \text{ sec.}^{-1}$,

and x = depth in cm.

The solution of the law applicable to this case of surface diffusion is given by the equation (40),

$$C = C_0/2 \left[\operatorname{erf} \left(\frac{h+x}{2\sqrt{Dt}} \right) + \operatorname{erf} \left(\frac{h-x}{2\sqrt{Dt}} \right) \right] \quad (\text{Eqn. 4})$$

where C_0 = initial concentration of active material (counts per min./cm.),

C = concentration at a distance x cm. from centre of active deposit,

$2h$ = width of deposit in cm. (i.e. deposit covers width from $-h$ to $+h$),

D = surface diffusion coefficient in $\text{cm.}^2 \text{ sec.}^{-1}$,

t = time in seconds

and $\operatorname{erf.}$ = Gauss' error function.

The diffusion equation can be solved by the use of Stefan's tables which are given on page 64 of Jost's "Diffusion" (41). Stefan used the error function integral of the one dimensional diffusion equation (Eqn. 4) and tabulated the concentration distribution for a semi-infinite system. The distribution in a finite system can be

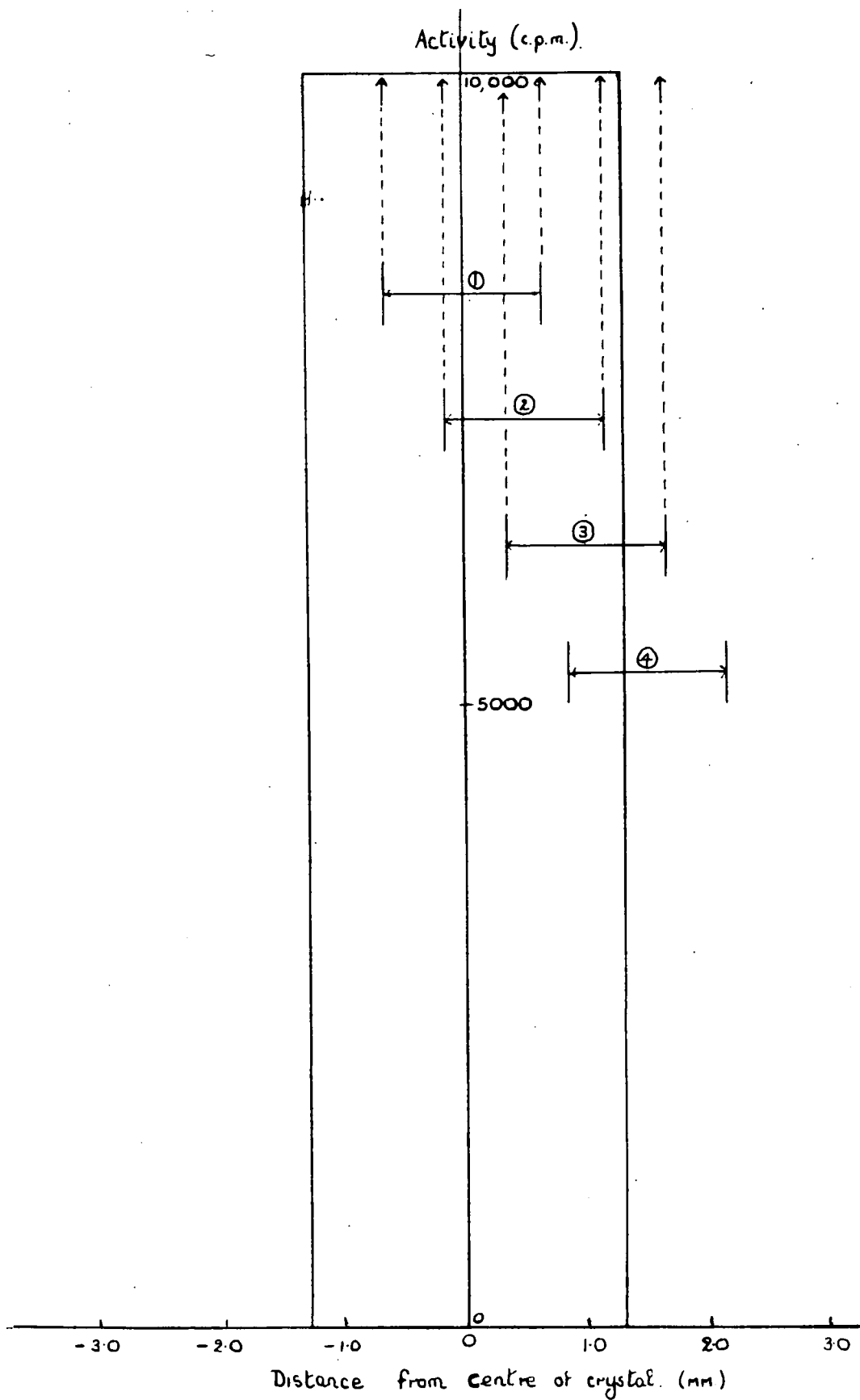


Fig. 36. Initial distribution of activity on crystal surface.

obtained from the semi-infinite solution by reflection.

The tables, which refer to only one half of the system, assume that a quantity of 10,000 is contained in a strip of width $2h$ (i.e. the total width of the active deposit is $4h$.) at the time $t = 0$. The tables then list the content of each consecutive strip of width h as a function of the argument $h/2\sqrt{Dt}$. A histogram could then be drawn of the distribution of activity in strips of width h against x , the distance from the centre of the complete system, and by reflection of this histogram around the $x = 0$ axis, the distribution of activity in the complete system was obtained, Fig. 38.

The use of these tables in the determination of the surface diffusion coefficient will now be shown.

It was assumed that the activity of the strip was 20,000 counts per minute so that there was an activity of 10,000 counts per minute in the distance $2h$ (i.e. half the strip-width).

From experimental measurements it was known that the strip width was 2.6 mm.

$$\therefore 2h = 1.3 \text{ mm.}$$

Before diffusion, the 10,000 counts per minute activity would be contained in this width of 1.3 mm., Fig. 36. This figure has been drawn to a scale of 2 cm. equal to 1 mm. of actual crystal.

A. Initial surface scan. —
B. Surface scan after diffusion. - - -

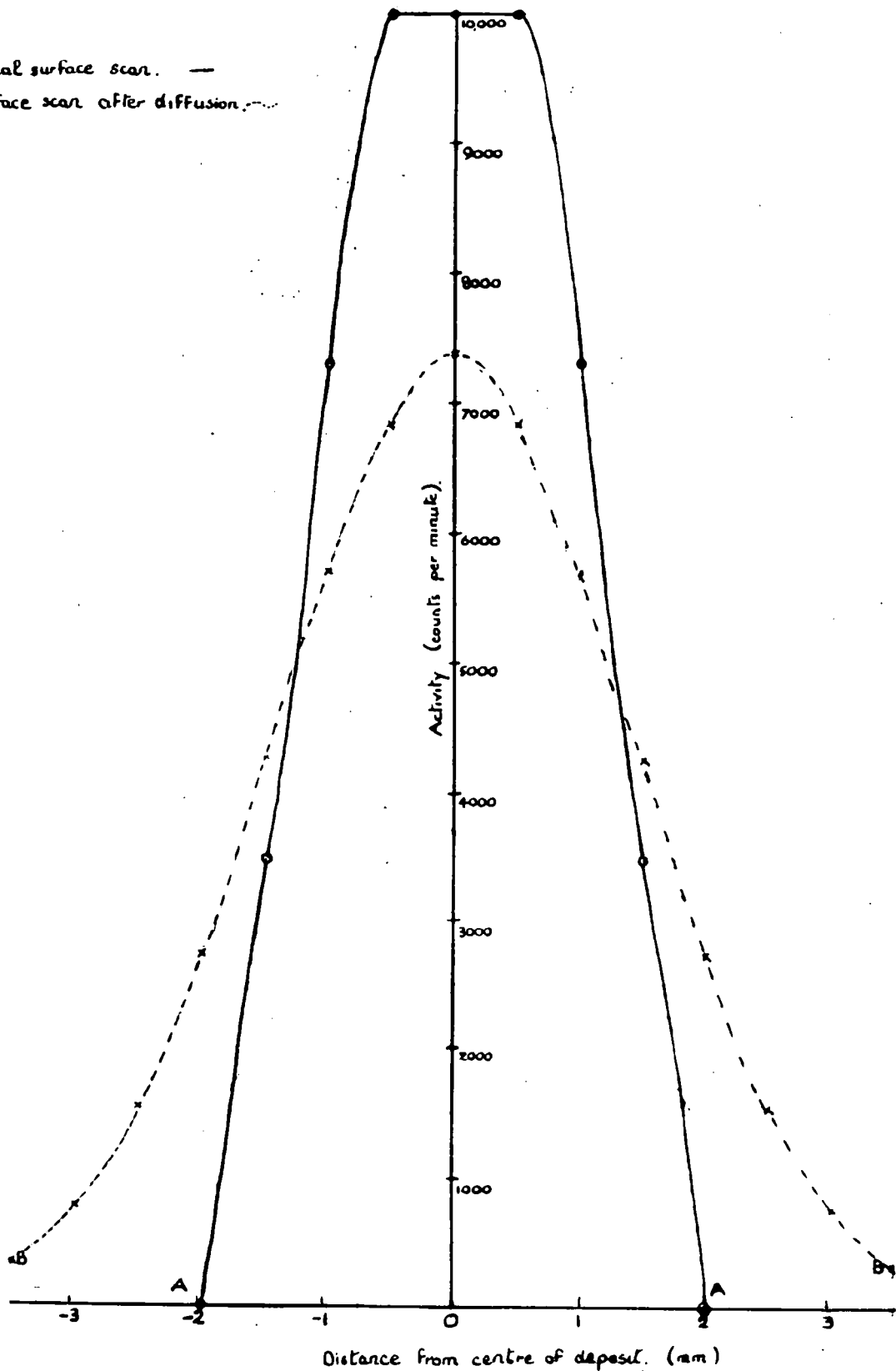


Fig. 37. Theoretical distribution of surface activity before and after diffusion.

Therefore, if the middle of the counter slit was at $x = 0$, (position ①), then it would see half of the 10,000 count on the left hand side of the centre of the deposit and half of the 10,000 count on the right hand side of the centre of the deposit. Hence, at $x = 0$, the counter would give 10,000 counts per minute.

Now, if the crystal was moved along 0.5 mm., (position ②), the counter would see $3/26$ th of the 10,000 count on the left hand side of the centre of the deposit and $23/26$ th of the 10,000 count on the right hand side. Hence, at $x = .5$ mm., the counter would give 10,000 counts per minute.

The crystal was then moved along a further 0.5 mm., (position ③), so that the centre of the counter slit was at $x = 1$ mm. The counter would now see $19/26$ th of 10,000 counts on the right hand side of the centre of the deposit and the remaining $7/26$ th would see no activity. Hence, at $x = 1$ mm., the counter would give $19/26 \times 10,000$ counts per minute.

In this way, the distribution of activity in counts per minute registered by the counter could be plotted against the distance from the centre of the deposit on the crystal. The complete curve, shown in Fig. 37, was obtained by reflection of the right hand side.

A value of the diffusion coefficient was then chosen and, since the time of diffusion was known, the value of

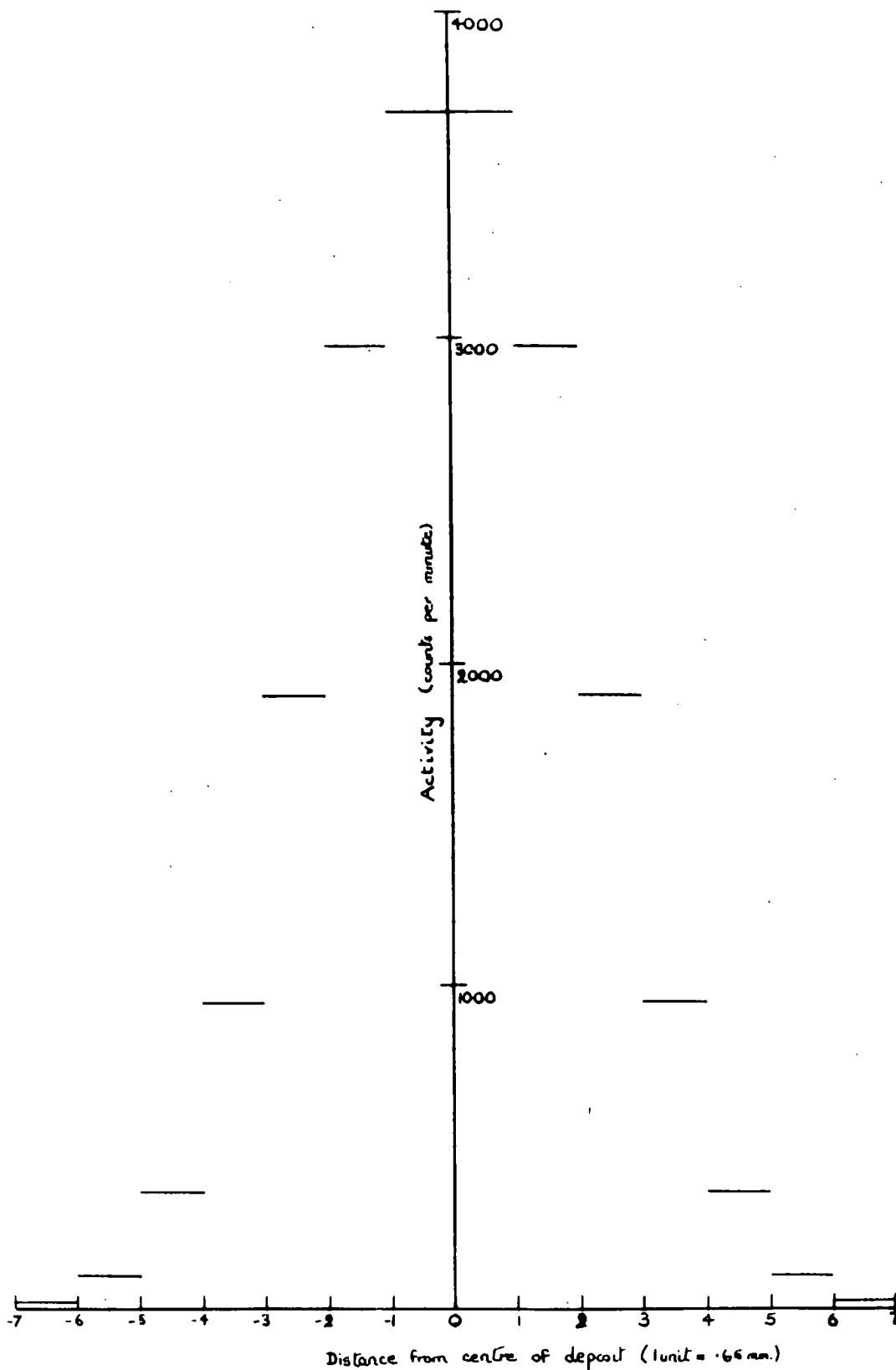


Fig. 38. The activity histogram for $h/2\sqrt{D.t} = 0.42$.

$h/2\sqrt{Dt}$ could be calculated. By use of Stefan's tables, the appropriate histogram for this value of $h/2\sqrt{Dt}$ could be plotted.

In the case of the surface diffusion in the present work, the crystal was heated for 214 hours at 506°C. A value of the surface diffusion coefficient, D , was chosen which was about a hundred times the bulk diffusion coefficient.

$$\text{Let } D = 8 \times 10^{-9} \text{ cm.}^2 \text{ sec.}^{-1}$$

$$t = 7.705 \times 10^5 \text{ sec.}$$

$$\therefore \frac{h}{2\sqrt{Dt}} = \frac{.065}{2\sqrt{8 \times 10^{-9} \times 7.705 \times 10^5}}$$

$$= .42.$$

The histogram appropriate to this value of $h/2\sqrt{Dt}$ was plotted using Stefan's tables, Fig. 38, after which the distribution of activity over the surface was determined by the method, previously described. The graph of this distribution of activity after diffusion is shown in Fig. 37.

A series of these calculations were made using different values of the surface diffusion coefficient and the appropriate graphs of the distribution of activity plotted. By comparison of these with the shape of the graph for the actual measurements it was possible to determine the surface diffusion coefficient.

The method was limited by the available data to calculations with a surface diffusion coefficient not less

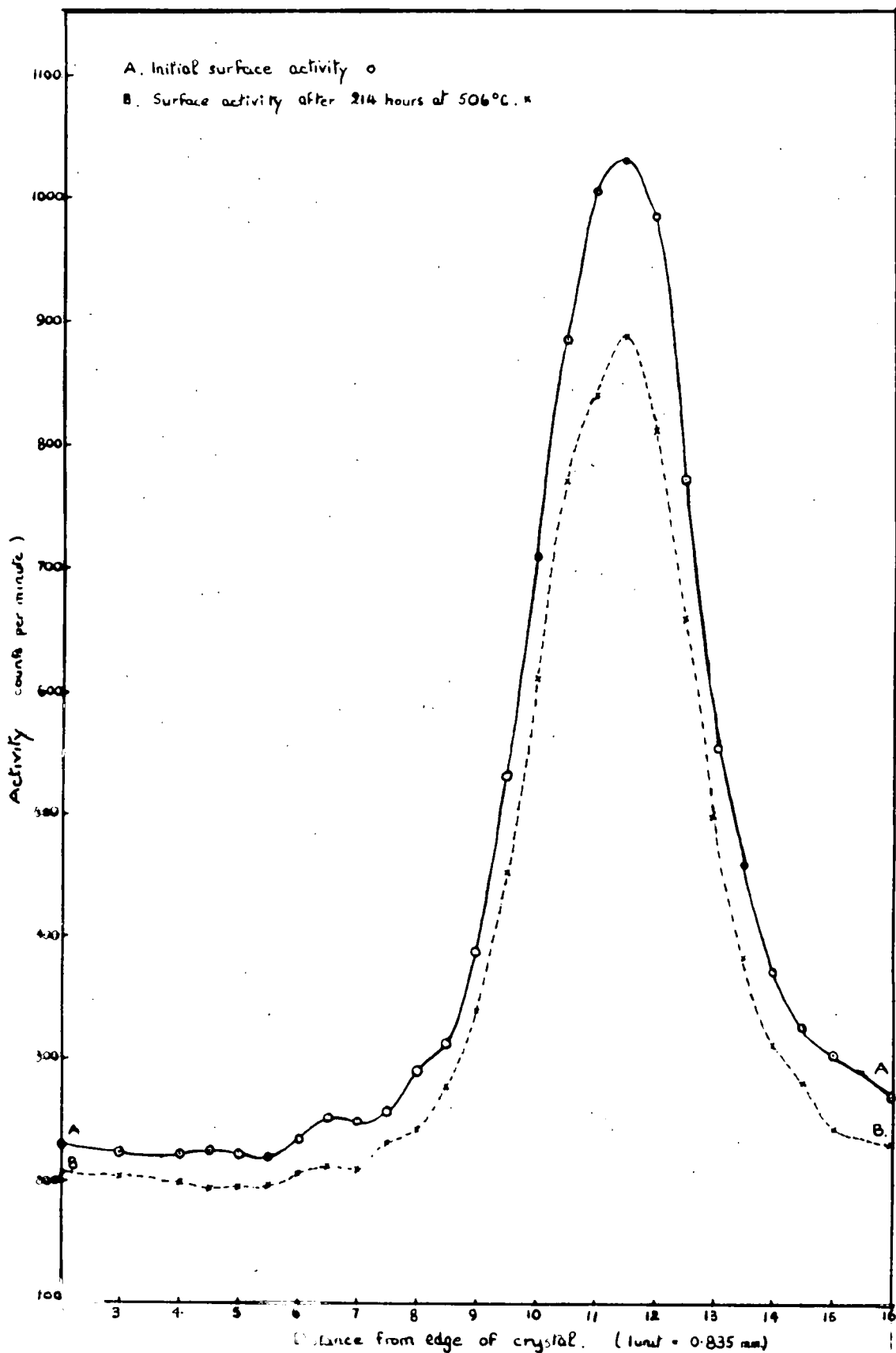


Fig. 39. Variation of activity over surface for crystal 5E.

than 10^{-9} cm.² sec.⁻¹. It was also doubtful whether it would be possible, using the present apparatus, to detect changes in the distribution of activity over the surface if the surface diffusion coefficient was less than 10^{-9} cm.² sec.⁻¹.

5.6. THE RESULTS OF THE SURFACE DIFFUSION MEASUREMENTS.

A series of trial experiments were carried out on crystal 1 in order to develop the technique and conditions for measurement of surface diffusion.

The results of these experiments have shown that with the present system a total surface activity of over 10,000 counts per minute was needed to obtain a statistical accuracy of approximately 1.5 per cent for the surface scan.

It was also observed that moisture condensed on the crystals during the surface counting so that in the final experiment the complete counting apparatus was desiccated with silica gel.

The important measurement of the surface diffusion coefficient was carried out on a piece of crystal 5, which was the crystal used in the final bulk diffusion experiments. The conditions of diffusion were maintained as near as possible to these experiments on bulk diffusion.

The crystal was maintained at a temperature of 506°C for 214 hours while the pressure of nitrogen in the diffusion vessel was approximately 2.7 atmospheres at this working temperature.

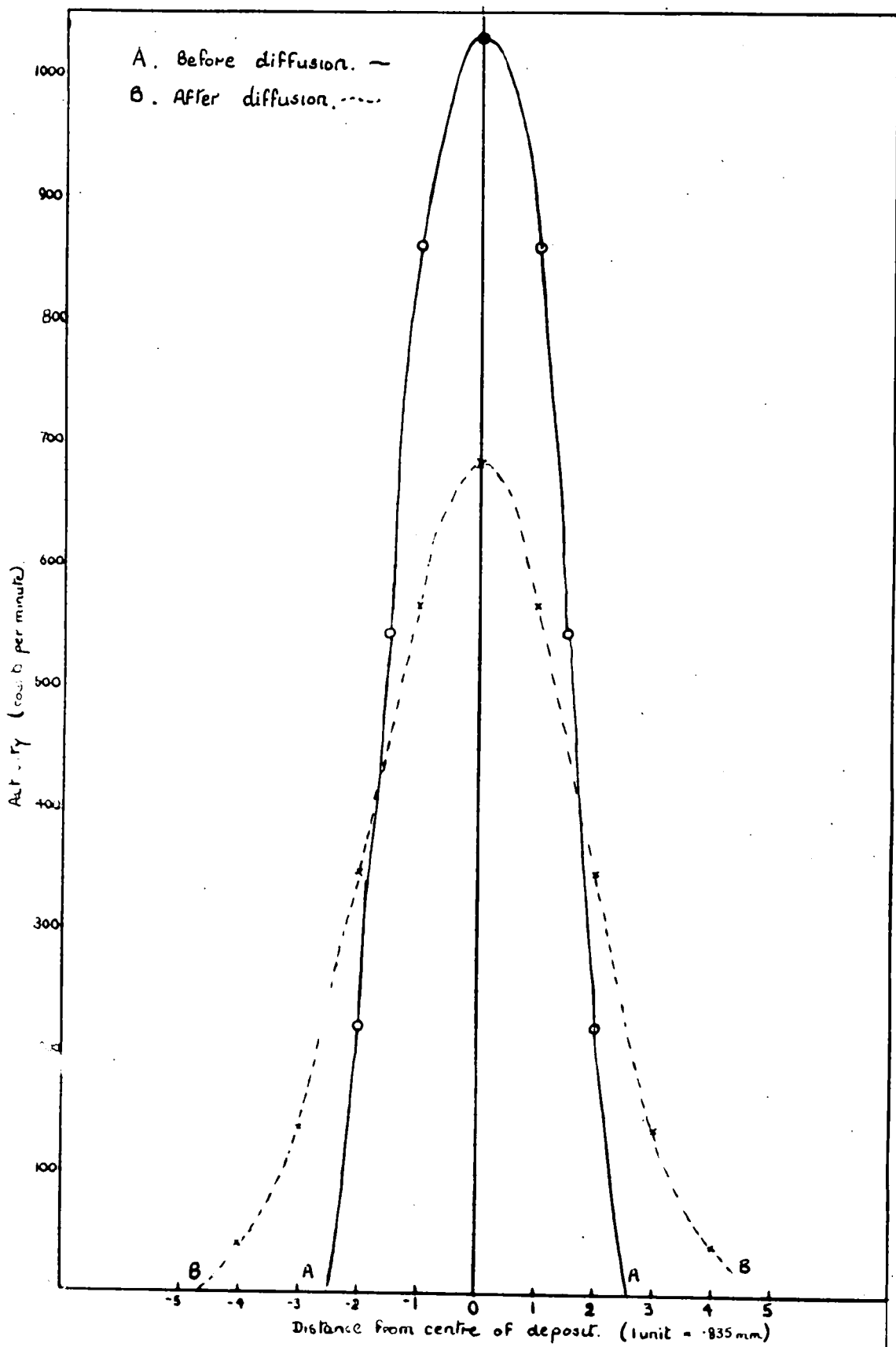


Fig. 40. Variation in activity over surface with $D = 8 \times 10^{-9} \text{ cm.}^2 \text{ sec.}^{-1}$

The results of the surface diffusion measurements, which have been plotted graphically as count rate against distance from the initial counting position on the crystal, are shown in Fig. 39 . Bulk diffusion has not been allowed for in the results but even without this correction it is obvious that the shape of the graph of activity is unchanged by the heating.

Comparison of Fig. 39 with the theoretical curves of the distribution before and after 214 hours heating at 506°C with a surface diffusion coefficient 100 times the bulk diffusion coefficient, (i.e. $8 \times 10^{-9} \text{ cm.}^2 \text{ sec.}^{-1}$), drawn on the same scale and with the same activity peak shows that there would certainly be a measurable change after this time, Fig. 40 .

It was therefore concluded that the surface diffusion coefficient must be either less, or of the same order, or up to ten times the bulk diffusion coefficient at this temperature.

CHAPTER 6.

THE SURFACE PATTERNS ON CLEAVED FACES OF
SINGLE CRYSTALS OF SODIUM CHLORIDE.

6. THE SURFACE PATTERNS ON CLEAVED FACES OF SINGLE CRYSTALS OF SODIUM CHLORIDE.

6.1. INTRODUCTION.

The construction of a vacuum apparatus for evaporation of deposits of sodium chloride on to the crystal faces was envisaged as serving a dual purpose. It was necessary to have a method of evaporation of active sodium chloride on to the crystal for diffusion measurements but also it was conceived that a study of the crystal surfaces might be possible by microscopic examination of this evaporated deposit.

This idea arose from the work of Kern and Pick (42) who observed the changes in surface structure when single crystals of the alkali halides were heated on the stage of a phase-contrast microscope to 700° - 800° C. They have published photographs of the lamellae patterns which appeared and have attributed these to evaporation from grain boundaries and other dislocations.

It was decided, therefore, to carry out the reverse of their procedure and to evaporate on to the crystal a deposit of sodium chloride, then examine it microscopically before and after heating the crystal plus deposit. From the observations of Yamaguti (43), who noted that when sodium chloride was evaporated on to a single crystal face the crystallites tended to form continuations of the underlying layers, it would appear probable that the grain boundaries

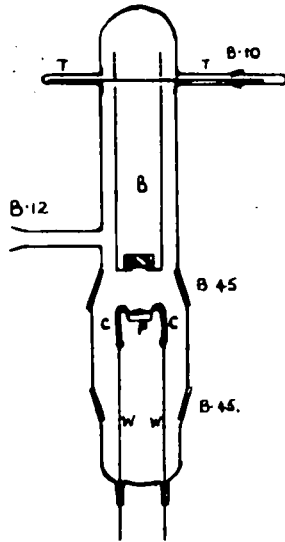


Fig. 41. The evaporation vessel.

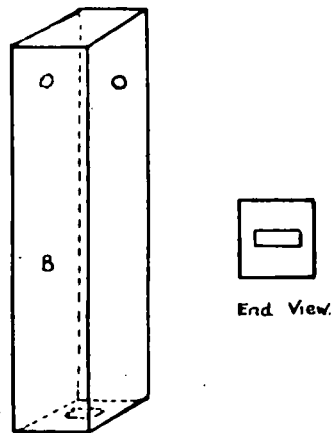


Fig. 42. The crystal container.

and dislocations at the crystal surface might show up on microscopic examination, after heat treatment of the crystal.

6.2. THE EVAPORATION VESSEL.

The vessel in which sodium chloride was to be evaporated on to the crystal surfaces is shown in Fig. 41. It was constructed of Pyrex glass and could be attached to the main vacuum line through the B.12 socket. The crystal was housed in a rectangular brass box, B, 1 in. square by 6 in. in length, whose base had an aperture drilled in it, Fig. 42. The box mounting shielded the crystal against evaporation of sodium chloride on to all the surfaces and the aperture in the base of the box allowed well defined deposits of any shape to be made on any desired face of the crystal. The shape of the aperture depended on the type of measurement to be made; a box with a circular aperture (1 cm. in diameter) in the base was used when evaporations were made for bulk diffusion measurements, while a rectangular aperture (1.5 cm. x .2 cm.) was used in the case of surface diffusion measurements. The box was suspended by a brass rod which passed through the B.10 joint, the two holes in opposite sides of the open upper end of the box and into the side tube, T. This upper vessel, containing the crystal holder, was connected to the lower vessel, containing the evaporation apparatus, by a B.45 cone and socket joint.

The evaporation of the sodium chloride took place from a small platinum boat, P, 2.5 cm. in length and .7 cm. wide,

the ends of which were fitted into slots in the ends of two thick copper wires, C, and these slots were closed onto the platinum by hammering. The copper leads were silver-soldered to two tungsten leads, W, which were sealed into the two limbs in the bottom of the vessel. This vessel was constructed in two parts so that there was easy access to the platinum boat. The heating current was supplied to the leads from the mains through a variac and a step-up transformer. The joints were lubricated with Dow Corning silicone grease, which is stable up to temperatures of 225°C , and the apparatus fitted together. When in position the platinum boat was approximately 1 cm. from the aperture in the box.

6.3. THE EVAPORATION TECHNIQUE.

A freshly cleaved crystal slice was placed in the box and about 50 mgms of dry sodium chloride were placed in the platinum boat. The evaporation vessel was assembled and the vessel connected to the vacuum line. When the pressure vessel reached sticking vacuum, the heating current was switched on and the boat maintained at a temperature of approximately 200°C for fifteen minutes to remove any moisture present, after which the temperature was gradually raised to red-heat over a period of fifteen minutes. The current was then switched off and the vessel brought down to atmospheric pressure. After removal of the crystal from the apparatus it was found to have on it a

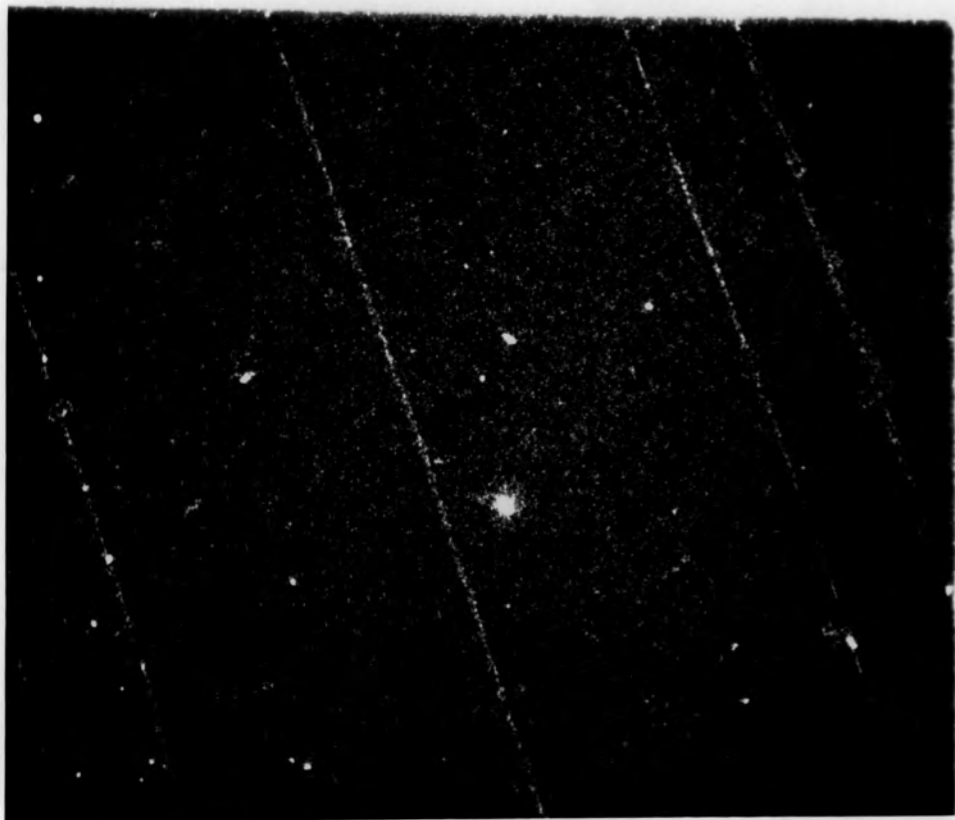


Plate E. Evaporated film on glass.

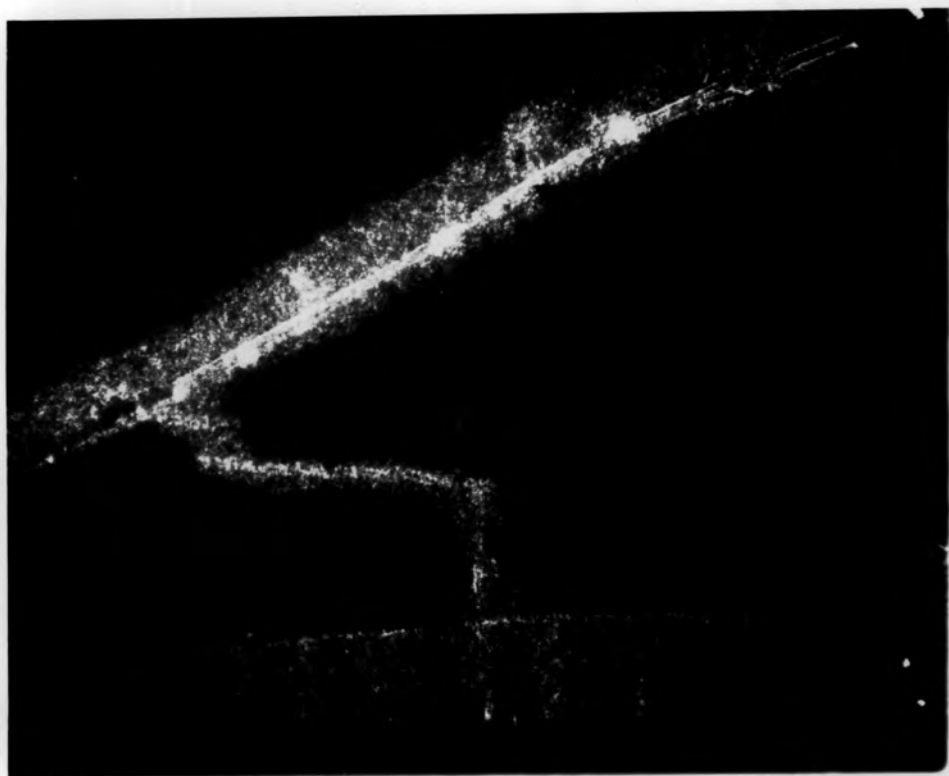


Plate F. Evaporated film on mica.

clearly defined deposit, which weighed about 20 mgms. The remainder of the sodium chloride, in the case of active depositions, was recovered by washing the vessel with distilled water and evaporating the washings to dryness.

The strength of the active sodium chloride used in the evaporations was 5×10^{-5} mc. per mgm.

6.4. THE RESULTS.

The crystals were treated as described in the previous section and then viewed under a microscope with 60 x magnification. Only a very few crystals showed a surface pattern immediately after the deposition but if the crystals with their deposits were then heated at 400° - 450° C in air for forty-eight hours, surface markings became visible on nearly all the crystals. These patterns were photographed with a 75 x magnification.

The patterns produced have been shown to be a function of the substrate and not the deposit by carrying out the evaporations on glass and mica surfaces. After diffusion the deposits were viewed under a microscope and showed no surface pattern (Plates E and F).

A typical pattern produced in the deposit on a sodium chloride crystal after six hours heating at 400° C is shown in Plate A.

A series of experiments on the same single crystal have been carried out to determine the effect of chilling the crystal in liquid nitrogen. Plate B shows the surface pattern



Plate A.



Plate B.

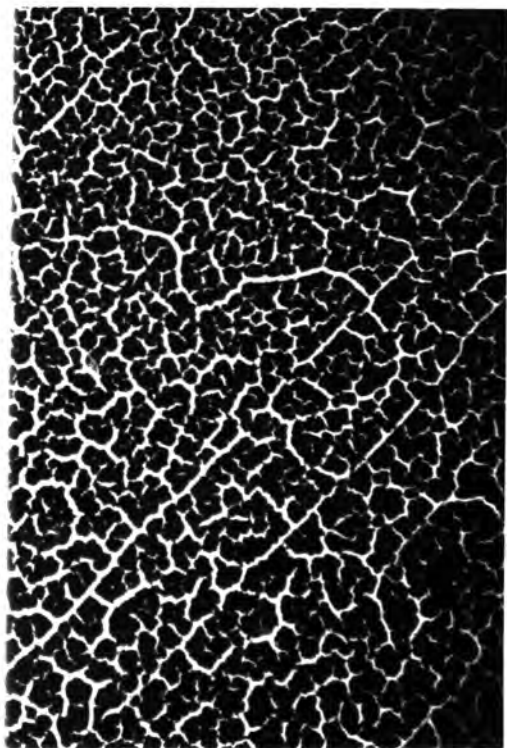


Plate C.

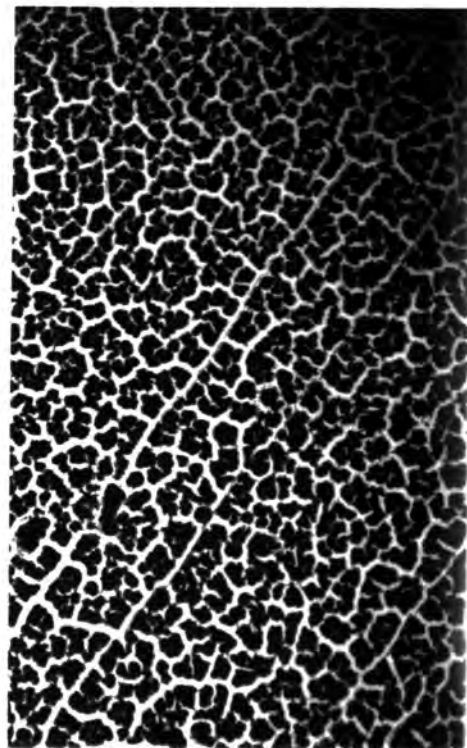


Plate D.

of the untreated crystal produced by heating the crystal, with its deposit, for six hours at 400°C . The same crystal was then chilled in liquid nitrogen and a new face obtained by cleaving, so that the effect of this treatment in the centre of the crystal could be observed. A deposit of sodium chloride was then evaporated on to this freshly cleaved face and the crystal heated at 400°C for six hours. The appearance of the deposit is shown in Plate C. The crystal was then heated for a further six hours at 400°C and the deposit again viewed, Plate D.

The results of these investigations show that the pattern produced in the deposit is a property of the crystal surface and appears to show the mosaic structure of the crystals. The area of these crystallites in the untreated crystal vary from $2.4 \times 10^{-4} \text{ cm.}^2$ to $3.2 \times 10^{-5} \text{ cm.}^2$. On chilling, these crystallites are further subdivided producing more boundaries in the crystal. The average area of the crystallites in the chilled specimen is $8 \times 10^{-6} \text{ cm.}^2$. Further heating of the crystal does not appear to have any effect on the number of boundaries.

CHAPTER 7.

AUTORADIOGRAPHIC STUDIES OF DIFFUSION IN
SINGLE CRYSTALS OF SODIUM CHLORIDE.

7. AUTORADIOGRAPHIC STUDIES OF DIFFUSION IN SINGLE CRYSTALS OF SODIUM CHLORIDE.

7.1. INTRODUCTION.

The investigations on the effect of fine structure on diffusion in single crystals of sodium chloride have been described in Chapter 4. In these experiments, crystal pieces of the same single crystal have been subjected to a series of heat treatments designed to alter the size of the mosaics without freezing in vacancies in the crystal, and then the self-diffusion coefficient of sodium in them measured. These treatments would be expected to alter the diffusion rates if there was grain boundary diffusion in the crystals, since this type of diffusion is usually more rapid than bulk diffusion. A series of measurements have also been made to determine the surface diffusion coefficient of sodium on these crystals in order that an estimate could be made of the rate of grain boundary diffusion.

However, the only satisfactory way to detect grain boundary diffusion in the crystal, provided it proceeds at a different rate to bulk diffusion, would be by autoradiography of sections of the crystal, through which diffusion has taken place.

7.2. DETAILS OF THE AUTORADIOGRAPHY TECHNIQUE.

a) Outline of the Method.

A circular deposit of active sodium chloride, labelled with sodium-22, was evaporated on to a freshly cleaved

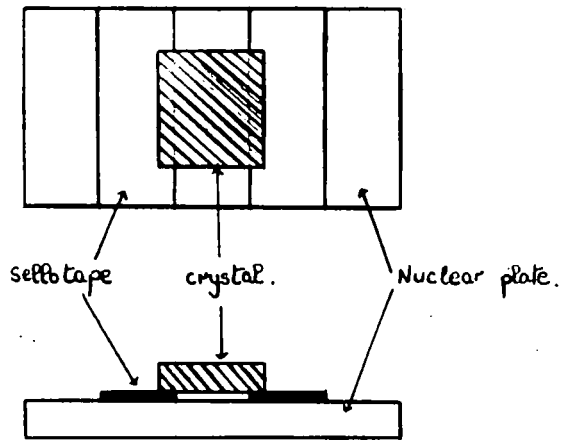


Fig. 43. The nuclear plate arrangement.

surface of a single crystal, 2 cm. x 2 cm. x .2 cm. in size. The crystal was then sealed in a pyrex tube under a pressure of one atmosphere of oxygen-free nitrogen and placed in a temperature controlled furnace. After allowing diffusion to take place for a known time the crystal was removed and cooled to room temperature. The procedure is fully described in section 4c of Chapter 4.

The active crystal face was counted with a Geiger counter to estimate a suitable exposure time and the active face then exposed to the nuclear plate as in Fig. 43. After development, the plate was examined under a microscope with a 450 x magnification. The plate showed a continuous blackening so the upper surface of the active face was removed by grinding and another exposure taken. The process of grinding the face, then exposing to a nuclear plate and after development viewing under the microscope was continued until all the activity was removed from the crystal. Great care was taken in the later stages of grinding because the crystals were easily damaged.

If the grain boundary diffusion was more rapid than bulk diffusion, a point would be reached in the removal of thin layers of the crystal, where the depth of crystal penetrated by the volume diffusion mechanism would have been ground away so that only the activity in the grain boundary would be left. On exposure and subsequent development of the plate the grain boundaries would be

expected to show up as areas of concentrated electron tracks giving a type of mosaic pattern, though it would obviously not be as distinct a pattern as those obtained by other methods, because of the scattering of the β^+ particles in the nuclear emulsion.

7.3. THE EXPOSURE AND DEVELOPMENT OF THE NUCLEAR PLATES.

The plates used in these experiments were ILFORD G.5 nuclear plates, which were glass-backed and had an emulsion thickness of 50μ . The plates were stored in lead castles until required, but could only be used for about six weeks after their manufacture.

The active face of the crystal was counted and then laid active face down on the plate. Direct contact between the crystal and the emulsion, produced pressure markings and these were eliminated by having the crystal edges resting on narrow strips of Sellotape, which adhered to the plate, Fig. 43. Trial experiments were carried out to find a suitable exposure time and it was found that with an activity of 1300 counts per minute, seven hours exposure was needed. The necessary exposure time for each crystal could then be calculated from this data by simple proportion. The crystal was exposed for the calculated time in a darkened desiccated box, surrounded by lead blocks.

After exposure, the plate was developed by immersing in ID-19 developer for thirty minutes and then transferred

to a solution of 30 per cent strength acid fixer. The fixing usually took ninety minutes and when this was completed, the fixer was gradually diluted down to 0.25 per cent over a period of four hours, then the plate was washed with water for thirty minutes. The development was, of course, carried out in a dark room as these plates were light sensitive.

7.4. THE GRINDING OF THE CRYSTALS.

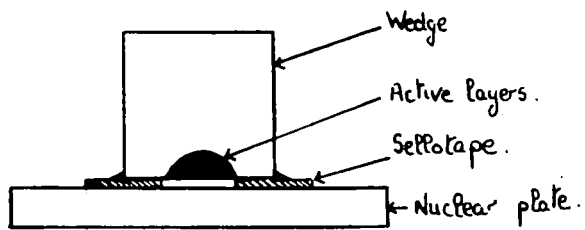
The crystals were ground on a glass plate using liquid paraffin as the lubricant. The abrasives used were carborundum and "Sira" powder, which was obtainable from the United Kingdom Optical Company. The former was used for the coarse grinding and the latter for taking off very fine layers of the crystal in the later stages. After grinding, the crystals were cleaned with tissue paper.

7.5. THE SENSITIVITY OF THE METHOD.

β -particles coming from a point source of radioactive matter emerge in all directions and are randomly scattered in an absorbing medium such as an emulsion. There must necessarily be a limit to how close two radioactive point sources can be without their images becoming indistinguishable from one another on a nuclear plate. A series of experiments were therefore carried out to determine the limits of proximity of two radioactive sources for resolution on a nuclear plate.

This was carried out by painting a layer of sodium

Side View.



End View.

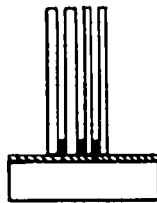


Fig. 44. The wedge.

chloride, labelled with sodium-22 on to one side of a number of microscope cover slips of varying thicknesses, and evaporating these sodium chloride layers to dryness. The slips were then glued together to form a wedge, each radioactive layer being separated from the next by the thickness of the cover slip. Any collimating effect of the wedge was removed by rubbing the edges down with sandpaper until active sodium could be detected at the edges, Fig. 44.

The wedge was then placed edge down on the plate but kept from contact with the plate by two strips of Sellotape at the ends, Fig. 44. The wedge was maintained in place by having the ends waxed to the Sellotape. After exposing for a suitable time, the plate was developed and fixed as previously described.

The result of the experiment is shown in plate G (75 x magnification). The sources, A and B, were separated by a cover slip of thickness $400\ \mu$, while B and C were separated by $200\ \mu$. As can be seen from the plate G it is just possible to distinguish two active sources separated by a distance of $200\ \mu$.

The method therefore will only be able to detect grain boundary diffusion, provided it is more rapid than bulk diffusion, if the grain boundaries are more than $200\ \mu$ apart.

7.6. THE RESULTS.

The autoradiography studies have been carried out on crystals 4, 5A and 5B, which were used in the diffusion experiments.

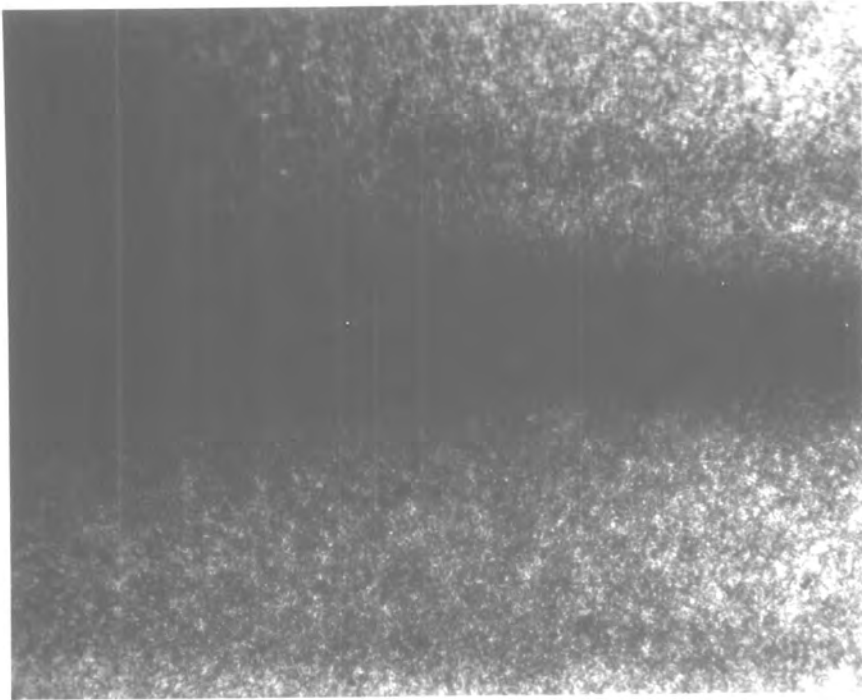


Figure 1. Micrograph showing granular texture.

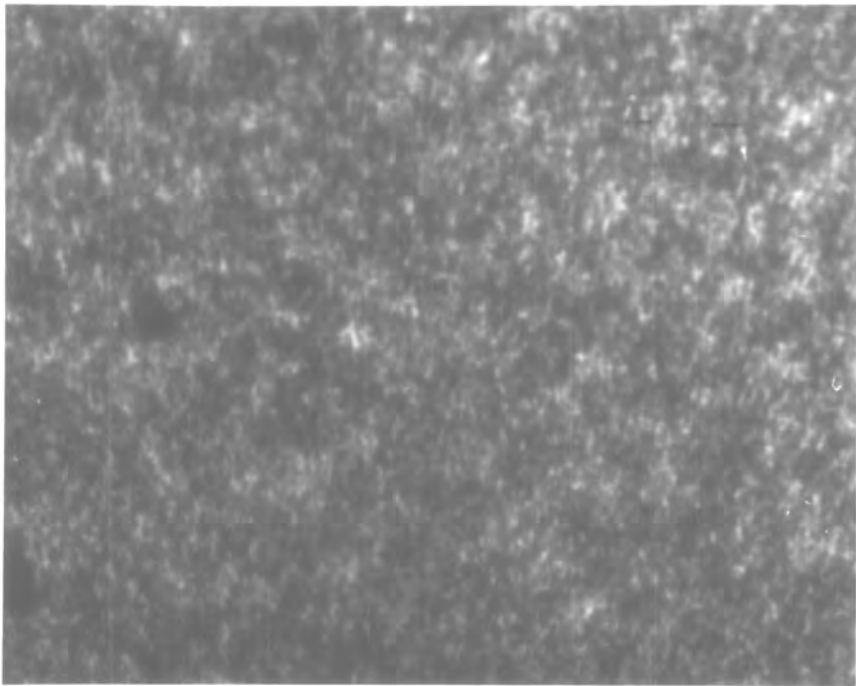


Figure 2. Micrograph showing granular texture.

In the experiments on crystal 4 and 5A, the grinding has been carried out from the face on which the active deposit was evaporated. Exposures were taken of the ground face when the activity detected at this face was 1000, 800, 600, 400, 200, and 100 counts per minute.

The plates when viewed under a microscope, with a 450x magnification, did not show any indications of grain boundary diffusion. Photographs are shown of the plates obtained by exposing the ground face of crystal 4, when its activity was 100 counts per minute (Plate H) and the ground face of crystal 5A, when its activity was 200 counts per minute (Plate I). In these photographs the plates have been magnified 75 times. As can be seen from these photographs there is no definite evidence of selective diffusion in grain boundaries.

In the experiment on crystal 5B, the face, opposite to the one on which the active deposit was evaporated, has been removed by grinding. Exposures were taken of the ground face when the activity detected at this face was 300, 500, 700 counts per minute. No evidence of any grain boundary diffusion was shown when the plates were viewed under a microscope with a 450x magnification. The plate obtained by exposing the ground face of crystal 5B, when its activity was 500 counts per minute is shown in Plate J (75x magnification).

It has been observed by examination of the plates, that there was no increase in the area of the active deposit after

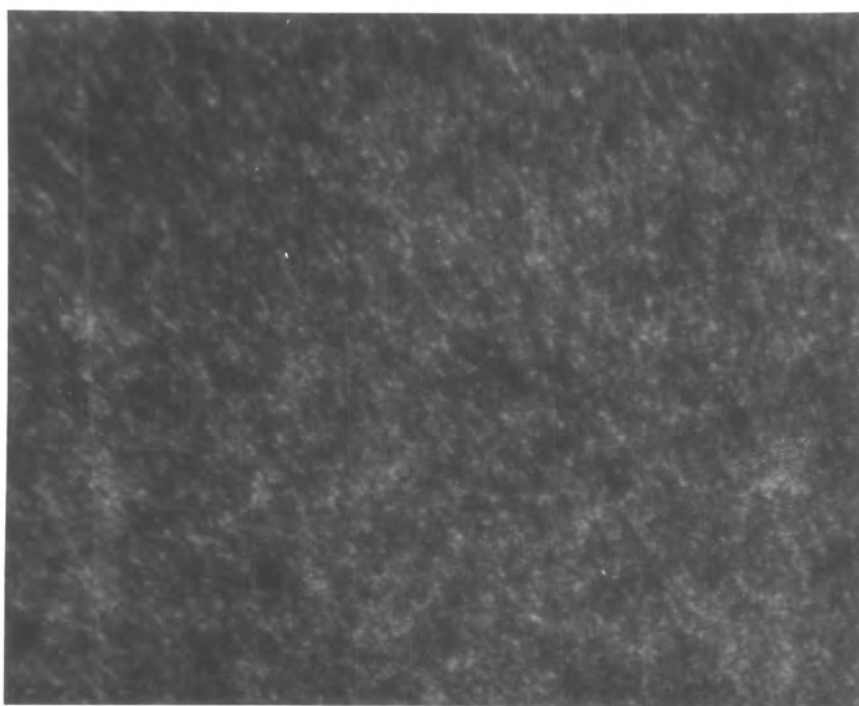


Plate I. Autoradiograph of crystal 5A.

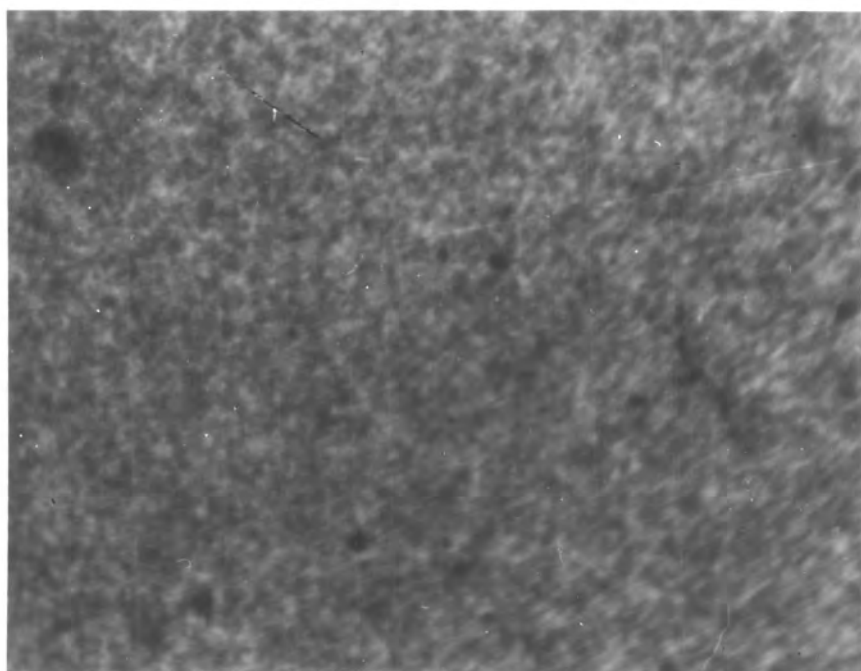


Plate J. Autoradiograph of crystal 5B.

grinding so that it can be assumed that the grinding does not spread activity over the crystal face. It should have been possible, therefore, to have detected grain boundary diffusion, provided the distance between these boundaries was greater than 200μ and provided the grain boundary diffusion was more rapid than the volume diffusion.

These results will be discussed in a later chapter.

CHAPTER 8.

THE DISCUSSION OF RESULTS.

8.

THE DISCUSSION OF RESULTS.

The aim of the work described in this thesis was the investigation of the effect of changes in crystal fine structure on the self-diffusion and conductivity in pieces of the same single crystal of sodium chloride. These changes were to be brought about by firstly, annealing the crystal pieces at 600°C and secondly, cooling other pieces rapidly in liquid nitrogen from room temperature to -195°C . This latter process would not be expected to "freeze in" vacancies in the crystal.

Two points of view with regard to the changes that would be expected in the self-diffusion and conductivity by this type of treatment will now be presented.

8.1. THE MOSAIC BLOCK THEORY.

It is generally observed that the energy of activation for surface diffusion processes is less than that for grain boundary diffusion, which is in turn less than that for bulk diffusion. If this is true of diffusion in sodium chloride, then the changes in fine structure brought about by the heat treatments would make themselves evident in changes in the apparent bulk diffusion coefficient: these structure changes would alter the amount of grain boundary and surface diffusion in the crystal. The same conclusions are true of conductivity, which is in fact, the diffusion of ions in the crystal under an applied electric field. Chilling the crystal,

which should lead to an increase in the number of grain boundaries in the crystal, would be expected to lead to an increase in the self-diffusion and conductivity. The reverse effects would be expected on annealing the crystal since this would tend to increase the perfection of the crystal structure.

Reddington has observed some of these effects in his measurements of the diffusion of barium in barium oxide crystals(44). He has found that quenching of the crystal from about 1475°K increases the barium ion self-diffusion rate while annealing of the crystal from this temperature reduced this self-diffusion rate.

8.2. THE THEORY OF SEITZ.

Seitz (45), on the other hand, has proposed an entirely different concept to interpret the results of Cunnell and Schneider (30), who have measured the effect of quenching from a high temperature on the conductivity of alkali halide crystals. They observed that the conductivity was lower in specimens which were cooled from 750°C to room temperature over a period of 36 hours than in "normally" treated specimens. They have, however, found that the conductivity was the lowest of all in the quenched crystals i.e. those cooled down from 750°C to room temperature by removing them from the furnace and leaving them to cool in air.

These results have been explained by Seitz who proposed that the quenching process was not rapid enough to retain

the vacancies generated in the non-structure sensitive range. Only those vacancies associated with the multivalent ions in the crystal were retained. The quenched specimens contained quenching strains and, therefore, possessed dislocations which might trap some of the positive vacancies, hence lowering the conductivity and the self-diffusion rate.

Seitz has speculated on the effect of annealing on the crystal conductivity: he thinks that on annealing it is possible that some of the impurities and the vacancies associated with them "precipitate" so that they no longer contribute to the conductivity. The conductivity should therefore be lower than in the untreated specimen.

One result of Seitz's concept would be that annealing would not lower the self-diffusion coefficient because the intervalent ion-vacancy complex still allows the vacancy to contribute to the diffusion process.

The views expressed above, therefore, are in complete disagreement with one another as far as quenching is concerned but they agree on the effect of annealing on the crystal conductivity.

8.3. THE RESULTS OF THE PRESENT WORK.

The results of the work for this thesis might be expected to produce evidence in favour of one or other of these concepts. A summary of the results obtained and the conclusions drawn from these observations are given below.

a) The study of the surface patterns produced by evaporation



- shows that chilling of the crystal specimens in liquid nitrogen leads to an increase in the number of boundaries at the surface. It is very probably that these boundaries extend into the crystal, as has been shown by the theoretical calculations of Lennard-Jones (22).
- b) The results of the surface diffusion investigation indicate that, at the temperature of 506°C , if there is any surface diffusion at all, it cannot proceed at a faster rate than ten times the bulk diffusion. It is, therefore, very probable that the rate of grain boundary diffusion is not larger than ten times the volume diffusion rate, if indeed it is any more rapid.
- c) The results of the autoradiography show that it is unlikely that grain boundary diffusion proceeds at a faster rate than the volume diffusion. This method is limited to a crystal in which the grain boundaries are more than 200μ apart. When comparison is made with the crystallite sizes obtained from the evaporation studies, it would appear, however, that grain boundary diffusion should be detected by autoradiography if it does proceed at more rapid rate than bulk diffusion.
- d) The changes of the diffusion rate with chilling and annealing shows that the self-diffusion coefficient is increased by both treatments. It has also been observed that the diffusion rate increases with length of heating.
- e) The conductivity measurements show that the conductivity

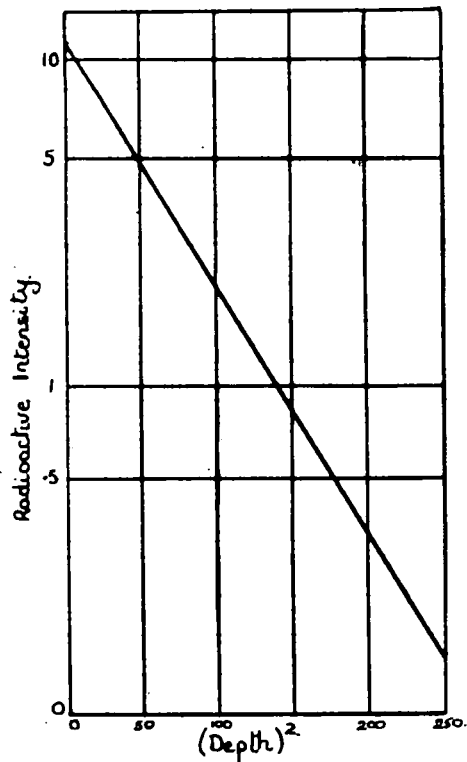


Fig. 45. Distribution of activity in the crystal.

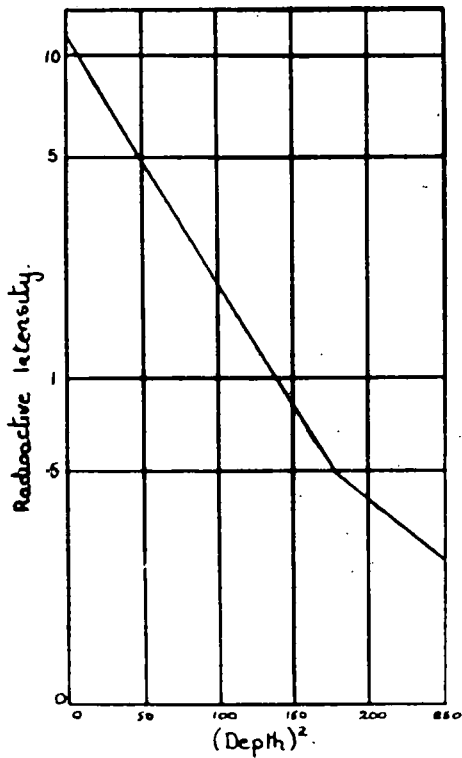


Fig. 46. Distribution of activity due to bulk and grain boundary diffusion.

of a crystal specimen is increased by annealing in two of the three specimens examined. This increase in conductivity is dependent on the length of annealing.

The chilling of the crystal in liquid nitrogen has also increased the conductivity in two out of the three specimens, on which measurements were made.

The third specimen, which has given anomalous results, has already been discussed in section 9 of Chapter 3.

8.4. COMPARISON OF THE RESULTS WITH OTHER WORKERS.

a) Diffusion.

It is possible to examine Mapother, Crooks and Maurer's work (1) on volume diffusion and draw some conclusions about grain boundary diffusion. When this is done, the results are in complete agreement with the present work. Their method of investigation, although it is subject to the disadvantages of possible loss of material during microtoming, has the advantage that it should be able to show this grain boundary diffusion if it proceeded at a different rate to the volume diffusion. They have calculated the diffusion coefficient from the equation: $C = \frac{C_0}{(\pi Dt)^{1/2}} e^{-x^2/4Dt}$ (Eqn. 5) by plotting $\log. C$ against x^2 , Fig. 45. If grain boundary diffusion did take place at a faster rate than volume diffusion, then this graph would be expected to have a "tail" (Fig. 46) due to this extra penetration by grain boundary diffusion. No evidence of this is shown in their work and, in this way, it agrees with the present work.

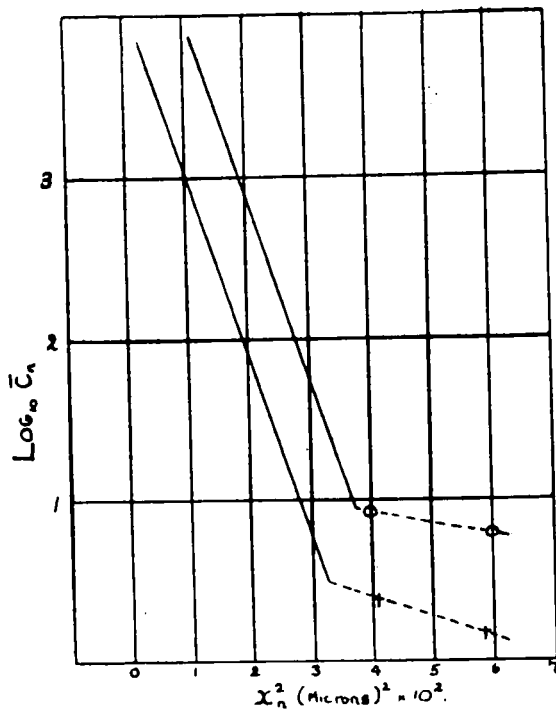


Fig. 47. Low temperature diffusion measurements of Schamp and Katz.

The results also agree with those of Laurent and Bénard (46) who have shown that the self-diffusion coefficient of sodium in sodium chloride crystals is independent of the number of grain boundaries. They have measured the self-diffusion of sodium in single crystals and in polycrystals, whose grain sizes varied from 50μ to 3000μ , of sodium chloride. The self-diffusion coefficient was found to be the same in all cases, thus showing that grain boundary diffusion must proceed at the same rate, or less than that of bulk diffusion.

In contrast to this situation for cation mobility there may, however, be evidence of grain boundary diffusion of the anion in sodium bromide crystals. It can be observed in a close examination of the results of Schamp and Katz (3), although the authors do not mention it, that for the bromide ion diffusion in single crystals of sodium bromide, in the low temperature range, the graph of $\log. C$ versus $(\text{depth})^2$ has a tail, Fig.47. This may be due to grain boundary diffusion proceeding at a more rapid rate than bulk diffusion.

Further evidence of anion diffusion in sodium halide crystals has come from the work of Laurent and Bénard (46) in their experiments on the chloride ion diffusion in single and polycrystals of sodium chloride. They have found that the chloride ion diffusion in single crystals is more rapid than in polycrystals and it is slowest in the polycrystal which has the smallest grain size. This, in fact, points to the grain boundary diffusion being slower than bulk diffusion.

b) Conductivity.

The conductivity results do not agree with the observations of Etzel and Maurer (4), who have found that the conductivity of the "pure" sodium chloride crystals was not affected by annealing or by quenching. Schneider and Cunnell (30), on the other hand, have shown that quenching of the pure sodium chloride crystals reduced their conductivity as described in an earlier section of this chapter.

Comparison of the present conductivity results with those of other workers, whose conductivity measurements are described above, shows that the results of the present work are in complete disagreement with regard to the effect of annealing of the crystals, while no results have been previously reported of the effect of chilling the crystals in liquid nitrogen.

8.5. COMPARISON OF THE RESULTS WITH THE PREVIOUS THEORIES.

The results of the present work cannot be reconciled with either of the theories discussed earlier in this chapter. Considering the simple mosaic theory, an increase in the self-diffusion coefficient and the conductivity would be expected on chilling the crystal in liquid nitrogen. Annealing the crystal, however, should lead to a decrease in the self-diffusion coefficient and the conductivity, which is the converse of the experimental observations. This theory must, therefore, be discarded.

It is also impossible to interpret this increase in the self-diffusion coefficient and the conductivity both on

annealing and chilling the crystal with the theory proposed by Seitz (45). In this theory, the effect of annealing would be expected to lead to a decrease in the conductivity while the self-diffusion coefficient should be unchanged. Chilling of the crystal in liquid nitrogen would be expected to decrease both the conductivity and the self-diffusion coefficient.

Before any new hypothesis is offered to explain these results, it seems worthwhile to digress from the main theme to consider the important effects of altermvalent ions on the conductivity and self-diffusion in chilled and annealed crystal specimens.

8.6. THE PRESENCE OF ALTERVALENT IONS IN THE CRYSTAL.

A series of experiments have also been carried out on the effect of annealing and quenching on crystals of sodium chloride containing added divalent impurities. Etzel and Maurer (4) have shown that the conductivity of sodium chloride crystals containing added cadmium impurity was reduced on annealing at temperatures above 400°C. This reduction increased with time but they have been able to show that a least part of this reduction was due to the electrodes which were applied to the crystal before annealing. They also observed that the conductivity of the quenched crystals was higher than that of

the crystals which were cooled slowly. These results have been confirmed by Goodfellow (29) with measurements on single crystals of sodium chloride containing added manganese impurity.

These results have been explained by Schneider and Caffyn's recent theory (47). They propose that on annealing, the divalent impurity forms aggregates or clusters near or at the internal boundaries. These impurity ions will be associated with some positive ion vacancies and the impurity aggregates may trap some unassociated vacancies, thus reducing the conductivity. On further heating, followed by quenching, a more uniform distribution of the impurity would be obtained and some of the positive ion vacancies, previously trapped at the internal boundaries, would be freed. This would lead to an increase in the conductivity.

When this theory is applied to the self-diffusion, it would be expected that there would be a decrease in the self-diffusion on annealing due to this trapping of some of the positive ion vacancies, while quenching of the crystal should lead to an increase in the self-diffusion coefficient.

It is concluded from this discussion, that attention must be given to the effects of altermvalent impurity ions in the crystal when the crystal is annealed or quenched. Since a spectroscopic examination of the "pure" crystals (Chapter 2), revealed an impurity content of approximately .001 per cent, any interpretation of the annealing or

quenching would be expected to incorporate this impurity effect. This will be discussed in the next section.

8.7. INTERPRETATION OF THE PRESENT WORK.

The results which have been obtained in the present work cannot be explained in terms of the existing theories and so another concept is now tentatively suggested to explain both the conductivity and the diffusion results.

It has previously been observed (1) that "pure" sodium chloride crystals contain a small amount of divalent ions present as impurities. Cottrell (48) has previously pointed out that foreign atoms in a solid solution distort the crystal locally and so there would be a certain amount of strain in a single crystal of sodium chloride due to these impurity ions. Furthermore strain will be produced in these crystals during the growing process and the short time of annealing after the growing will probably not relieve this strain to any appreciable extent.

This distortion of the crystal because of strain would probably partially inhibit the movement of vacancies and ions in the crystal, and so if by some treatment this strain is relieved then the mobility of the vacancies would probably increase. It seems not unreasonable to suggest that either annealing or a moderate shock treatment might have this effect.

Experiments on the evaporation patterns on the crystal faces has shown that the chilling of the crystal in liquid nitrogen does in fact lead to an increase in boundaries.

These boundaries would probably be formed at the points of distortion in the lattice so reducing the strain in the crystal. This would release some vacancies trapped by the distortion and would increase the mobility of the vacancies in the area of the distortion. The self-diffusion and the conductivity would therefore be expected to increase on chilling and this is in fact what has been experimentally observed.

Annealing of the crystal would also be expected to reduce the strain in the crystal. This is also demonstrated by the difficulty in cleaving a crystal which has not been annealed for any length of time.

One possible view of this reduction of the strain on annealing is that the divalent impurity ions would diffuse rapidly towards, and some would reach, the grain boundaries in the crystal and so reduce the distortion. This is very probable for as Mapother, Crooks and Maurer (1) have shown the diffusion rate of the divalent cations is several hundred times that of the sodium ion. The heating of the crystal at 600°C would also break up some of the impurity ion-vacancy complexes. Lidiard (49), on a theoretical basis has shown that dissociation of the complexes occurs fairly rapidly with increase in temperature when the divalent impurity ion concentration is not greater than .01 per cent. It is possible that the rate of cooling after annealing is too rapid to allow all of the divalent ions, which were previously present as complexes, to reassociate with positive ion vacancies.

These extra vacancies would therefore increase the conductivity, although they would have no effect on the diffusion rate since they already contribute to the diffusion when they are associated with the divalent impurity ion. However the reduction of the strain in the crystal due to the diffusion of the impurity ions to the grain boundaries would increase both the conductivity and the self-diffusion.

Evidence in favour of these proposals has come from the comparison of the directly measured self-diffusion coefficient and that calculated from the conductivity measurements by use of the Nernst-Einstein relationship (Eqn.1). The ratio of D_{observed} to $D_{\text{calculated}}$ was 2.29, 1.59 and 1.29 for the untreated slice, the slice cooled in liquid nitrogen, and the slice annealed for $254\frac{1}{2}$ hours at 620°C respectively. This discrepancy between D_{observed} and $D_{\text{calculated}}$ * may be due to the presence in the crystal of divalent impurity-vacancy complexes, which contribute to the diffusion but not to the conductivity. These results therefore show that both chilling and annealing of the crystal decreases the impurity ion-vacancy complex contribution to the diffusion.

The effect of the lowering of the conductivity with quenching in the "pure" sodium chloride crystals, observed by Cunnell and Schneider (30), could therefore be explained

* It should be pointed out, however, that other explanations have been given for the discrepancies between D_{observed} and $D_{\text{calculated}}$ (50, 51).

by assuming that this quenching process would set up quenching strains in the crystal. These strains would then probably reduce the mobility of the vacancies, hence reducing the conductivity and the diffusion. The cooling of the crystals at a slower rate would be expected to cause less strain in the crystal and so the conductivity and diffusion would be higher than for the quenched crystal.

It is difficult to account for the results of the annealing and quenching of single crystals, containing added divalent impurities, on this concept. One possible explanation is that, since these crystals contain of the order of 0.1 per cent divalent impurity, the annealing process would not reduce the strain in the crystal because it is very likely that clusters of the impurity form at the grain boundaries and these would be of such a size that they would introduce strains in the neighbouring crystallites. As Schneider and Caffyn (47) have suggested, a certain number of unassociated positive vacancies may be trapped in these clusters so reducing the conductivity. Also, on the basis of the views of Lidiard (49), because of the higher impurity content, the heating might not be expected to break up the impurity ion-vacancy complexes

The quenching of the crystal would produce a more uniform distribution of the impurity. This redistribution should decrease the strain in the crystal but it would be countered by the quenching strains which would also be

produced. Since it is experimentally observed that quenching increases the crystal conductivity, it must be assumed that the overall strain in the crystal is reduced.

8.8. SURFACE DIFFUSION AND GRAIN BOUNDARY DIFFUSION.

The results of the surface diffusion and autoradiography experiments indicate that the order of magnitude of the rates of surface diffusion, if it does take place, and grain boundary diffusion are approximately of the same order as the volume diffusion. This estimate is in agreement with the views of Roberts (52), though Gyulai (53) has found some evidence of surface mobility in sodium chloride crystals grown from the vapour. Laurent and Bénard (46) have also shown that grain boundary and volume diffusion are of the same order.

These results for surface migration, and grain boundary diffusion are in marked contrast to that reported for the diffusion of active barium in and on barium oxide crystals (44) and for the diffusion in and on metals. Langmuir (54), for example, has reported that in the case of diffusion of thorium in and on crystals of tungsten, the surface diffusion was more rapid than grain boundary diffusion, which was more rapid than volume diffusion. Hoffman and Turnbull (55) have also reported a grain boundary diffusion for silver in silver crystals 10^6 times as great as the bulk diffusion, while the surface diffusion at this temperature has been shown to be of the same order as the grain boundary diffusion (56).

Winegard and Chalmers (56), who have carried out these surface diffusion measurements of silver on silver crystals, have

proposed that both the surface diffusion and the grain boundary diffusion proceed by a vacancy mechanism. They account for the increased rate of surface and grain boundary diffusion by assuming there is a greater concentration of vacancies at this surface and grain boundaries.

The lack of surface mobility on cleaved surfaces of sodium chloride crystals is surprising because experiments on the specular reflection of helium from these surfaces (57) indicate a smooth surface with a "roughness" of only 1\AA . The surface mobility should therefore not be inhibited by steps on the crystal face.

De Boer (58), in a series of calculations, has shown that there is a very small difference in absorption energies for sodium ions on top of chloride ions (23.1 K.cals/mole) and in the centre of the lattice (26.0 K.cals/mole) and so facile migration might have been expected. However, the calculations also indicate that the corner and the edges will have higher heats of absorption and, therefore, act as traps for surface mobile ions. It may be that the presence of steps in the crystal surface, which are not detectable by the specular reflection of helium, do act as inhibitors of surface movement.

Another possible explanation is that the surface migration does take place by a vacancy mechanism (c.f. silver on silver crystals), but because the crystal slices used in the present work were taken from the centre of a single

crystal, there would be no increased concentration of vacancies at these cleaved faces. The rate of surface diffusion would be expected to be of the same order as the bulk diffusion.

It is therefore concluded that for sodium chloride crystals, although the grain boundaries and dislocations in a crystal do affect the self-diffusion and conductivity, actual migration along these grain boundaries, and on the crystal surface, makes no significant contribution to the diffusion. This situation should be compared with that for metals in which grain boundary and surface diffusion are of considerable importance.

8.9. FUTURE WORK.

The hypothesis presented in this chapter could be tested by measurement of the self-diffusion of sodium in quenched specimens of sodium chloride crystals and also by an investigation of the effects of annealing, quenching, and chilling in liquid nitrogen on the self-diffusion of sodium in single crystals containing added divalent impurity. Also the surface diffusion measurements have been only able to determine an upper limit for the surface diffusion coefficient and so a more accurate method of measurement is required. It would seem probable that an autoradiographic technique might be suitable for this.

It is felt that a further investigation is required into the dependability of various electrode coatings for the conductivity measurements. The effect of the various

coatings on the crystal conductivity on annealing should also be studied, since Etzel and Maurer (4) have shown that the conductivity of a crystal, containing added divalent impurity, is reduced by annealing for periods of one hour or less. It would seem probable therefore that the conductivity would depend on the length of heating time during a conductivity run and a more careful study of this is required.

Furthermore, it would be most interesting to study the effect of the addition of divalent negative impurities to the crystal on the conductivity and the anion self-diffusion. Morrison (59), who has very kindly allowed us a preview of a paper soon to be published, points out that there is a possibility of a vacancy pair mechanism for the anion self-diffusion in sodium chloride.

In view of the observations on the effect of annealing and quenching on the crystal conductivity and self-diffusion, it would seem advisable, that in all future work on the sodium chloride crystals, a standard growing and annealing procedure should be used. A more accurate comparison could then be made of the results of different workers.

CHAPTER 9.

THE APPENDIX.

9.

THE APPENDIX.9.1. THE LABELLING OF SODIUM.

a) Both radioactive isotopes of sodium have been used in these experiments; they were sodium-24, (a $\beta^- + \gamma$ emitter with a β^- -particle energy of 1.38 MeV and a half-life of 14.8 hours) and sodium-22 (a $\beta^+ + \gamma$ emitter with a β^+ -particle energy of .536 MeV and a half-life of 2.6 years).

The sodium-24 was available from the A.E.R.E., Amersham, as solid sodium chloride with an activity of 1 mc./mgm.. This was diluted by adding 1 gm. of inactive sodium chloride. Two samples of sodium-22 were obtained from the A.E.R.E., Amersham, in the form of solutions of sodium chloride with an activity of 0.2 mc./ml.. This was diluted with solid inactive sodium chloride to give an activity of 5×10^{-5} mc/mgm. and the solution evaporated to dryness. Another sample of sodium-22 was obtained from the cyclotron at Birmingham University. The sodium had been produced by deuteron bombardment of a magnesium target and so the active sodium had to be separated from the magnesium. This separation is described in part b) of this section.

b) The Separation of Sodium-22 from the Magnesium Target.

Reagents.

1. Glacial acetic acid - analytical reagent grade.
2. Nitric acid - analytical reagent grade.
3. Uranyl acetate reagent - 20 gms uranyl acetate + 15 ml. glacial acetic acid + water to 250 ml.

4. Ethanol - 95%.
5. Hydrogen peroxide - 100 vol. - M.A.R. grade.
6. Dibutyl phosphate - alkali and acid washed.

Proceédure.

The magnesium target was dissolved in the minimum volume of dilute acetic acid in a 500 ml. flask under reflux.

The whole solution was transferred to a 500 ml. beaker and treated with 200 microgrammes of sodium carrier (added as sodium chloride) and the solution evaporated carefully to remove all excess liquid. The evaporation was carried out under vacuum and no heat was applied to the solution. The crystalline residue was redissolved in the smallest possible volume of redistilled water. 50 ml. of the uranyl acetate reagent (3 above) was well mixed with the solution, followed by 100 ml. of 95% ethanol. The mixture was cooled to below 10°C. in an ice-water bath and stirred with a mechanical stirrer for 30 - 40 minutes. The almost opaque solution was kept overnight at about 20°C. and then yielded a clear solution with a well-crystallised precipitate of the triple acetate.

The precipitate was isolated on a No. 3 porosity sintered glass Gooch crucible, and washed with several small volumes of 95% ethanol, (the filtrate and washings were retained for counting). The precipitate was then dissolved in 0.5 N. nitric acid and the resulting solution evaporated nearly to dryness. The residue was taken up in 10 ml. of 0.5 N nitric

acid, and the bulk of the uranium was precipitated as the peroxide by adding hydrogen peroxide reagent. The uranium peroxide was separated from the sodium-22 solution on a sintered glass Gooch crucible and washed with 0.5 N nitric acid; the filtrate and washings were combined and evaporated to dryness. The residue was dissolved in 5 ml. of 0.5 N nitric acid and this solution, plus 5 ml. of water washings, was shaken with two lots of 2 ml. of dibutyl phosphate reagent (diluted with an equal volume of ether) to remove any remaining uranium. Traces of dibutyl phosphate were removed from the aqueous layer by a final extraction with 10 ml. of ether.

The aqueous layer was evaporated to dryness and then made up to 10 ml. with redistilled water and a little hydrochloric acid to give a pH of 1 - 2. The solution was diluted with solid inactive sodium chloride to give an activity of 5×10^{-5} mc./mgm. and then evaporated to dryness.

9.2 CALCULATION ON THE NERNST-EINSTEIN RELATIONSHIP.

A summary of the results of the comparison of the directly measured self-diffusion coefficient and the self-diffusion coefficient, calculated from the conductivity measurements using the Nernst-Einstein equation, has been given in Chapter 4. The complete calculations are shown below.

The Nernst-Einstein relationship states that,

$$\frac{\sigma}{D} = \frac{Ne^2}{kT}$$

where σ is the conductivity measured in $\text{ohm}^{-1}\text{cm}^{-1}$,

D is the self-diffusion coefficient measured in $\frac{\text{cm}^2}{\text{sec}^{-1}}$.

N is the number of ion pairs per cm^3 ,

e is the electronic charge,

k is the Boltzmann constant in erg.deg^{-1} ,

and T is the absolute temperature in degrees.

The numerical tables give the following values for the constants

$$\text{Avagadro constant} = 6.0249 \times 10^{23} \text{ moles}^{-1}.$$

$$e = 1.602 \times 10^{-20} \text{ e.m.u.}$$

$$k = 1.3804 \times 10^{-16} \text{ erg.deg}^{-1}$$

$$\text{Therefore } N = \frac{\text{Avagadro constant}}{\text{Mol.wt in grams}} \times \text{density} = \frac{6.0249 \times 10^{23}}{58.45} \times 2.165$$

$$= 2.232 \times 10^{22}$$

Since σ is expressed in $\text{Ohm}^{-1} \text{ cm}^{-1}$, the factor 10^9 must be introduced to convert from electromagnetic units.

$$\begin{aligned} \therefore \frac{\sigma}{D} &= 10^9 \frac{Ne^2}{kT} = \frac{10^9 \times 2.232 \times 10^{22} \times (1.602 \times 10^{-20})^2}{1.3804 \times 10^{-16} \times T} \\ &= \frac{4.15 \times 10^7}{T} \end{aligned}$$

Comparisons have been made of the ratio of D_{observed} to $D_{\text{calculated}}$ for crystals 3, 5A, 5B, 5C.

Crystal 3.

$$\sigma \text{ at } 502^\circ\text{C} = 3.428 \times 10^{-6} \text{ ohm}^{-1} \text{ cm}^{-1} \quad (\text{From Fig. 18})$$

$$D \text{ at } 502^\circ\text{C} = 1.26 \times 10^{-10} \text{ cm}^2 \text{ sec}^{-1}$$

$$\frac{\sigma}{D} = \frac{4.15 \times 10^7}{T}$$

$$D = \frac{\sigma \cdot T}{4.15 \times 10^7}$$

$$D_{\text{calculated}} = 6.401 \times 10^{-11} \text{ cm}^2 \text{ sec}^{-1}.$$

Crystal 5A.

$$\sigma \text{ at } 511^{\circ}\text{C} = 1.82 \times 10^{-6} \text{ ohm}^{-1} \text{ cm}^{-1} \quad (\text{From Fig. 20})$$

$$D_{\text{observed}} \text{ at } 511^{\circ}\text{C} = 7.9 \times 10^{-11} \text{ cm}^2 \text{ sec}^{-1}$$

$$D_{\text{calculated}} \text{ at } 511^{\circ}\text{C} = 3.438 \times 10^{-11} \text{ cm}^2 \text{ sec}^{-1}$$

Crystal 5B.

$$\sigma \text{ at } 511^{\circ}\text{C} = 2.884 \times 10^{-6} \text{ ohm}^{-1} \text{ cm}^{-1} \quad (\text{From Fig. 20})$$

$$D_{\text{observed}} \text{ at } 511^{\circ}\text{C} = 8.7 \times 10^{-11} \text{ cm}^2 \text{ sec}^{-1}$$

$$D_{\text{calculated}} \text{ at } 511^{\circ}\text{C} = 5.45 \times 10^{-11} \text{ cm}^2 \text{ sec}^{-1}$$

Crystal 5C.

$$\sigma \text{ at } 511^{\circ}\text{C} = 3.802 \times 10^{-6} \text{ ohm}^{-1} \text{ cm}^{-1} \quad (\text{From Fig. 20})$$

$$D_{\text{observed}} \text{ at } 511^{\circ}\text{C} = 9.28 \times 10^{-11} \text{ cm}^2 \text{ sec}^{-1}$$

$$D_{\text{calculated}} \text{ at } 511^{\circ}\text{C} = 7.183 \times 10^{-11} \text{ cm}^2 \text{ sec}^{-1}$$

REFERENCES

1. Mapother, Crooks and Maurer J.Chem.Phys. 18, 1231,(1950).
2. Morrison et.al. Phil.Mag. Ser.8, 1, 393,(1956).
3. Schamp and Katz. Phys.Rev. 94, No.4,828,(1954).
4. Etzel and Maurer. J.Chem.Phys. 18,1003,(1950).
5. Seitz. Rev.Mod.Phys. 18,No.3,384,(1946)
Rev.Mod.Phys. 26, 7,(1954).
6. Turbandt. Handbuch der Experimental Physik
Vol.II, Part I.
7. Nernst. Z.Physik.Chem. 2, 613,(1888).
8. Einstein. Ann.Physik. 17, 549,(1905).
9. Smekal. Z.Elektrochem. 34,476,(1928):
Handb.Phys.XXIV/2,876,(1933).
10. Jost. Diffusion and Chemische Reaktion
in Festen Stoffen; (Steinkopff,
Dresden 1937). p.77.
11. Koch and Wagner. Z.Phys.Chem. 38B,295,(1937).
12. Hilsch and Pohl. Trans.Faraday.Soc. 34,883,(1938)
13. Amelinckx, Van Der Vorst,
Gevers Dekeyser. Phil.Mag.46, 450,(1955).
14. Humphreys-Owen and Furth. Nature 167, 715,(1951): Proc.
Phys.Soc. B.69, 350,(1956).
15. Schneider and Parker. Nature 178, 327,(1956).
16. Taurel. Compt.Rend 234, 2443 and 2530,
(1952).
17. Mark. Naturwissenschaften, 13,1042,
(1925).
18. Komar. Nature 137, 397,(1936).

19. Jones and Smith Proc.Phys.Soc. B69,878,(1956).
20. Guinier and Tennevins. Acta.Crysta.Camb. 2 133,(1949).
21. Amelinckx. Acta Metallurgica 2,848,(1954).
22. Lennard-Jones and Dent. Proc.Roy.Soc. 121A,247,(1928).
23. Renninger and Ewald. International Conference of Physics (Physical Society,1935), p.57.
24. Goldsztaub.and Kern. Bull.Soc.Franc.mineral 75, 297, (1952).
25. Barrer. Diffusion in and through solids (Cambridge University Press,1951) p.312.
26. Von Hevesy. Z.Phys.Chem. 101,337,(1922).
27. Tamman and Veszi Zeit.anorg.Chem. 150, 355,(1926)
28. Smekal and Quittner. Z.Phys. 55, 298, (1929).
29. Goodfellow. Ph.D.Thesis, University of Durham (1955).
30. Schneider and Cunnel. Phys.Rev. 95, 598A, (1954):
31. Menzies and Skinner. Disc.Faraday Soc. 5, 366,(1949).
32. Albert, Montariol, Reich and Chaudron. Radioisotope Conference Vol II (Butterworth's Scientific Publications), p.75.
33. Schulman. J.Phy.Chem. 57, 749,(1953).
34. McFee. J.Chem.Phys. 15, 856,(1947).
35. Lehfeldt. Z.Phys. 85, 717,(1933).
36. Stone. Chemistry of the solid state.- Edited by Garner. (Butterworth's Scientific Publications 1955), p.33.
37. Steigman, Shockley and Nix. Phys.Rev. 56, 13,(1939).
38. Jost. Diffusion in solids,liquids, gases.(Academic Press Inc. 1952. p.17.

39. Sherwood. Private communication.
40. Jost. Diffusion in solids, liquids, gases (Academic Press Inc. 1952) p.23.
41. Jost. Ibid. p.64.
42. Kern and Pick. Zeit.fur Phys. 134, 610, (1953).
43. Yamaguti. Proc.Math.Soc. Jap. 23, 433, (1941)
44. Reddington. Phys.Rev. 87, 1066, (1952).
45. Seitz. Rev.Mod.Phys. 26, p.13 (1954).
46. Laurent and Bénard. Compt.Rend. 241, 18 (1955).
47. Schneider and Caffyn. Proc.Phys.Soc.Suppl., 74, (1955).
48. Cottrell. Strength of Solids (London, Physical Society, 1948) p.30.
49. Lidiard. Phys.Rev. 94, 29, (1954).
50. Bardeen and Herring. Imperfections in Nearly Perfect Crystals-Shockley (Wiley 1952) p.28
51. Compaan and Haven. Trans.Faraday Soc. 52, 786, (1956)
52. Roberts Private communication.
53. Gyulai. Z.Physik. 125, 1-17, (1948).
54. Langmuir. J.Franklin Inst. 217, 543, (1934).
55. Hoffman and Turnbull. J.Applied Phys. 22, 634, (1951).
56. Winegard and Chalmers. Canad.J.Physics 30, 422, (1952).
57. Fraser. Molecular Rays (Cambridge 1931) p.82.
58. De Boer. Advances in Colloid Science Interscience N.Y. 1950, Vol. III p.
59. Morrison. Private communication.

